Publication 15

MORPHOMETRIC NERVE STUDIES

John P. Fraher

MB BCh BAO BSc PhD

DSc Thesis

University of Edinburgh

1991

Volume 2

PROGRESS IN NEUROBIOLOGY
IN PRESS.

THE CNS-PNS TRANSITIONAL ZONE OF THE RAT.

MORPHOMETRIC STUDIES AT CRANIAL AND SPINAL LEVELS

John P. Fraher,
Anatomy Department,
University College,
Cork,
Ireland.

CONTENTS

1. INTRODUCTION

The central and peripheral parts of the nervous system differ in many respects, such as in the nature of their myelinating cells and supporting tissues and in the form and composition of their myelin sheaths. The interface between their territories lies in the CNS-PNS transitional zone. Peripheral to this, myelin sheaths are produced by Schwann cells and the supporting tissues include fibroblasts, collagen fibrils and root sheath cells. Central to the interface, myelin sheaths are produced by oligodendrocytes and nerve fibres are to some extent separated from one another by astrocytes. Astrocytes also make up the CNS-PNS barrier. There is a close fit between this and the fibres penetrating it, which helps to maintain a relatively tight seal between the two tissue compartments.

The boundary between the CNS and PNS therefore represents a biological interface characterized by a sharp discontinuity in a variety of tissue types. Considerable variation is found between different locations in the morphology of the transitional zone. For example, central tissue forms a prominent dome projecting distally into dorsal and into some ventral spinal nerve rootlets, whereas the boundary is placed deep to the level of the spinal cord surface at the attachment of some cervical ventral rootlets. In addition, during development, the boundary undergoes considerable movement and oscillation and continually changes its shape and position, as central and peripheral nervous tissues interact with one another as they establish their mutually exclusive territories. A thorough explanation of the developmental events which have such different end results in the

various locations is a prerequisite for understanding the morphogenetic mechanisms whereby the two tissue classes interact.

Studies on CNS-PNS transitional zone structure date back to at least the middle of the nineteenth century. Early studies have been reviewed by Berthold, Carlstedt & Corneliuson (1984). It was clear from the earliest investigations that central nervous tissue extended distally into many nerve roots (Virchow, 1858; Obersteiner & Redlich, 1894) which therefore consisted of proximal segments containing neuroglia and distal segments composed of peripheral nervous tissue.

Skinner (1931) carried out a detailed histological investigation of the extent of the glial outspread in various cranial nerves, mainly using human material. He noted that glial tissue generally extended further distally in sensory than in motor nerves, and that the glial projection tended to be dome shaped. He observed that the CNS-PNS junction was highly irregular, there being apparent interdigitation of the two tissue compartments at their interface. He identified both astrocytes and oligodendrocytes in the portion of the root composed of central nervous tissue. Tarlov (1937a,b) published two papers on the structure of the nerve root. His observations confirmed and extended many of those of Skinner (1931). He noted considerable variation in the length of the glial projection, between different cerebrospinal nerves, between the rootlets of the same nerve and between the right and left sides. He identified presumed glial islands in the peripheral tissue segment of the root. Both he and Skinner (1931) considered that oligodendrocytes comprised the majority of the neuroglial cells in the root. He described systematic variation in the length of the glial projections, concluding that these are longer in sensory than in motor

roots, but only for the cranial nerves taken as a group, and only for the roots of spinal nerves at a given level along the neuraxis. He noted further that there is a gradient among the spinal nerve roots whereby the length of the glial segment increases in a rostrocaudal direction to the level of the upper sacral segments, below which it decreases.

Foncin (1961) carried out the first ultrastructural study on the transitional region, including the transitional node, in the rat. He showed that an apparent deficiency of myelin in the transitional zone, the Aufhellungszone (Obersteiner & Redlich, 1894), was artefactual, due to pronounced splitting of the oligodendrocytic myelin sheath on the central side of the CNS-PNS interface. In a systematic light and electron microscopic study, Němeček, Pařízek, Špaček & Němečková (1969) also examined variation in the distal extent of the glial projection. They too noted considerable interdigitation of peripheral and central nervous tissue at the transitional zone. They described the border between the central and peripheral tissue compartments as being formed by a barrier of astrocytes and observed that the internode central to the transitional node was myelinated by an oligodendrocyte and that distal to it by a Schwann cell. Maxwell, Kruger & Pineda (1969) in a study on the transitional zone of the Macaque trigeminal sensory root, found that astrocytes and not oligodendrocytes were the principal glial components of the transitional zone. They noted that the part of the root composed of central nervous tissue had essentially the structure of white matter and that the astrocyte processes of the glial projection were homologous to, and continuous with, the glia limitans forming the surface of the CNS generally.

The light and electron microscopic appearance of the transitional zone of cat S1 dorsal roots was described in a series of studies by Berthold and Carlstedt (1977a,b,c) and Carlstedt (1977b). These provided a detailed account of the structure of the glial projection and the distribution of the various tissue components within it. A number of studies indicated that the essential structure of the transitional region has similar features in a variety of mammals including man (Sindou, Quoex & Baleydier, 1974). Thus, Snyder (1977) showed that the organisation of dorsal root transitional zones in cats and monkeys resembles that in the rat (Nathaniel & Nathaniel, 1963; Nathaniel & Pease, 1963; Steer, 1971). Schlaepfer, Freeman and Eng (1979) utilised ultrastructural and histochemical techniques to identify and characterise the glial elements in human and bovine nerve roots. Moll and Meier (1983) described the transitional zones of dorsal and ventral cervical spinal nerve roots in both normal and Jimpy mutant mice using light and electron microscopy. They showed that, despite a severe deficiency of central myelin in Jimpy animals, there was no central migration of Schwann cells to remedy the defect.

It became clear from early ultrastructural studies (Foncin, 1969) that good fixation of the central nervous tissue component of the transitional zone is particularly difficult to achieve. Maxwell et al. (1969) also observed that central myelin in the zone was often poorly preserved. They ascribed this to distorsion of the myelin due to stresses associated with either manipulative trauma or fixation procedures. This was also evident from other early ultrastructural studies, such as those of Ross and Burkel (1971) and Steer (1971). Carlstedt (1977a) carried out a systematic and detailed study on fixation

procedures, as a result of which good preservation of both central and peripheral tissue componenets of the cat transitional zone was achieved. In the rat it was found that a combination of vascular perfusion and irrigation of the subarachnoid space through cranial and sacral burr-holes resulted in very satisfactory fixation of both central and peripheral components of the zone (Kaar, O'Sullivan & Fraher, 1983).

This review primarily summarizes a systematic series of studies on the development and mature form of the CNS-PNS transitional zone of rat cranial and spinal nerves. In general, the material examined was prepared for electron microscopy (Fraher & Kaar, 1984; Kaar et al., 1983). Specimens were sectioned in most cases by means of alternating sequential series of thin and semithin sections in transverse and/or longitudinal planes. This allowed determination of the three-dimensional form of the transitional zone both during development and at maturity and also of the growth, myelination and maturation of the fibres traversing it.

2. DEFINITIONS

In the rat, most spinal and cranial nerves break up into roots in the vicinity of the central nervous system. In general, each root is attached to the neuraxis by a group of rootlets (Fig. 1a,b). The fibre bundle which comprises each rootlet is continued into the CNS. Accordingly, each rootlet has an intramedullary segment within the CNS, an emergent segment where it passes through the CNS surface, and a free segment peripheral to this (Fig. 1c). The free segment traverses the pia mater and, more distally, lies in the subarachnoid space. Free rootlets commonly join together in groups to form aggregated rootlet bundles (Fig. 1a,b) which in turn combine, giving the roots which unite to form the spinal and cranial nerve trunks. The area of brainstem or spinal cord surface through which motor rootlets emerge is termed the exit zone; that to which sensory rootlets are attached is termed the attachment zone.

In general intramedullary rootlets are composed of central nervous tissue and the distal portions of free rootlets of peripheral nervous tissue. Where the two tissue classes meet they interdigitate and overlap so that a segment of the rootlet contains both. This is the CNS-PNS transitional zone (Fig. 1d). Central nervous tissue projects distally beyond the plane of the CNS surface into a majority of rootlets as a central tissue projection (Fig. 1d). A large part of the transitional zone therefore lies in the free rootlet in these cases. Less commonly, this projection is absent and the zone lies at about the level of the CNS surface.

Each myelinated axon passing between the CNS and PNS possesses a transitional node (Fig. 1e). The myelin sheath enveloping the axon distal to this is formed by the transitional Schwann cell, which is the most proximal Schwann cell of the PNS. The sheath central to the transitional node is formed by a transitional glial unit, one of a number which extend from the perikarya of a transitional oligodendrocyte. Transitional nodes lie on the CNS-PNS interface, and so are distributed throughout the zone.

On emerging from the neuraxis, dorsal rootlets curve ventrally and ventral rootlets curve dorsally. Accordingly, each rootlet has a superficial and a deep surface with respect to the neuraxis. The rootlets also run laterally as they approach one another to form aggregated rootlet bundles. As a result each has a rostral and a caudal surface, termed the collateral surfaces. The central tissue projections which they contain possess similarly named surfaces.

3. TRANSITIONAL ZONE STRUCTURE

3.1. Types of Transitional Zone

The transitional zone may lie in a variety of locations in the rootlet. Its position, form and extent differ widely between individual nerves and even in some cases between the constituent rootlets of a given nerve. In the majority of cases it lies either at approximately the level of the surface of the CNS, or immediately distal to this within the proximal part of the free rootlet. In some instances, however, it may extend deep into the CNS, as in dorsolateral vagal rootlets, or it may lie within the nerve at a considerable distance peripheral to the surface of the CNS, as in the cochlear nerve. The central nervous tissue component is covered by a specialised thickening of the glia limitans, the distal surface of which is commonly irregular. This interdigitates closely with the peripheral nervous tissue distal to it. The CNS-PNS interface is therefore undulant. Transitional zones may be classified into eight main types as follows, according to the morphology, position and extent of the mass of astrocytic tissue which forms their main bulk (Fig. 2).

A transitional zone which lies at and slightly deep to the surface of the neuraxis is classed as type 1 (Figs. 2, 3a-d). The thickening of the glia limitans is invaginated by the central ends of transitional Schwann cells of myelinated fibres (see below). From its superficial surface slender astrocytic processes extend distally into the rootlet among the transitional Schwann cells, forming a glial fringe. Around the perimeter of the fibre bundle at and deep to the plane of the CNS surface, the transitional zone is commonly surrounded by a thick collar of astrocytic tissue which is not traversed by any nerve fibres. From

its deep extremity astrocytic tissue may be prolonged as a centrally tapering wedge-shaped projection, which is traversed by the distal parts of the transitional oligodendrocytes.

In type 2 transitional zones, central nervous tissue extends distally into the free rootlet as a central tissue projection (Figs. 2, 3e). This tapers distally and so is approximately cone- or wedge-shaped. In cross section it is generally flattened dorsoventrally. Its surface is formed by the thickened glia limitans and its core resembles central white matter. Peripheral nervous tissue comprises the complementary portion of the free rootlet over the length of the transitional zone. The central ends of transitional Schwann cells usually lie in grooves on its surface, at the proximal ends of which lie the transitional nodes (see below). Many central tissue projections have a markedly irregular surface and may branch towards their distal ends. Some larger examples may display more than one order of branching. In most cases the projection lies asymmetrically in the rootlet, being placed closer to its deep than to its superficial surface. Type 2 zones are generally confined to the rootlet and do not extend into the neuraxis as do type 1 zones.

Type 3 zones lie within the rootlet at a considerable distance beyond the surface of the neuraxis (Figs. 2, 3f-h). This is because a long segment of the free rootlet between the surface of the CNS and the transitional zone consists entirely of central nervous tissue The internal structure of the central tissue segment is similar to that of a CNS tract and its surface is bounded by a layer of astrocytic tissue continuous with the glia limitans covering the CNS surface surrounding the attachment of the rootlet to the neuraxis (Fig. 3g).

In type 4 zones there is also a prominent central tissue projection into the rootlet. However, this is markedly asymmetrical, so that it coincides over its entire length with the deep surface of the rootlet. It is therefore wedge-shaped (Figs. 2, 4a-d). Accordingly, the central-peripheral interface crosses the rootlet obliquely. As it is traced centrally this type of projection also makes up a progressively increasing proportion of the collateral rootlet surfaces.

In type 5 zones the glia limitans is markedly thickened over a circumscribed area and gives rise to a wedge-shaped (type 5a) or pedunculated (type 5b) elevation which projects above the level of the surrounding neuraxis (Figs. 2, 4e). This is traversed by the fibre bundle comprising the rootlet, which enters its deep aspect and emerges from one aspect of its free surface to run at a shallow angle to the surface of the CNS. As it traverses the projection the bundle is surrounded by a thick sleeve of glial tissue containing no nerve fibres. The transitional Schwann cells are invaginated into the projection (see below) and a glial fringe projects distally among them from its surface.

In type 6 zones peripheral nervous tissue is found at considerable distances deep to the CNS surface (Figs. 2, 4f-h). In the majority of cases PNS tissue generally extends centrally through a central tissue projection as one or more strands. It extends further centrally for considerable distances along the course of the intramedullary rootlet within which it expands to form a peripheral tissue insertion (Fig. 2).

Type 7 zones resemble the former insofar as peripheral nervous tissue forms a substantial proportion of the cross sectional area of the intramedullary rootlet over a considerable length deep to the plane of the CNS surface. However, it entirely lacks continuity with peripheral

tissue further distally and therefore constitutes a peripheral tissue island isolated deep to the surface of the neuraxis (Fig. 2).

In type 8 zones a prominent central tissue projection forms the entire cross section of the nerve trunk over a considerable distance (Fig. 2). Distal to this, the nerve is composed of separate bundles, arranged either as closely related fasciculi or as a leash of branches. Each such bundle contains a central tissue projection stemming from that in the main nerve trunk.

Each of the above types of zone may be modified by the occurrence in the free rootlet of an island of glial tissue lacking all continuity with the tissue of the CNS (Fig. 2). Such glial islands may consist only of astrocytic tissue or may in addition contain oligodendrocytes.

That part of the free rootlet immediately distal to the transitional zone is termed the proximal rootlet segment. This differs from typical peripheral nervous tissue in that its development lags behind that of more distal parts of the root. Even at maturity it retains a number of immature features (Fraher & Rossiter, 1983a,b; Fraher & Kaar, 1986).

3.2 Ultrastructure of the Transitional Zone

3.2.1 Astrocytic tissue - general features

Astrocytic tissue forms the bulk of the central tissue component of the transitional zone, which consists predominantly of a thick weave of astrocyte processes. A variable number of astrocyte perikarya also occur in it, depending on the size of the zone. Where this is large, such as in the central tissue projections of C7 dorsal rootlets (Fraher & Sheehan, 1987), numerous astrocyte perikarya are present, most commonly at the surface but also within the substance of the projection (Fig. 3e). Few if any occur within smaller transitional zones, such as those of lower cervical ventral rootlets or abducent rootlets. Instead they usually lie at the surface of the CNS around the margin of the zone and give rise to processes which enter it (Figs. 4e, 5c).

Astrocyte processes tend to be arranged concentrically around individual myelinated axons or unmyelinated axon bundles as these traverse the transitional zone (Figs. 5c, 10a). In general, they are separated by a basal lamina-lined cleft from myelinating Schwann cells which are invaginated into the zone (Fig. 5b). They also project into the transitional node gap, forming a disc-like partition between the CNS and PNS environments. In addition, considerable amounts of astrocytic material intervene between transitional nodes of neighbouring fibres. A short distance central to the transitional node, the transitional oligodendrocytic myelin sheaths become more closely apposed to one another as the astrocytic material separating the fibres decreases (Fig. 5b). As for the astrocytes, the perikarya of transitional oligodendrocytes lie around the periphery of small zones but are found, often in large numbers, within large central tissue projections.

Astrocytic processes, both singly and in the form of interlocking complexes, also extend distally into the rootlet to intermingle with the transitional Schwann cells, both from the surfaces of central tissue projections and in transitional zones which lie at or deep to the level of the surrounding CNS surface (Figs. 5b, 6a). The astrocytic glial fringe so formed is more sparse and open in the rat than in the cat, as described by Berthold and Carlstedt (1977a) and by Carlstedt (1981).

A continuous basal lamina covers the surface of the astrocytic limiting membrane of the transitional zone (Fig. 5b) including the glial fringe, from early development onwards. This follows all the irregularities of the zone surface and lines the invaginations for the transitional Schwann cells.

A high degree of complexity of astrocytic process arrangement is not confined to the transitional zone. For example, in the exit zones of at least a number of cranial nerves, the glia limitans forming the CNS surface in the intervals between the transitional zones of the rootlets is markedly thickened and irregular. This is especially the case where rootlets closely overlie the CNS surface, as in the oculomotor exit zone (Fig. 3f,g). Also, the glia limitans forms a prominent circumscribed pad of interdigitating astrocytic lamellae (Fig. 3a) surrounding many emerging abducent and upper cervical ventral rootlets (Fraher & Cremin, 1987, unpublished). In addition, in some instances astrocytic processes may extend distally as a thick sheath forming the surface of that part of the rootlet which consists entirely of CNS tissue, as in type 3 transitional zones (Fig. 3g). Furthermore, the glia limitans may be thickened in some places outside the limits of the exit zone. For

example, it forms a thickened strip along the ventral brainstem surface underlying the abducent nerve trunk distal to its exit zone.

3.2.2 Astrocytes in the vagal transitional zone

The arrangement of astrocyte perikarya and processes was examined in detail in rat dorsolateral vagal rootlets which had been sectioned to provide extensive series of thin sections and also of alternating sequential series of thick and thin sections (see Rossiter & Fraher, 1990). Less extensive serial ultrastructural studies indicate that the general arrangement of astrocytic tissue in other rat transitional zones, including those of C7 ventral rootlets (Fraher, 1978a), L5 ventral rootlets (Fraher & Kaar, 1986), C7 dorsal rootlets (Fraher & Sheehan, 1987) and the trochlear nerve (Fraher et al., 1988c) resembles that in vagal central tissue projections.

Typical features of vagal transitional zone astrocytes are illustrated in Figure 6c-e and summarized in Figure 7. Typically, one or more large transversely orientated primary processes project from each perikaryon (Fig. 6c,d), giving rise to longitudinally running secondary processes (Fig. 7a). These, and also those primary processes which arise from the ends of the perikaryon and which also run longitudinally, frequently extend for up to 30 μm in the long axis of the rootlet. Transversely orientated flattened tongue- and sheet-like processes stem from the primary and secondary processes and also directly from the perikarya (Figs. 6c,e, 7b).

The astrocytic limiting membrane forming the central tissue projection surface is generally 1-5 μm thick and consists of many layers of processes, ranging in appearance from irregularly interlocking to regularly stacked (Fig. 8a,b). It is generally considerably more

complex than the glia limitans of the brainstem surrounding the transitional zone (Fig. 8c). Gap junctions, stacks of desmosomoid adherent junctions and hemidesmosomes are common between the processes. Processes from neighbouring perikarya interdigitate extensively.

General features of the organisation of the vagal central tissue projection and peripheral tissue insertion are illustrated in Figure 9. Within the central tissue projection, astrocytic processes form a complex network which extensively partitions central and peripheral tissues. This segregates bundles of unmyelinated as well as centrally and peripherally myelinated axons, both from one another and each from others of its kind. The network consists mostly of thin laminar processes and the larger longitudinally running processes from which they arise (Fig. 7a,b). An individual myelinating Schwann cell internode is typically isolated in a basal lamina-lined invagination.

In the vagus, much less astrocytic tissue is found in peripheral tissue insertions than in central tissue projections. Internodes myelinated by Schwann cells share compartments with others of their kind and with unmyelinated bundles, both being embedded in an endoneurial matrix which lacks fibroblasts (Fig. 9c). Astrocytic tissue forms a barrier between its peripheral nervous tissue and the central tissue of the surrounding brainstem and also projects into the peripheral tissue insertion (Figs. 8d,e, 9c). Towards the superficial end of the insertion, astrocytic processes form an open network of septa dividing the peripheral nervous tissue into intercommunicating compartments. More deeply, the septa are much less well developed. Here, some astrocyte process profiles are dispersed among the

peripheral nervous tissue which is virtually unsegregated. The arrangement of astrocytic tissue in relation to peripheral tissue islands closely resembles that in insertions.

Thus, nerve fibres are better segregated in the central tissue projection than in the peripheral tissue insertions or islands. In the peripheral tissue insertion astrocyte processes play a unique morphological role. They take the place of sheath cells in the peripheral parts of the vagal rootlets and of endoneurial and perineurial cells elsewhere in the PNS.

The barrier between the peripheral tissue insertion and the brainstem typically consists of only one or two layers of astrocyte processes. It is covered on its inner surface by a basal lamina, where a narrow endoneurial space containing collagen fibrils generally separates it from Schwann cells of the peripheral tissue insertion. The barrier is commonly deficient. In places it contains perforations through which oligodendrocytic myelin sheaths are directly exposed to the endoneurial space of the peripheral tissue insertion and in some cases are exposed to myelinating or non-myelinating Schwann cells (Figs. 8f, 9c). Such communication between the CNS and PNS tissue compartments is unique to the vagal transitional zone. It has, however, been observed in adult rat spinal cord following neonatal X-irradiation (Blakemore & Patterson, 1975; Sims & Gilmore, 1983; Gilmore & Sims, 1986) and also following remyelination subsequent to demyelination induced by heat injury in the adult animal (Sasaki & Ide, 1989).

3.2.3 Transitional zone astrocytes have distinctive features

Astrocyte processes in the transitional zone demonstrate an unusual combination of features compared with those in other areas. For example, their large cylindrical primary processes resemble the radial glial processes in the spinal cord (Sims et al., 1985) which also contribute to the glia limitans. The pattern of the larger sheet-like primary processes and their longitudinally orientated secondary processes is similar to that of astrocytes within the optic nerve, which have traditionally been regarded as fibrous in nature (Skoff, Knapp & Bartlett, 1986). Many of the processes which contribute to the network within the transitional zone are small, thin and sheet-like and resemble lamellar processes of protoplasmic astrocytes as illustrated by Wolff (1965), Stensaas and Stensaas (1968) and Poritsky (1969). Processes of this form are not characteristic of those of fibrous astrocytes, such as separate nerve fibres from one another in white matter (Peters, Palay & Webster, 1976). They are, however, typical of the glia limitans of the brain (Haug, 1971; Bondareff & McLone, 1973; Braak, 1975; Williams, 1976; Suarez & Fernandez, 1983; Wagner, Barthel & Pilgrim, 1983; Uehara & Ueshima, 1988) and spinal cord (Sims et al., 1985). Individual astrocytes of the vagal transitional zone contribute to the surface boundaries of the central tissue projection or peripheral tissue insertion and also, as at the transitional zone of rat spinal ventral rootlets (Fraher & Kaar, 1984) give rise to processes contacting the transitional nodal axon. They therefore have features of both type 1 and type 2 astrocytes in the rat optic nerve (Miller & Raff, 1984; Miller, Fulton & Raff, 1989). Of these, type 1 mostly form the glia limitans and type 2 lie within the nerve and give rise to processes contacting the nodes (ffrench-Constant & Raff, 1986; Miller et al., 1989).

Transitional zone astrocytes are thus of a single type possessing a wide variety of processes which play a full range of morphological roles appropriate to transitional zone structure. This finding is consistent with the growing recognition of the structural (as well as immunochemical and functional) heterogeneity of astrocytes (Fedoroff, 1986; Privat & Rataboul, 1986; Skoff et al., 1986; Miller, 1988; Raff, 1989) as well as the limitations of the traditional fibrous/protoplasmic classification system (Privat & Rataboul, 1986; Miller, 1988; Miller et al., 1989).

Maxwell et al. (1969) commented on the infrequent occurrence of oligodendrocytes in the glial tissue of the Macaque trigeminal sensory root, and Berthold and Carlstedt (1977a) noted that in the cat oligodendrocytes are less numerous than astrocytes and are restricted to the core of the transitional zone. It is clear that in the rat at least, the presence or absence of oligodendrocyte perikarya in the transitional zone is closely related to the size of the nerve or rootlet. Where this is large, as in the case of the cochlear nerve, and where it contains a central tissue projection (Fraher & Delanty, 1987) oligodendrocyte perikarya are common. Large numbers also lie in that segment of the nerve which consists entirely of CNS tissue Irrespective of the location of the transitional oligodendrocytic perikarya, their myelin sheaths extend distally within transitional zones of all sizes as far as the CNS-PNS interface from an early stage in maturation (see below).

3.3 Transitional Zone Schwann Cells

A variable length of the transitional Schwann cell is closely related to the astrocyte processes forming the CNS-PNS interface. The arrangements for myelinated and non-myelinated fibres differ.

3.3.1 Myelinating Schwann cells

The central end of the transitional myelinating Schwann cell commonly lies in an invagination or in a groove walled by astrocytic tissue. The former arrangement is characteristic of type 1 and type 5 and the latter of type 2 transitional zones. These invaginations (Figs. 5b,c,10a) may be 50 μm or more deep and are found at lower cervical and upper thoracic ventral rootlet zones (Fraher, 1978a; Fraher & Kaar, 1982). They also occur in other locations where they tend to be shorter, for example in dorsal spinal rootlets (Steer, 1971; Berthold & Carlstedt, 1977a; Carlstedt, 1981; Moll & Meier, 1983; Fraher & Sheehan, 1987) and in cranial nerves (Maxwell et al., 1969; Nemecek et al., 1969; Ross & Burkel, 1971; Fraher et al., 1988a,b,c; Rossiter & Fraher, 1990). The wall of the invagination is composed of astrocyte processes, which in many instances are circumferentially arranged. Its inner aspect is covered by a layer of basal lamina. The invagination contains the central end of the transitional Schwann cell, consisting of its paranode and a variable length of the adjacent part of the internode, depending on the depth of the invagination. The transitional node lies at the deep end of this (Fraher & Kaar, 1984; Fraher et al., 1988a). Here, astrocyte processes project into the node gap and separate the transitional Schwann cell from the paranode of the oligodendrocyte bounding the node centrally. The CNS and PNS environments are further separated from one another by the basal lamina which forms a disc-like projection into the node gap between the astrocyte

processes and the Schwann cell (Fig. 5b). At this point, the basal lamina lining the invagination is continuous with that covering the transitional Schwann cell by being reflected onto the latter. Around this it forms the most proximal part of the sleeve which is continuous distally, uninterrupted, along the series of Schwann cells enveloping the myelinated axon. Within the invagination, the gap between the basal laminae contains collagen fibrils, the number of which increases during development. Many of these cross the gap and interconnect the two layers of basal lamina. In their deeper parts the invaginations are surrounded by complete astrocytic walls. More superficially these become incomplete and are continuous distally with the astrocytic processes forming the glial fringe.

In type 1 transitional zones, the invaginations are generally closely packed, so that the zone resembles a honeycomb, and the mouths of the invaginations lie approximately in the plane of the CNS surface. Their average depth is around 30 μm in the adult. The appearance and arrangement of astrocytic invaginations are clearly shown in specimens in which the ventral rootlets have been experimentally avulsed (Bristol & Fraher, 1989) from the spinal cord (Fig. 11). In many instances (Fig. 11d,e) individual fibres rupture at the transitional node and the transitional Schwann cells are pulled out of their invaginations, showing the honeycomb-like arrangement of the astrocyte processes.

In those rootlets possessing central tissue projections the relationship of the central end of the transitional Schwann cell to the astrocytic tissue is somewhat different from that described above. Each lies in an individual open-sided groove on the surface of the projection (Figs. 10b, 12b,c). The groove varies in length from 20 μm in lumbar

ventral rootlets to over 50 μm in some examples in the dorsolateral vagal rootlet. Most transitional nodes lie at the central ends of the grooves.

While one or other of the above arrangements is found generally, transitional Schwann cells in dorsolateral vagal rootlets display some more unusual features. For example, the central ends of about one fifth of myelinated transitional Schwann cells are unrelated to either a groove or an invagination and are surrounded by endoneurium up to the level of the node (Fig. 10c). Also, many share grooves up to 70 μm long on the central tissue projection surface with groups of unmyelinated axons or with other similar myelinated fibres (Fig. 10d). In addition, some are accompanied by basal lamina-covered complexes of astrocytic processes and Schwann cell-enveloped unmyelinated axons (Fig. 10e).

3.3.2 Nonmyelinating Schwann cells

Transitional nonmyelinating Schwann cells also have an intimate relationship with the astrocytes of the transitional zone. Many large unmyelinated axons pass between the CNS and PNS at, or even distal to, the general surface of the zone (Figs. 13a, 14a,b). In such cases, a collar of astrocyte processes commonly extends distally into the rootlet for several micrometers around the axon or axon bundle. Where this meets the central end of the transitional Schwann cell, the two frequently interdigitate. Often, no basal lamina intervenes between the two cell types. In some cases the two cells fail to come into close apposition with one another and basal lamina closely surrounds the bare axon segment intervening between them.

The CNS-PNS transition of unmyelinated axon bundles as, for example, in vagal dorsolateral rootlets is characterized by extensive interdigitation and overlap of central and peripheral tissues (Figs. 13b,

14c-f), even at locations 200 μm deep to the brainstem surface where the unmyelinated bundles finally enter the CNS. As the bundle is traced centrally, its enveloping Schwann cell processes extend below the plane of the central tissue surface (Fig. 14c). The resulting invagination is bounded externally by astrocytic tissue. In its superficial part this is separated from the Schwann processes by a cleft, both surfaces of which are covered with basal lamina. Further centrally the cleft disappears and the Schwann sleeve becomes directly apposed to the surrounding astrocytic tissue (Fig. 14d). The processes terminate gradually with increasing distance centrally (Fig. 14e,f). Those towards the periphery of the bundle end furthest distally. Those towards its centre have generally terminated completely 60 μm deep to the central tissue surface. This manner of central-peripheral transition of unmyelinated axons is considerably more elaborate than in either of the other two locations in which it has been the subject of serial section study, namely, the cat S1 dorsal root (Carlstedt, 1977b) and the cat trigeminal motor root (Risling et al., 1986).

4. VARIATIONS IN TRANSITIONAL ZONE MORPHOLOGY

The various types of transitional zone (see 3.1) are found in differing combinations and proportions in the nerves examined. In some cases all the rootlets of a given nerve possess transitional zones of one and the same type. For example, the ventral C7 rootlets possess type 1 zones. By contrast, transitional zones differ between individual rootlets of the majority of cranial and of some spinal nerves. This section gives an account of the variation found in transitional zone morphology in selected cranial and spinal nerves (Fig. 15a).

4.1. Spinal Nerves

4.1.1. C2 ventral rootlets

Second cervical ventral rootlets and their transitional zones vary considerably in form. Upper rootlets run ventrocaudally within the cord (Fig. 15b). Some continue in this course as they emerge and contain type 2 transitional zones. Others possess type 5b zones. Their central tissue projections contain numerous astrocytic perikarya and are markedly pedunculated (Fig. 15c). Large parts of these lack nerve fibres and may be closely apposed to bloodvessels or fused with corresponding portions of adjacent projections (Fig. 15d). The fibre bundles turn laterally within those projections before emerging from them. More caudal rootlets cross the anterolateral white fasciculus approximately transversely. Some of these possess type 1, others type 5 transitional zones.

The transitional nodes of adjacent fibres differ markedly in level relative to the cord surface. In type 1 zones most lie deep (some as much as 55μm) to the plane of the surrounding cord surface. In type

2 zones all nodes lie within the free rootlet, some up to 100μm distal to the exit zone. In type 5 zones most nodes lie superficial to the cord surface, through a small number are deep to it.

4.1.2. C7 ventral rootlets

The C7 ventral rootlets possess archetypal type 1 transitional zones (Fraher, 1978a; Fraher & Kaar, 1982) (Figs. 2, 5). The central ends of the transitional Schwann cells are invaginated below the cord surface to an average depth of about 30 μm and some cases up to 50 μm. Here they lie in an astrocytic honeycomb. This is clearly evident when the rootlets are avulsed experimentally (Fig. 11) (Bristol & Fraher, 1989).

4.1.3 Upper Thoracic ventral rootlets

Upper thoracic ventral rootlets are short. They emerge from the spinal cord in a ventrocaudal direction and immediately join an aggregated rootlet bundle. All but the smallest tend to contain central tissue projections (Figs. 15f, 16a,b). Most of these are slender and extend distally into the aggregated rootlet bundle in which they follow an irregular course. Some terminate freely, while others fuse within the aggregated bundle with those of adjacent rootlets. This arrangement is unusual, though it is also found in C7 dorsal rootlets (Fraher & Sheehan, 1987) (see Section 4.1.5). These central tissue projections vary markedly in length. In a small sample measured, values ranged from 120 μm to over 700 μm (mean: 240 μm).

The slender projections are traversed by unmyelinated axons. These are the central continuations of small myelinated axons (of diameter averaging 3 μm) which lose their myelin sheaths on entering the central tissue projection (Fig. 16a-c).

These projections intermingle with large axons myelinated by Schwann cells (mean diameter: 10 μm), which generally have their transitional nodes at or (in some cases a considerable distance) deep to the plane of the spinal cord surrounding the ventral rootlet attachment. The transitional zones of such rootlets therefore constitute a mixture of type 1, for the large fibres, and type 2, for the small fibres. In some larger rootlets the large fibres traverse the CNS-PNS interface through a type 2 transitional zone.

Upper thoracic ventral rootlets are thus distinctive in that the modes of transition of large and small myelinated axons differ markedly from one another. The presence of long unmyelinated segments between the central end of the transitional Schwann cell and the CNS surface represents the persistance of an immature trait, found early in transitional node development (Fraher & Kaar, 1984).

4.1.4 Lumbar ventral rootlets

The fourth and fifth lumbar ventral rootlets contain type 2 transitional zones (Fraher & Kaar, 1986; Bristol & Fraher, 1987), averaging 160 and 70 μm long respectively. Each of these lies almost entirely in the free rootlet. It contains a typical prominent central tissue projection (Fig. 2). The central ends of most transitional Schwann cell internodes lie in open-sided grooves, around 20-30 μm long, on the surface of this (Fig. 12b). Though most transitional nodes lie at the proximal ends of these grooves, a few lie in shallow invaginations, 5-10 μm deep. A small number of mature oligodendrocyte perikarya lie in the central tissue projection, though most of those responsible for myelinating the transitional oligodendrocytic internodes lie within the CNS, central to the zone.

4.1.5 C7 dorsal rootlets

The transitional zone of a typical C7 dorsal rootlet is also of type 2. However, its central tissue projection is larger and more elaborate than that of the L5 ventral rootlet. It consists of a proximal segment, shaped like a dorsoventrally flattened wedge (Fig. 15e). From this, one or more long, tapering conical processes extend distally and in some cases branch. The presence or absence of branching bears no clear relationship to projection length. Thus, among the longest examples, some are unbranched while others possess second or third order branches. Distal to the levels at which rootlets become apposed and join with one another, their central tissue projections commonly fuse, or are separated only by layers of collagen fibres (Fig. 25a). The mature form of the central tissue projection of the rat C7 dorsal rootlet is considerably more complex and variable than that of the cat S1 dorsal rootlet, which is described by Berthold and Carlstedt (1977a), as having a regular, approximately conical shape.

4.2 Cranial Nerves

4.2.1 Motor nerves to extraocular muscles

(a) Oculomotor nerve

The oculomotor nerve is composed of large numbers of rootlets of widely differing size (Fraher et al., 1988b). The emergent segments of most of these run laterally immediately deep to the glia limitans (Fig. 15g). As they do so, many form plexuses with one another and each produces a progressively more prominent ridge on the brainstem surface. They separate from this at a shallow angle to become the free rootlets, which converge and join together to form the nerve trunk.

Transitional zones of types 1 to 5 are found in oculomotor rootlets. While a number of smaller rootlets contain type 1 zones, a central tissue projection extends distally into the majority. Rootlets fall into four main classes, each of which tends to be associated with a distinct type of projection (Fraher et al., 1988b). The longest projections are of type 3 (Fig. 3f-h). In these, especially close to the central end of the free rootlet, the glia limitans forms a thick covering surrounding the fibre bundle (Fig. 3g).

In rootlets possessing type 4 transitional zones peripheral nervous tissue extends proximally ventral to the central tissue projection into the emergent segment. Here it forms a thin, gradually tapering strip, commonly over 50 μm long. Accordingly, the transitional zone lies in both emergent and free parts of the rootlet. It has a very extensive central-peripheral interface which makes for marked separation of transitional nodes. Furthermore, the central ends of many of the transitional Schwann cells are deeply invaginated into the central tissue projection. These arrangements minimise or exclude the likelihood of crosstalk between nodes on fibres innervating the majority of extraocular muscles and therefore reinforce the precise control of eyeball movement. Type 5 zones are found in relation to the smaller rootlets.

(b) Trochlear nerve

Intramedullary trochlear rootlets are few in number. They curve dorsally around the periaqueductal grey matter and decussate with those of the opposite side. Continuing laterally, they run on the dorsal brainstem surface and unite to form a single bundle which creates a conspicuous ridge there before becoming the free nerve

trunk. The transitional zone is generally of type 2, but in some cases it is of type 3, when the proximal free portion of the nerve consists entirely of central nervous tissue (Fig. 15k). The projection is generally large, dorsoventrally flattened and distally tapering. The transitional nodes tend to be concentrated close to its blunt distal extremity.

The trochlear transitional zone (Fraher et al., 1988c) resembles that of a C7 dorsal spinal rootlet (Fraher & Sheehan, 1987) in some ways. Both are of similar size and emerge dorsally from the neuraxis. Their central tissue projections are similar in form and dimensions, though those of the trochlear nerve tend to be unbranched. They are substantially longer than those of L4 (Bristol & Fraher, 1987) or L5 (Fraher & Kaar, 1986) ventral rootlets. They are also considerably longer than oculomotor central tissue projections (Fraher et al., 1988b).

(c) Abducent nerve

Intramedullary abducent rootlets run ventrally and emerge through the corpus trapezoideum. The most caudal rootlets curve rostrally to run approximately parallel to the brainstem surface as they traverse it. They then become confluent to form the nerve trunk (Fig. 15h). The remaining rootlets pierce the brainstem surface approximately at right angles before bending sharply rostrally as they fuse with the trunk.

The transitional zones of caudal rootlets are of type 5a. In these, the fibres emerge through the rostral face of a wedge-shaped central tissue projection (Fig. 15h). The remaining zones are of type 1 and closely resemble those of C7 ventral rootlets (Fraher, 1978; Fraher & Kaar, 1982). Most of their transitional Schwann cells invaginate the CNS surface and the nodes lie up to 20 μm deep to it. They contain a

more prominent glial fringe than the C7 rootlets. Their transitional zones extend into both intramedullary and free rootlet segments. Abducent transitional zones possess a number of distinctive features. Some traverse a thick, circumscribed astrocytic pad as they emerge from the CNS (Fig. 3a). In some cases the glia limitans forms a thick strip where the abducent trunk runs rostrally in close relation to it beyond the exit zone.

It is evident therefore that the transitional zones of the three nerves innervating the extraocular muscles of the rat differ markedly from one another in terms of the number, morphology, size and arrangement of their rootlets and in terms of their transitional zone and central tissue projection morphology. The transitional zones of the trochlear nerve and of rostral abducent rootlets resemble in many respects those of dorsal and ventral lower cervical spinal rootlets, respectively. The oculomotor zones, however, differ markedly from all of these in many ways. Most noteworthy is the occurrence of a number of different types of central tissue projection as well as a very wide variation in rootlet size. Thus, despite their similar developmental origin, their purely or largely motor nature, and many features of their peripheral innervation, the morphology of the transitional zones of the nerves to the extraocular muscles differ widely from one another. The wide variety of forms of transitional zone found in these three nerves includes all of the major types noted elsewhere, except for those of the facial and vagus nerves.

4.2.2 Trigeminal nerve

The sensory root of the trigeminal nerve is the largest of all the rat cranial nerves. It emerges running in a rostral direction, from the

ventrolateral aspect of the brainstem, in close relationship with the trigeminal motor root. It contains a type 3 transitional zone (Fig. 15i). The distal surface of the central tissue projection is smooth and convex distally. The succeeding part of the root, which is composed of peripheral nervous tissue is compact. Central tissue projections do not extend into individual fascicles of the nerve.

4.2.3 Facial nerve

The attachment zone of the facial nerve (including the nervus intermedius) is close to that of the vestibular nerve. In the vicinity of the brainstem the facial nerve consists of a number of rootlets or fascicles of differing sizes. One is generally substantially larger than the others.

The transitional zone is usually of type 8 (Fig. 15o) . Typically, the central tissue projection makes up the entire cross section of the proximal part of the nerve and of each of the fascicles or branches to which this gives rise. In these it generally lies asymmetrically and tapers distally. Its distal end tends to be irregular or undulant and is commonly branched. The projections within the various fascicles are offset relative to one another so that at a given level some consist entirely of central and others of peripheral nervous tissue.

The nervus intermedius consists of a series of fascicles as it approaches the brainstem surface. These form two groups, of which one set possesses a type 8 transitional zone. The central tissue projection into each fascicle is short while that of the stem consisting of the fused fascicles is relatively long. Each of the fascicles comprising the second group contains a central tissue projection. The majority of these are of type 3 and the rootlet segment consisting entirely of CNS

tissue is surrounded by a markedly thickened layer of astrocyte processes and perikarya.

4.2.4 Cochlear nerve

The cochlear nerve transitional zone is of type 3. The nerve possesses a relatively very long central tissue projection. This occupies the entire cross section of much of its length and therefore resembles typical CNS tissue. It extends distally almost to the lateral limit of the modiolus, within which its distal end curves rostrally. Cochlear nerve branches arise directly from the projection (Figs. 15j, 16d,e). Short central tissue projections pass distally into some of these. Although some branches initially run close together, especially where they surround the distal end of the main projection, they are only loosely bound to one another and do not reunite to form a compact peripheral nerve trunk, as occurs in the cat (Berthold, Carlstedt & Corneliusson, 1984). Thus, the cochlear nerve possesses no segment where the nerve trunk consists entirely of peripheral nervous tissue. It is unique in this. Furthermore, it differs from all rat spinal and cranial nerves except the facial and from almost all rootlets in that a substantial length of its trunk consists entirely of CNS tissue.

The most proximal cochlear nerve branches arise from the lateral aspect of the projection and run to the basal turn of the cochlea. The projection is not symmetrical about its long axis. Its medial part extends further distally than the remainder and it comes to lie medially and caudally within the leash of its branches.

4.2.5 Vestibular nerve

The rat vestibular ganglion consists of dorsal and ventral parts, joined by an isthmus. Many small nerve bundles emerge from the deep

aspect of the dorsal part (Fig. 15l). These are short and in general each enters the brainstem separately. Some follow a relatively straight course. Others are markedly tortuous and loop around, interdigitate with, or even intersect one another in the shallow gap between the ganglion and the underlying brainstem. The attachment zone of this part of the nerve is very irregular. Its glia limitans is markedly thickened and gives rise to many highly irregular central tissue projections of widely differing shapes. The nerve bundles traverse many of these as they enter the CNS. Some resemble those of type 4, type 5a or type 5b zones. However, many projections contain no nerve fibres and take the form of ridges, veils or branching complexes of astrocyte processes which extend into the gap between the ganglion and the attachment zone. These are particularly evident at the level of the isthmus.

Fibre bundles emerging from the ventral part of the ganglion form rootlets which enter the CNS through a large tongue-shaped central tissue projection (Fig. 15l-n). This has a smoother and more regular surface than that of the attachment zone underlying the dorsal part of the ganglion. Its base is attached to the brainstem. Its free part is flattened and tapers distally. Rootlets emerging from the ganglion are compactly arranged. They run approximately at right angles to the long axis of the projection and merge gradually with its superficial surface which is consequently stepped (Fig. 15m,n). Small type 2 or type 4 central tissue projections extend into some of these rootlets from the main projection.

The central ends of many transitional Schwann cells are invaginated into the thick glia limitans of all parts of the transitional

zone, as in type 1 zones (Fig. 5). However, many invaginations are oblique to the projection surface and as a result the transitional node lies close to the surface of the glia limitans. In addition, a substantial minority of transitional nodes lie superficial to the general plane of the surface of the glia limitans. In these cases, a sheath of astrocyte processes extends distally around the oligodendrocyte up to or beyond the level of the node.

4.2.6 Vagus nerve

The rat vagus nerve possesses dorsolateral, intermediate and ventrolateral rootlets (Rossiter & Fraher, 1990) (Fig. 17a). The dorsolateral rootlets are likely to be predominantly sensory (Kalia & Sullivan, 1982; Miceli & Malsbury, 1985; Bieger & Hopkins, 1987). They have a uniquely complex morphology (Rossiter & Fraher, 1990). Each contains a prominent central tissue projection which branches distally and has a highly irregular surface (Fig. 17b-f). Its transitional zone therefore possesses type 2 features. In addition, however, one or more strands of PNS tissue extend centrally in the rootlet (Figs. 9a, 17g-j), each either in a groove on the surface of the central tissue projection or in a tunnel piercing it, commonly for over 200 μm (and in some cases for over 500 μm) along the intramedullary segment deep to the brainstem surface. There the peripheral tissue expands considerably (Fig. 17g) to form a cylindrical or spindle-shaped peripheral tissue insertion. These transitional zones are of type 6. In some rootlets the peripheral nervous tissue deep to the brainstem surface constitutes an island buried deep within the CNS and so the zone is of type 7 (Figs. 2, 17k). Over 85% of rootlets possess a peripheral tissue insertion or island in their intramedullary courses. In other rootlets the continuity

of peripheral tissue in the intramedullary segments with that distal to the transitional zone is established only through a cross connection with the peripheral tissue insertion of a neighbouring rootlet (Fig. 171). The occurrence of an insertion is usually associated with the presence within the rootlet of several contiguous groups of small myelinated and unmyelinated fibres. Conversely, rootlets lacking a peripheral tissue insertion or island contain a high proportion of evenly distributed closely packed large diameter myelinated fibres. The interface between the insertion or island and the surrounding central nervous tissue is highly irregular. Groups of centrally myelinated vagal axons encroach upon it as ridge-, bridge- or finger-like projections of central tissue (Figs. 9c, 17g,h).

Despite the wide variation in transitional zone morphology in nerves other than the vagus, the almost universal arrangement elsewhere (Fraher, 1978a; Berthold et al., 1984; Bristol & Fraher, 1987; Fraher & Delanty, 1987; Fraher & Sheehan, 1987; Fraher et al., 1988b,c) is that myelinated fibres cross the central-peripheral interface only once. Such an interface, however irregular, is topologically equivalent to a planar surface. The vagal central-peripheral interface is topologically more complex than this. This is because the insertion or island is continuous with the rootlet distal to the projection by means of more than one strand of peripheral nervous tissue. Therefore, even though the CNS-PNS interface consists of a single surface, its essential form cannot be reduced to that of a plane. Where a peripheral tissue island is present, the interface is more complex still, consisting of two distinct surfaces, namely, that of the central tissue projection and that of the island. The former is open, being continuous with that of the surrounding CNS. The latter, by contrast, is closed and is

topologically equivalent to that of a sphere, unless it is crossed by a bridge of central nervous tissue, when it is equivalent to a torus.

(a) Axon ensheathment in the vagal transitional zone

At the level of the dorsolateral vagal central tissue projection, a majority of myelinated axons acquire oligodendrocytic sheaths and are enveloped in this manner over their entire course further centrally (Fig. 18a). However, in accordance with the highly irregular and convoluted form of the vagal CNS-PNS interface, many axons pass between the PNS and CNS more than once in their course through the vagal transitional zone. As they do so, they are surrounded by alternating central and peripheral myelin sheaths (Fig. 18a). They are enveloped by transitional Schwann sheaths distally and by oligodendrocytic sheaths within the central tissue projection. Central to this, in the peripheral tissue insertion or island, they are again enveloped by one or more intercalated Schwann cells. Such alternation is exhibited by 20% of axons. Figure 19 shows a series of transverse sections through a typical example of such a fibre.

The majority (85%) of axons on which alternation occurs are enveloped by a single intercalated Schwann cell in the peripheral tissue insertion or island. However, more complex patterns are found whereby some possess as many as three pairs of alternating central and peripheral myelin sheaths or up to four serially arranged intercalated internodes (Table 1). Morphologically, intercalated internodes closely resemble those of typical mature myelinating Schwann cells. They are, however, considerably shorter than those lying distal to the central tissue projection (Fraher & Rossiter, 1991). Accordingly, Schwann cell perikarya are relatively abundant in the peripheral tissue insertion

(Fig. 8d). The nodes located where axons pass between the central and peripheral tissue compartments resemble typical CNS-PNS transitional nodes (Fraher & Kaar, 1984).

Vagal unmyelinated axon bundle transition is characterized by extensive interdigitation and overlap of central and peripheral tissues, even at locations 200 μm deep to the brainstem surface where the unmyelinated bundles finally enter the CNS. Less than 20% of unmyelinated bundles undergo direct PNS-CNS transition. As the bundle is traced centrally, its enveloping Schwann cell processes extend below the central tissue projection surface as described in 3.3.2 above. The majority (over 80%) of unmyelinated bundles enter the CNS in that fashion, but re-emerge into a peripheral tissue insertion or island further centrally (Fig. 18b). As they do so they again become gradually enveloped by Schwann cell processes in a sequence similar, through in reverse order, to that in which they enter central nervous tissue. Further centrally the bundles re-enter the CNS as before. A substantial proportion of unmyelinated bundles alternate between the CNS and PNS more than once. Within the insertion or island, the unmyelinated bundles form plexiform patterns resembling those described by Aguayo et al. (1976) in the peripheral nervous system.

Many axons possess alternating myelinated and unmyelinated segments. These occur in varying combinations. Approximately 17% of peripheral unmyelinated axons become invested by an oligodendrocytic myelin sheath on entering the central tissue projection. On some stretches of central axons a short myelinated segment is interposed between unmyelinated segments (Fig. 20). Over 25% of axons with an

intercalated Schwann cell internode have a central and/or peripheral unmyelinated segment at other levels.

Intermittently myelinated peripheral axon segments are also found in the atrial endocardium of the dog (Yokota, 1984), in the sciatic nerve of Xenopus laevis (Smith, Chan & Schaap, 1985), in the superior cervical ganglion of the mouse (Kidd & Heath, 1988) and in dorsal spinal roots of the lizard, Lacerta muralis (Pannese, Ledda & Matsuda, 1988). On most such vagal axons the marginal cytoplasmic collar of the myelinating Schwann cell abuts on the sleeve of Schwann processes enveloping the unmyelinated segment at a heminode, in a manner similar to that found by Yokota (1984), Kidd and Heath (1988) and Pannese et al. (1988). However, on some, the sleeve of Schwann processes is overlapped by the myelin sheath, a pattern which occurs frequently in the sciatic nerve of Xenopus laevis (Smith et al., 1985) and in mouse superior cervical ganglion (Kidd & Heath, 1988).

4.2.7 Accessory nerve - spinal rootlets

The spinal accessory trunk extends rostrally from the fifth cervical segment, approximately equidistant from the dorsal and ventral rootlet exit zones. Its exit zone is a strip of cord surface underlying the trunk and the rootlets gradually merge with this, having first turned rostrally (Nugent et al., 1991).

Most intramedullary rootlets are small, being similar in size to ventral cervical rootlets at the same cord levels. They run laterally and rostrally from the junction of the dorsal and ventral grey columns, through the lateral funiculus. As they approach the cord surface they bend sharply rostrally and emerge through it (Fig. 15r,s). In doing so they traverse a pad of astrocytic material (Fig. 3c,d). Some small

rootlets pursue a marked dorsally convex course through the lateral funiculus and then run tangentially in the glia limitans (Fig 15r), before emerging obliquely to form the free rootlet.

In the majority of rootlets the transitional zone is of type 5a and a glial fringe projects distally into the rootlet from the wedge-shaped glial projection. It resembles that typical of caudal abducent rootlets (Nugent et al., 1991). These zones also share many features with those of lower cervical ventral rootlets (Fraher, 1978a). For example, they lie close to the level of the surrounding cord surface and many of the transitional nodes lie deep to this. These features are in marked contrast to those of the cervical dorsal transitional zones (Fraher & Sheehan, 1987). A short central tissue projection of at most a few tens of micrometres in length extends into the free segment in a small proportion of rootlets. In this they resemble some upper cervical ventral rootlets (Fraher & Cremin, unpublished observations).

Thus, despite their emergence in a location intermediate between the dorsal and ventral spinal rootlets, spinal accessory rootlets possess transitional zones closely resembling those of ventral rootlets at the same cord level.

4.2.8 Hypoglossal nerve

Hypoglossal transitional zones resemble those of the oculomotor nerve. Intramedullary rootlets run laterally immediately deep to the brainstem surface before deviating ventrally to emerge as free rootlets (Fig. 15p,q). These lie at first within the pia mater, where they are separated by inter-radicular spaces. As they pierce the pia they join aggregated rootlets bundles in series. These in turn converge within the subarachnoid space as they approach the hypoglossal canal.

Many rootlets which deviate sharply to traverse the brainstem surface at right angles possess type 1 transitional zones (Fig. 15p). Many others traverse the brainstem surface obliquely. These possess type 2, 3 or 5 transitional zones (Fig. 15q) and their central tissue projections vary considerably in length. Astrocytic tissue forms a prominent collar around free rootlets containing type 3 zones. Where the intramedullary segment runs parallel to the brainstem surface, it lies within a marked thickening of the glia limitans which therefore envelops its deep as well as its superficial aspect. Where the free rootlet closely overlies the brainstem the glia limitans also forms a thickened pad.

The great majority of transitional Schwann cells are invaginated into the astrocytic tissue of the transtional zone, which is therefore deeply honeycombed.

4.3 Patterns of Transitional Zone Morphology

Though the central tissue projections into the dorsal rootlets in the rat (Fraher & Sheehan, 1987) and cat (Berthold & Carlstedt, 1977a; Carlstedt, 1981) resemble in some ways those in rat L5 ventral rootlets, there are also a number of differences between them. Firstly, the projections in dorsal rootlets (Skinner, 1931; Tarlov, 1937a,b; Němeček et al., 1969; Fraher & Sheehan, 1987) are larger than those in ventral rootlets. Secondly, projections are more highly organised in dorsal than in ventral rootlets. In the latter they lack the core and mantle zones described by Berthold & Carlstedt (1977a) and by Carlstedt (1981), and also the regular layer of astrocyte cell bodies on the surface of the projection, which instead is composed largely of astrocyte processes.

Even though transitional zone morphology varies widely a number of patterns may be discerned within this variation. The possibility that transitional zone morphology could be related to the function of the nerve fibres contained in the rootlet may be examined using the oculomotor, trochlear and abducent nerves. Though the first of these possesses an autonomic component lacking in the other two, all three nerves share many features. Their motoneurons all belong to the somatic efferent class and the voluntary musculature innervated by them is similar in general function, motor unit size and developmental origin. A numerical study of the oculomotor nerve (Fraher, 1989) indicates that its autonomic outflow may be restricted to its medial rootlets. Its remaining rootlets, which are therefore likely to be composed largely of motoneuron fibres, possess transitional zones which vary widely in form and size, belonging to all types except 6 and 7. By contrast, the transitional zones of the abducent nerve are of types 1 or 5, while the single zone generally found in the trochlear nerve is of type 2 (Fraher et al., 1988b,c). It is unlikely therefore that transitional zone form is related purely to fibre function.

Another possibility is that the position of the attachment of a given nerve to the CNS in the dorsoventral axis might determine transitional zone form. This is suggested by two observations. Firstly, the zones of the dorsally attached trochlear nerve are of type 2 (Fraher et al., 1988c), like those of C7 dorsal spinal rootlets (Fraher & Sheehan, 1987), even though the former are motor and the latter sensory. Secondly, the zones of abducent and C7 ventral rootlets, both of which are ventrally attached, are of type 1 (Fraher, 1978a; Fraher et al., 1988c). Accordingly, if location determines transitional

zone form, then spinal accessory rootlets should possess zones intermediate in form between types 1 and 2. This, however, is not the case. Spinal accessory transitional zones resemble those of ventral cervical rootlets at the same cord level (Fraher & Cremin, unpublished; Nugent et al., 1991).

It could also be that transitional zone morphology is related to rootlet size. Thus, among the sensory cranial nerves, the dorsolateral vagal rootlets are large and contain extensive central tissue projections (Rossiter & Fraher, 1990). Also, the cochlear nerve lacks rootlets but contains a type 3 transitional zone, consisting of a very long central tissue projection, which comprises the entire nerve trunk (Fraher & Delanty, 1987). The transitional zone lies towards the distal end of this, where the cochlear nerve branches spring from its surface. In addition, the sensory root of the trigeminal nerve, which is the largest of all cranial nerve roots in the rat, also lacks rootlets and possesses a substantial central tissue projection and a type 3 transitional zone. Analysis of cranial nerves thus suggests that the presence or absence of a central tissue projection and therefore the location of the transitional zone within the rootlet or at the surface of the neuraxis, respectively, may be associated with the size of the fibre bundle which passes through the CNS surface. In fact, it is only the smallest rootlets that consistently lack a projection. Such a relationship would be in agreement with differences in transitional zone morphology between the relatively large dorsal and small ventral rootlets at lower cervical cord levels. It also accords with the finding that in the upper thoracic region large ventral rootlets contain prominent central tissue projections, while these are commonly absent from small rootlets. The

presence of long central tissue projections in lumbar ventral rootlets is the sole exception to the otherwise rather well-defined association between transitional zone morphology and rootlet size.

It is generally agreed that at a given level along the spinal cord the central tissue projection into the dorsal rootlet is longer than that into the ventral (Skinner, 1931). This is the case for rat lower cervical rootlets (Fraher, 1978a; Fraher & Sheehan, 1987). However, it is not true that central tissue projection length increases gradually in a rostrocaudal direction along the spinal cord, as has been stated (Skinner, 1931). Thus, while central tissue projections are present in some rat ventral rootlets at upper cervical levels (Fraher & Cremin, unpublished observations), they are absent at lower cervical levels (Fraher, 1978a). They reappear in upper thoracic rootlets. Here, central tissue projection length undergoes a sudden sharp increase and mean values are greater than at lumbar levels (Table 4). Furthermore, mean lengths may differ considerably between serially adjacent rootlets (Kaar, 1984; Bristol, 1989).

4.4 Central Tissue Projection Asymmetry

Like the rootlets in which they lie, central tissue projections have superficial, deep and collateral surfaces (see Section 2). They are generally flattened dorsoventrally and so are oval or rectangular on cross section. They are also generally markedly asymmetrical in position within the rootlet. In most cases they are displaced away from its central axis towards its deep surface. The degree of asymmetry is commonly such that the deep surface of the rootlet is made up to some extent by that of the central tissue projection (Figs. 3e, 15e). In the

extreme case, the entire deep surface of the projection coincides with that of the rootlet as in type 4 transitional zones. Peripheral tissue distribution complements that of central tissue. It extends further proximally on the superficial than on the deep surface of the projection. It commonly extends into the emergent segment, for 200 μm or more in some cases (as in the C7 dorsal rootlet). As a result its surface area is considerably greater than if it were confined to the rootlet. Its transitional nodes are correspondingly widely spaced, reducing or excluding the likelihood of crosstalk between them. They are therefore preferentially located on the superficial surface of the projection. In occasional large oculomotor rootlets and ventral lumbar rootlets projection asymmetry differs from that generally found. In these, the projection lies asymmetrically towards the superficial or collateral, rather than the deep, rootlet surface.

Central tissue projection asymmetry is present from the outset and becomes progressively more marked during development in those areas studied: L5 ventral and C7 dorsal spinal rootlets and the cochlear nerve (Fraher & Kaar, 1986; Fraher & Delanty, 1987; Fraher & Sheehan, 1987). In accordance with this, the central tissue projection forms progressively larger proportions of the deep and collateral surfaces as age advances.

5. NODE DENSITY IN THE TRANSITIONAL ZONE

Since each myelinated fibre possesses a node of Ranvier as it traverses the transitional zone (Fraher, 1978a; Fraher & Kaar, 1984; 1986; Bristol & Fraher, 1987), it is to be expected that the density of nodes within the zone is particularly high. Also, since intramedullary rootlets contain relatively short internodes, their node densities are likely to be higher than those in the ventral rootlets (Fraher, 1978b).

Node density in the rat lumbar ventral rootlet transitional zone was compared with that in the central and peripheral parts of the nervous system. Absolute density was calculated at three different positions along L4 ventral motoneuron axon bundles: in the transitional zone, in the intramedullary rootlet and in the ventral root (Fraher & Bristol, 1990). Each of these was serially sectioned transversely. The total number of nodes within a segment of each was counted, the volume of the segment was calculated by computerised reconstruction and the number of nodes per unit volume was determined. This procedure was carried out for nodes of large (predominantly alpha) and small (predominantly gamma) fibres separately. These were readily separable from one another, since in rat L4 ventral rootlets the fibre calibre distribution is bimodal (Bristol, 1989). Each fibre was allocated by an iterative method to the large or small class (Cox, 1966; Dempster, Laird & Rubin, 1977; Kaar & Fraher, 1985). Using the serial sections, each node was readily identified as belonging to one or other of these classes, and was identified throughout subsequent analysis as a large or a small node.

In addition, transitional node distribution within both upper cervical (C2) and lumbar (L4) transitional zones was examined

morphometrically. Node position was determined from serial sections and three-dimensional node distribution was plotted on computerised reconstructions using a Kontron IPS system. Calculation of the absolute distances between all possible pairs of nodes was carried out by computer. From these, the distance between each node and its nearest neighbour was calculated - the nearest neighbour distance. This measures the true distance between node centres and so is a more exact measure of spacing than node density estimates got by simply calculating node number per unit volume, which treats nodes as if they are uniformly distributed within the transitional zone or the central tissue projection. Moreover, density estimates take no account of node clustering, whereas nearest neighbour distances do.

5.1 Lumbar Nodes

The majority of nodes of both large and small L4 fibres are concentrated 50%-80% of the way along the proximodistal longitudinal axis of the transitional zone. Patterns of distribution of both types of node are similar.

Node density within the transitional zone averages nearly seven times that in the ventral root and more than twice that calculated for the intramedullary rootlet (Table 2a). These differences are statistically very significant ($P < 0.001$). Overall node density in the central tissue projection ($26.3/10^5\ \mu m^3$) is approximately twice that in the transitional zone ($13.8/10^5 \mu m^3$). It is greatest in the smaller rootlets (Table 2b) and increases more than five-fold in a proximodistal direction along the central tissue projection (Table 2c).

The high node density in the transitional zone is because each fibre possesses a node as it traverses that relatively short segment of rootlet. Transitional nodes therefore approach being in register with one another to a degree which is inversely proportional to transitional zone length. No such restrictions on node distribution apply along fibre bundles centrally or peripherally. The greater node density in the transitional zone compared with that in the intramedullary rootlet is likely to be an underestimate for two reasons. Firstly, all the transitional nodes lie at the surface of the central tissue projection which has an irregular conical shape and so comprises about half the volume of the transitional zone (Fraher & Kaar, 1986; Bristol & Fraher, 1987). Secondly, the method used overestimates intramedullary node density because some astrocytic and oligodendrocytic material within the perimeter of the bundle was excluded in calculating intramedullary bundle volume. For these reasons it is likely that node density in the central tissue projection averages at least five times that in the intramedullary rootlet and that node density in the latter differs rather less than calculated from that in the ventral root.

The overall mean nearest neighbour distance between L4 transitional nodes was 12.8 μm (range 2.5 to 52.7 μm) (Table 3a). Though considerable variation is found, nodes are furthest apart in the proximal third of the zone and are closest together in the middle and distal thirds, in which they are similarly spaced. About 6% of all nodes are less than 5 μm apart and about 40% are less that 10 μm apart, from node centre to node centre. The true distance between adjacent nodal axolemmae is considerably less than this, depending on nodal axon diameter. Table 3b gives estimates of the degree to which large and

small nodes are paired with one another (small-large) and each with others of its kind (small-small and large-large), (i) for all nodes, irrespective of nearest neighbour distances, and (ii) for nodes which are relatively close together, i.e. with nearest neighbour distances of less than 10 μm. This shows that about 30% of small nodes and about 20% of large nodes have nearest neighbours of a similar kind less than 10 μm distant. Thus, a larger proportion of nodes of small fibres are more closely aggregated with each other than is the case with large fibres. This is counter to the relative proportions of numbers of nodes of the two size classes within the rootlet (small:large :: 1:1.5).

The extent to which nodes are clustered together may be estimated using the nearest neighbour distance of each node relative to its longitudinal position in the transitional zone. This shows that in some rootlets there is definite clustering, whereas in others none is apparent. This confirms the visual impression from three-dimensional reconstructions (Fig. 21) that nodes occur most frequently in the middle third of the projection. These reconstructions also show that nodes tend to be more common on those parts of the central tissue projection surface which are orientated closest to the transverse plane of the rootlet. They are commonly absent from extensive areas of the projection surface, even those which are relatively transversely orientated. Fewer tend to be located on the dorsal than on the ventral aspect of the projection, in accordance with its asymmetric position in the rootlet. In general, though large and small nodes tend to be intermingled in some cases, there is a clear tendency for each type to be aggregated into clusters on the central tissue projection surface, especially towards its distal end.

These observations suggest that, if node densities in the intramedullary rootlet and in the ventral root resemble values generally occurring in the CNS and PNS, respectively, the possibility of electrical interaction between myelinated fibres is greater in the transitional zone than in any other part of the nervous system. The morphometric estimates of node density and clustering suggest that if interaction occurs it is most likely to take place between the nodes of small fibres in small rootlets. However, any tendency for fibre interaction at the transitional zone is likely to be offset by the presence of large numbers of concentrically arranged astrocyte processes surrounding the peripheral paranodal and nodal segments of motoneuron axons (Fraher, 1978a). These may serve to insulate transitional nodes more effectively than the less elaborately arranged astrocyte processes related to central nodes.

5.2 Cervical Nodes

Node distribution was examined in type 5 transitional zones of C2 ventral rootlets (Fraher & Cremin, unpublished). The coordinates of node position were calculated and plotted relative to the plane of the cord surface surrounding the zone and also to a parasagittal plane normal to this. Figure 22 shows node distribution for a typical zone, projected onto the median longitudinal plane of the rootlet. While nodes of neighbouring fibres may lie at markedly different levels relative to the cord surface, there is a general tendency for those of lateral fibres in the rootlet to lie deeper than those of medial fibres. The general plane in which the nodes lie is thus orientated to face ventrolaterally. It therefore tends to lie transverse to the plane of the rootlet as the

latter changes direction to run laterally as it emerges from the cord. On average, the most superficial node was found to lie 19μm above the plane of the cord surface and the deepest 13μm below it.

6. TRANSITIONAL ZONE MORPHOMETRY

6.1 Rootlets

Over the range of rat spinal nerves studied, motor rootlets tend to be considerably smaller but more numerous than sensory rootlets. Thus, the L4 and L5 ventral roots are each formed from around 60 rootlets (Kaar, 1984; Bristol, 1989) and upper cervical ventral roots from around 30. By contrast, each rat C7 dorsal root possesses only four to eight rootlets (Fraher & Sheehan, 1987). Average spinal motor rootlet size, estimated as myelinated fibre number, ranges from 14 in upper cervical rootlets to 30 in L5. All of these rootlets are substantially smaller than C7 dorsal rootlets.

Some cranial nerves follow these patterns closely. Thus, the abducent (Fraher et al., 1988c) and spinal accessory (Nugent et al., 1991) nerves are formed from an average of 19 and 33 rootlets respectively. These contain considerably fewer myelinated fibres than the dorsolateral vagal rootlets, which in addition contain large numbers of unmyelinated axons, and number only 7 to 12 (Rossiter, 1989). The oculomotor and hypoglossal nerves are exceptions among motor nerves, since their rootlets vary considerably more in size than in all others examined (Fraher et al., 1988b; Fraher, 1989). Each oculomotor nerve includes one especially large rootlet.

6.2 Transitional Zone Dimensions

The length of the transitional zone, i.e., its longitudinal dimension in the long axis of the rootlet, varies markedly both between individual nerves and between the rootlets of a given nerve. Table 4 gives the values for a selection of cranial and spinal nerves. It shows that zones

in ventrally attached rootlets tend to be much shorter than in those which are dorsally attached, though this is by no means always the case. Ventral rootlets also tend to be smaller than dorsal. Transitional zone length is related to rootlet size within a given nerve, though the strength of the relationship is relatively weak and varies from nerve to nerve. Thus, the proportion of the variance in transitional zone length attributable to a linear relationship between it and rootlet size was 35% in C7 dorsal rootlets (Fraher & Sheehan, 1987) and 66% in oculomotor rootlets (Fraher et al., 1988b).

It is clear from Table 4 that there is no rostrocaudal gradient of central tissue projection length among the cranial nerves. It is also likely that there is no clearly evident rostrocaudal gradient among ventral spinal rootlet transitional zone lengths. These are shorter in lower than in upper cervical rootlets. Furthermore, there is a sharp, rather than a gradual increase in zone length between lower cervical and upper thoracic ventral rootlets, i.e., at the transition between the motor outflow to the upper limb and that to the body wall musculature.

7. TRANSITIONAL ZONE SUPPORTING TISSUES

7.1 Rootlet Sheaths

The structure and arrangement of the sheaths surrounding those parts of rat lumbar ventral rootlets containing the transitional zone were examined during development and at maturity (Kaar & Fraher, 1986).

Immediately distal to its emergence from the cord, each L4 rootlet continues as a discrete entity for 100 μm or more (Fig. 23a). It lies within the intrapial space (Fig. 23c), which is limited superficially by the most superficial layer of the pia mater and deeply by the glia limitans. The part of the intrapial space which intervenes between neighbouring rootlets is termed the inter-radicular space (Fig. 23d). The inter-radicular spaces form a labyrinth around the emerging rootlets (Fig. 23c,d). This space is limited proximally by the cord surface. It tapers proximodistally as the rootlets converge and come into apposition before fusing to form or contribute to an aggregated rootlet bundle. With age the rootlets become more closely packed together and the space becomes correspondingly less extensive.

The sheath surrounding the initial segment of the rootlet consists at all stages of development and at maturity of a single layer of thin, flattened cells (Fig. 23d) which lack a basal lamina. Early in development the sheath contains fenestrations up to 10 μm wide. Through these, the rootlet endoneurium commmunicates with the subpial space and the blood vessels of the inter-radicular space are directly related to the rootlet fibres (Fig. 23d). During the early postnatal period the fenestrations become smaller and less extensive. Proximally, the rootlet sheaths generally end freely in the angle between the rootlet

and the cord surface and are separated by a considerable gap from the subjacent glia limitans. In this region, therefore, the endoneurial space of the rootlet and the intrapial space are in continuity.

Further distally, where rootlets are closely apposed, they are generally separated by a common layer, two to five cells thick, of sheath cells (Fig. 23d). Sheath cells contain abundant ribosomes, granular endoplasmic reticulum, mitochondria and Golgi complexes. Coated micropinocytotic vesicles are plentiful. Where cells overlap, their plasmalemmae show increased density in places and come to within 6-8 nm of each other.

An arrangement similar to that described above is found in cranial nerves which are attached to the brainstem by means of rootlets, such as the oculomotor, abducent and hypoglossal nerves. Many cranial nerve rootlets, including those of the facial, vestibular and vagus nerves , show a marked degree of subdivision of their component fibre bundles into small fascicles (Figs. 23e-h, 24b). Some of these contain only one myelinated fibre. Others contain only collagen fibril bundles. This subdivision is produced by a network of fine cytoplasmic processes. These arise from cells resembling those which comprise the rootlet sheath. They have polygonal perikarya and lack a basal lamina. In some places the processes are apposed to one another and may be linked by tight junctions. They form series of longitudinally running compartments. These are aligned with the astrocyte-lined channels transmitting the fibre bundles through the transitional zone further centrally. Thus, fibres are subdivided into the same groups for some distance on either side of the CNS-PNS interface. Within the central tissue compartment of the zone some fibre bundles are subdivided

further by astrocytic septa and so are even more compartmentalised than peripherally. Where the peripheral cytoplasmic processes approach the glia limitans, many end freely (Fig. 23g), though some turn aside to be closely applied to the surface of the glia limitans for some distance (Fig. 23h). As they are traced distally, neighbouring compartments become confluent and so fascicle size increases progressively to levels typical of peripheral nerves generally.

Some free rootlets, such as those of the abducent and hypoglossal nerves, run parallel and in close apposition to the glia limitans for some distance. Here the sheath cells and the astrocyte processes of the glia limitans may come into close apposition (Fig. 24a). Where they do so, the sheath cell processes may be invaginated between astrocyte processes in the form of pegs or the two may intermesh with one another intricately.

7.2 Connective Tissue

Endoneurial collagen is present in considerably smaller amounts in spinal nerve roots than in peripheral nerves generally (Gamble, 1976). This is also true of both spinal and cranial rootlets. In these, collagen fibrils run predominantly in a longitudinal direction. In general, they terminate blindly just distal to the CNS-PNS interface. However, some collagen fibrils are found within the invaginations containing the proximal ends of transitional Schwann cells (Figs. 10a, 14c). Some of these connect the basal lamina covering the Schwann cell with that on the surface of the astrocytic wall of the invagination. In many cases relatively tightly packed bundles of approximately parallel endoneurial collagen fibrils are inserted centrally into the astrocytic limiting

membrane of the CNS compartment of the transitional zone (Fig. 25b). Here these collagenous insertions lie in clefts between the astrocyte processes. Their frequency varies between nerves. They occur at both cervical and lumbar levels and are particularly numerous at the transitional zone of the vestibular nerve (Fraher, 1987 unpublished). Well developed bundles of collagen fibres form rings around the most proximal parts of many free rootlets (Fig. 25c). Where astrocyte processes form the surface of a rootlet as it runs parallel to the glia limitans, or where adjacent surfaces of two closely related rootlets are both formed of astrocyte processes, the two tissues may be closely apposed to one another or may be separated by intervening bundles of collagen fibrils (Figs. 24c, 25a).

7.3 Blood Vessels

The blood supply of the transitional zone is of interest for a number of reasons. Firstly, it needs to be sufficient to meet the metabolic requirements of the high concentration of nodes and paranodes in the zone. Secondly, the presence or absence of anastomoses across the interface could determine the viability of the tissue on one or other side of this if the blood supply is threatened by disease.

A morphological and morphometric examination was carried out on the blood vessels supplying the rat L5 ventral rootlet transitional zone from development to maturity (Kaar & Fraher, 1987). The pronounced developmental changes in transitional zone blood supply were correlated with concurrent maturation of adjacent tissues, in particular the transitional nodes.

Blood vessels do not occur within rootlets. They run instead parallel to them. At the cord surface they branch to form a closely-knit network in the inter-radicular spaces (Fig. 25e). In this location between 10 and 35% of the vessels or their branches traverse the cord surface (Fig. 25d). From here they continue centrally and run parallel and immediately adjacent to the intramedullary rootlets in the ventrolateral white funiculus. Some continue centrally as far as the grey matter.

The vessels related to the transitional zone are either capillaries or postcapillary venules (Fig. 26). Capillary walls consist of a single unfenestrated endothelial layer and an outer incomplete layer of pericytes (Fig. 26a). The junctions between endothelial cells vary. In some the edges are simply abutted together. In others, they are oblique, overlapped (Fig. 26b) or tongued and grooved (Fig. 26c). They commonly include a zonula occludens. Elsewhere they are separated by a 5-10 nm gap. A continuous basal lamina lies external to the endothelial cells. The walls of postcapillary venules resemble those of the capillaries except that the outer layer of pericytes is complete (Fig. 26d). Where each vessel penetrates the cord it is surrounded by a narrow, funnel-shaped perivascular space bounded by astrocyte processes continuous with the astrocytic limiting layer of the cord surface (Fig. 26e). Between 6 and 300 days this space increases in width at the cord surface from 0.5-1.0 μm to 2.0-5.0μm and in length from 5 μm to 30 μm.

The vascularity of the transitional zone was estimated as (i) the mean number of each type of blood vessel per rootlet, and (ii) the proportion of the length of each transitional zone which was related to

each type of blood vessel. (A vessel was said to be related to a rootlet if no other structure intervened between it and the rootlet sheath). On this basis each free rootlet has at least one capillary related to it at each age (Table 5). Some rootlets are related to more than one capillary and vice versa. During the first week postnatum the numbers of capillaries and rootlets are approximately equal. After this, capillary numbers increase. After 3 weeks they outnumber rootlets by up to 50%. About half the length of the transitional zone is directly related to one capillary or more up to 12 days postnatum. From 20 days on this length is over 90%. The mean distance from the capillary wall to the centre of the related rootlet (see Kaar & Fraher, 1987) increases progressively throughout life. Mean capillary diameter remains similar at around 8 μm at each age. Mean postcapillary venule diameter (16.6 μm) is considerably greater than this (Table 5) and shows some tendency to increase with age.

The blood vessels of the transitional zone resemble those occurring in the central nervous system (Caley & Maxwell, 1970; Phelps, 1972; Hannah & Nathaniel, 1974; Sturrock, 1981) and within the endoneurium of peripheral nerves (Thomas, 1963; Lundborg & Brånemark, 1968; Olsson, 1975).

Extensive communications exist between blood vessels in the vicinity of the transitional zone and those of the adjacent neuraxis in a wide variety of locations. They cross freely between the peripheral and central nervous systems at cervical and lumbar ventral spinal zones (Fraher, 1978a; Fraher & Kaar, 1986; Kaar & Fraher, 1987). The inter-radicular spaces between oculomotor rootlets contain numerous vessels which communicate freely with those in the midbrain. In

addition, the oculomotor rootlets are divided into a medial and a lateral group by one or more longitudinally running large veins and arteries. Central and peripheral vessels are also continuous with one another at the transitional zones of the abducent, trochlear (Fraher et al., 1988c) facial, vestibular, hypoglossal (Fraher, unpublished observations) and cochlear nerves (Fraher & Delanty, 1987). In general, the network of vessels in the inter-radicular space is also continuous peripherally with the vessels of the root. These arrangements differ from that at the dorsal rootlet attachment zone in the cat. Here, both during development (Carlstedt, 1981) and at maturity (Berthold & Carlstedt, 1977a) the blood vessels running proximally on the rootlet do not enter the cord but deviate to join vessels on the cord surface. Resulting from this lack of anastomotic communication, dorsal roots may be more susceptible to ischaemia than ventral roots.

This substantial increase in the capillary vascularisation of the ventral rootlet transitional zone between 12 and 20 days postnatum is associated with functional maturation of gamma fibres. The majority of these attain structural and therefore probably functional maturity over this interval (Fraher & Kaar, 1984; Kaar & Fraher, 1985). The age-related increase in vascularisation is somewhat offset by the progressive increase in the distance from the capillary wall to the centre of the rootlet, resulting from growth in rootlet cross-sectional area. However, the distance involved (approximately 40 μm) remains within the range for cells in general from capillaries (25-50 μm) given by Guyton (1981) and is considerably less than the value of 100 μm or more for nerve fibres in feline dorsal rootlets, given by Berthold & Carlstedt (1977a,b). Metabolite diffusion for all fibres in the rat

ventral rootlet transitional zone is therefore likely to be highly efficient. Efficiency is likely to be even greater because the present estimate does not include capillaries separated from rootlets by other capillaries, which would further enhance the diffusion process. The rich blood supply to the transitional zone may reflect its large nutritional requirements, in particular in relation to the high concentration of nodes.

These age changes in vascularisation of the transitional zone differ significantly from those of the adjacent cord, in which increased vascularity coincides with the onset of myelination and with a period of rapid increase in cord cross sectional area, after which vascularisation diminishes considerably (Sturrock, 1981, 1982). In the lumbar transitional zone the absence of such a decrease and the persistant high level of vascularisation may reflect sustained metabolic requirements of the central-peripheral transitional nodes. The presence of blood vessels within the large cochlear central tissue projection ensures that its tissues are sufficiently close to them for metabolic purposes. In the adult rat, its radius (around 250 μm) is five times greater than the upper limit of the range (Guyton, 1981) of distances of cells in general from blood vessels.

8. STRUCTURAL - FUNCTIONAL CORRELATES

The region of attachment of the rootlet to the CNS is likely to be placed under stress during relative movements between the neuraxis and its bony casing, once any slack due to sinuosity of the root and its component rootlets has been taken up. High levels of longitudinal stress may be transmitted centrally to cervical rootlets and their transitional nodes in violent traction injuries of the upper limb in man, and may lead to avulsion of the rootlets at the spinal cord attachment (Sunderland, 1978). Any tendency for the rootlet to break in the region of the transitional zone is likely to be resisted by the continuity between both the connective tissue and cellular components of the rootlet sheaths and corresponding elements of the pia mater (Kaar & Fraher, 1986). The endoneurial collagenous insertions may serve a similar function. These longitudinally running compact bundles of collagen fibrils project into clefts between astrocytic processes of the transitional zone and may help to anchor the rootlet to the CNS. They may protect the zone against traction injury by taking longitudinal stress which would otherwise be borne by the more delicate nerve fibres passing between the two tissue territories. In addition, those rootlets which run in close apposition to the underlying neuraxis may be further protected against traction by specialised contacts between the two. These include intricate interdigitation between rootlet sheath cells and the astrocyte processes forming the subjacent glia limitans. Furthermore, the transitional Schwann cells themselves may resist distal traction in two ways. Firstly, where they lie in grooves or invaginations of the CNS surface, the basal lamina surrounding them

and that of the astrocytes lining the groove are in some places fused with one another or linked by spiralling collagen fibrils. Secondly, the astrocytic invagination into which the central end of the transitional Schwann cell is inserted may act as a suction cup, resisting distraction of the internode. This mechanism may limit tension on the node, which is likely to be a point of weakness along the fibre, since it lacks the strength provided by the cytoplasm of the oligodendrocyte or, more particularly, the Schwann cell, as well as the basal lamina surrounding the latter. Because of its fluid crystalline characteristics, the mechanical strength provided by the myelin sheath may not be very significant in resisting longitudinal stress. The packing density of ventral motoneuron nodes in the transitional zone is likely to be seven times greater than in the ventral root and five times greater than in the intramedullary segments of these fibre bundles in the spinal cord (Fraher & Bristol, 1990). The transitional zone is therefore likely to be a particularly weak point mechanically along the fibre bundle. The relative vulnerability of the transitional node has been demonstrated in experimental traction studies of the transitional zone, in which fibre rupture commonly occurred at the node (Bristol & Fraher, 1989). However, this was by no means always the case, showing that the node is not markedly more vulnerable than the rest of the fibre.

The longitudinal offsetting of transitional nodes relative to one another in a region where they are very densely packed may help to reduce or exclude crosstalk between them. This is because the distance between a given pair of neighbouring nodes is on average greater than if all lay in the same transverse plane of the rootlet. The fact that most transitional nodes are displaced distally into the rootlet

or nerve trunk also reduces or excludes any possible crosstalk between them and fibres of the CNS proper.

As each rootlet travels between the CNS surface and its nucleus of origin or termination, its intramedullary segment intersects CNS fibre bundles which must deviate to accommodate it. This increases the transverse sectional dimensions of the cord or brainstem. It is noteworthy that in all nerves studied the transitional zones of large rootlets lie distal to the plane of the CNS surface and within the rootlet. This applies to the majority of rootlets of all sizes examined, except for small motor rootlets in some cranial and cervical spinal nerves. The cross sectional area of a given rootlet tends to be greater at the transitional zone than where it lies in the CNS. This is because large amounts of astrocytic tissue surround it and intervene between its constituent fibres in the zone. Positioning the transitional zone distal to the CNS surface therefore minimizes the additional enlargement of the CNS which would result from accommodation within it of the zones of the many rootlets (commonly over 100) which contribute to the formation of a typical root. This in turn reduces the cross sectional area of the neuraxis relative to that of the dural sac. As a result, the neuraxis is allowed more mobility within the latter and so is less vulnerable to damage in extremes of movement of the axial skeleton.

9. TRANSITONAL ZONE DEVELOPMENT

9.1 General Features

At first, the CNS-PNS transition is not clearly evident within the fibre bundles making up the presumptive rootlets since the axons comprising these are closely apposed to one another. However, axon segregation soon takes place as astrocyte processes derived from perikarya lying around the periphery of the bundles grow into them and segregate their component axons by forming an intricately interwoven matrix (Fig. 27a). Differences in cellular density central (where it is lower) and peripheral (where it is higher) to the plane of the surrounding CNS are commonly present from an early stage, as in the cochlear nerve (Fraher & Delanty, 1987) (Fig. 29h,i). Distal to the presumptive CNS-PNS interface, Schwann cells or their precursors are initially abundant. At and around the surface of the bundle these form prominent clusters (Fraher & Rossiter, 1983a,b) or sleeves (Fraher & Kaar, 1986) (Figs. 27b,c, 28a). The individual cells comprising these give rise to extensive processes which interdigitate with one another and encapsulate other cells of the cluster. They also give origin to a dense weave of fine processes which enter the axon bundle and isolate individual axons from one another by means of a dense matrix closely resembling that of the astrocytes, described above (Fig. 27c). This process appears to be more active in L5 ventral than in C7 dorsal rootlets (Fraher & Kaar, 1986; Fraher & Sheehan, 1987). At later stages, cells successively separate from the clusters. As they do so their fine processes are withdrawn and the matrix disappears. At the same time each cell comes to envelop an axon segment in the manner typical of a promyelin Schwann cell, though the length of axon enfolded

is relatively short (Fig. 28b). At this stage the perikaryon of the transitional Schwann cell is closely related to the surface of the CNS, though each is covered by basal lamina, and so remain separated. At lower cervical levels many Schwann cell perikarya lie in shallow depressions in the cord surface (Figs. 27d, 28b). The short cytoplasmic process extending centrally from the perikaryon at this stage commonly becomes closely apposed to transitional zone astrocyte processes and may extend between these deep to the CNS surface.

With maturation the Schwann cell elongates and enfolds a progressively longer stretch of axon. As it does so, its perikaryon comes to lie correspondingly further distal to the CNS surface. Nevertheless, the central end of the Schwann cell remains closely related to the astrocyte processes of the glia limitans (Figs. 27e, 28b,c). It lies in a shallow cylindrical invagination in the transitional zone, lined by basal lamina which is reflected distally onto the promyelin Schwann cell. As myelination commences and proceeds, the Schwann cell maintains a similar relationship with the central nervous tissue, but comes to be gradually more deeply invaginated below it (Figs. 27f, 28d,e). Central myelination of each such axon is brought about by a transitional oligodendrocytic glial unit which begins to enfold it at a considerable depth below the CNS surface. Consequently a long stretch of axon is enveloped by astrocytic processes between the distal end of the glial unit and the proximal end of the Schwann cell. Thus, prior to myelination the central segments of ventral motoneuron axons are fully segregated from one another by the matrix of astrocyte processes as they traverse the transitional zone. In this they resemble developing peripheral axon segments, which are also fully isolated from

one another by establishing a 1:1 ratio with a promyelin Schwann cell before mesaxonal spiralization and cytoplasmic extrusion result in compact myelin formation. Such extensive segregation is not typical of central axon segments in general prior to myelination (Peters et al., 1976). As central myelination progresses the glial unit gradually extends distally along the axon segment towards the transitional node, stripping the astrocyte processes off it as it does so. These processes persist and continue to surround the distal end of the transitional oligodendrocyte, separating it from neighbouring fibres.

A few slender astrocyte processes continue to be closely related to the axon at the level of the CNS-PNS transitional node (Fig. 28e). These separate the distal cytoplasmic compartment of the oligodendrocyte from the transitional node gap. This intimate relationship of astrocyte processes to the transitional node resembles that found at central nodes generally (Hildebrand, 1971a,b; Raine, 1984; Waxman & Black, 1984; Waxman, 1986). The node gap also contains an infolded disc of basal lamina where that lining the astrocytic invagination is continuous with that covering the transitional Schwann cell. Transitional nodal development has been described in detail elsewhere (Fraher & Kaar, 1984). The transitional nodal axon specialisations resemble those found at peripheral nodes (Wiley-Livingston & Ellisman, 1980). Developmental changes in the paranodal segments of both the Schwann cell and the oligodendrocyte resemble relatively closely those occurring in relation to peripheral and central nodes, respectively (Berthold, 1968a,b; 1974a,b; Allt, 1969; Webster, 1971; Fraher, 1973; Peters et al., 1976; Hirano & Dembitzer, 1978). Accordingly, neither the Schwann cell nor the oligodendrocytic

glial unit substantially modifies its developmental behaviour in relation to node formation, even though each lies at opposite ends of one and the same node. However, the transitional Schwann cell lies in the proximal rootlet segment. It differs from Schwann cells in the rootlet generally in a number of ways (Fraher 1978a,b; Fraher & Kaar, 1985). For example, it may remain unmyelinated while myelination is advancing rapidly in those distal to it; when it does produce myelin its sheath is commonly thinner than that of serially adjacent internodes on the same axon; its sheath may show considerable longitudinal variation in thickness and may possess a decremental segment along which it gradually diminishes in thickness in the direction of the node. Furthermore, its internodal length may be considerably shorter than the average for levels distal to the proximal rootlet segment (Carlstedt, 1981; Fraher & Rossiter, 1983b). Thus the proximal rootlet segment manifests a number of persistent immature features.

Some of the presumptive Schwann cells which comprise the clusters or sleeves surrounding the rootlets do not segregate axon segments. Instead they come to lie within the proximal rootlet segment isolated from axonal contact. Their numbers, however, seem to decrease during maturation (Kaar, 1984; Rossiter, 1988, unpublished observations).

9.2. Spinal Nerve Rootlets

9.2.1. C7 ventral rootlets

The development of the C7 ventral rootlet transitional zone follows the pattern described above relatively closely. At birth, astrocyte processes of the zone extend distally into the rootlet for a short distance. In the period immediately after birth these become more

numerous. They arise from perikarya lying around the edge of the zone, at the spinal cord surface. They progressively segregate the great majority of axons from one another so that by about 3 days postnatum each eventually traverses the zone in an individual tunnel. This is bounded by a multilayered sheath of processes, which may help to insulate it until myelination occurs. Astrocyte processes form a shallow dome which at 3 days postnatum projects into most rootlets for around 10 μm. It presents an undulant surface to the PNS tissue distal to it. From this a loose glial fringe extends a little further peripherally. Subsequently the dome sinks into the underlying cord and projects into a progressively smaller proportion of rootlets (less than half at 12 days) as development proceeds. By 21 days astrocyte processes generally extend little, if at all, above the plane of the cord surface. However, occasional strands of interwoven processes project distally among the rootlet fibres for up to 30 μm, but contain no axons.

In the immediate postnatal period transitional Schwann cell perikarya are prominent in the outer third of the zone (Fig. 27d). Many lie below the plane of the surrounding cord surface. By 4 days the perikarya have disappeared from the zone. This is likely to come about because as the Schwann cells elongate distally and their perikarya migrate out of the zone into the proximal rootlet segment as described above (9.1). Their proximal ends continue to invaginate the cord surface for a short distance (Fig. 27e). The average depth of the invagination increases gradually from about 5 μm at 3 days to 23 μm at 12 days.

Stereological methods were used to analyse quantitatively age changes in the proportions made up by the various tissue components of

the rat C7 ventral transitional zone in the period of most marked changes in zone development, i.e. between 1 and 12 days after birth (Fraher & Kaar, 1982). These are summarized in Table 6. Astrocyte processes form its major component, and are most densely packed in its middle and inner thirds throughout the period examined. As the zone changes its location between 4 and 12 days after birth by sinking into the spinal cord, the composition of each level within it remains fairly constant and there is little or no change in the distance between the inner and outer margins of the zone; its depth remains remarkably constant at about 20 μm. These findings suggest that the change is due less to reorganisation of the components of the dome itself than to differential radial spinal cord growth, as a result of which the zone sinks into the cord. This explanation of the mechanism by which the C7 transitional zone becomes more centrally positioned during development is supported by the increase in the rate of radial growth of the cord which takes place shortly after 7 days, accompanying the onset of myelination in the tracts of the ventrolateral funiculus adjacent to the transitional zone (Fraher 1976, unpublished) and in the corticospinal tracts (Samorajski & Friede, 1968; Shonbach, Hu & Friede, 1968; Matthews & Duncan, 1971).

9.2.2. C7 dorsal rootlets

The shape and complexity of the C7 dorsal rootlet central tissue projection change considerably with age (Fraher & Sheehan, 1987). The central-peripheral interface is initially approximately planar and is at the same level as that of the surrounding cord (Figs. 29a, 30e). The projection first appears at 4 days postnatum. From then until about the end of the second week it elongates rapidly, especially towards the

beginning of this period (Fig. 30f). Astrocyte perikarya are present within it from the earliest stage. Early projection outgrowth is disorganised and as a result the central-peripheral interface is jagged (Fig. 29b,c). Consequently, transitional nodes of adjacent fibres lie at markedly different levels in the longitudinal direction, commonly separated by distances of up to 30 μm. During the third postnatal week, reorganisation occurs at the expense of elongation. The projection assumes a more regular form and comes to be shaped like a dorsoventrally flattened wedge. As it does so, it decreases in length (Fig. 30f,g). Its surface becomes smoother than previously and remains so subsequently. At the same time, its shape becomes more complex. One or more distally tapering conical extensions grow peripherally from its distal margin. By 20 days it has developed the features typical of maturity (Fig. 30h). Nevertheless, after this it continues to elongate and the overall dimensions of each segment increase progressively with age. The projection comes to comprise around 75% of the ventral and 50% of the collateral surfaces of that segment of the free rootlet which contains the transitional zone.

Rootlet size, estimated as cross-sectional area (Table 7), varies markedly (commonly by an order of magnitude) between the component rootlets of each C7 dorsal root studied. The larger rootlets tend to lie towards the middle of the attachment zone. Mean cross-sectional area increases over all the age intervals studied. Central tissue projection length also varies widely between rootlets. It generally tends to increase with age except for a relatively minor decrease between 12 and 20 days (Fig. 30f,g; Table 7). The greatest rate of increase takes place between 6 and 12 days.

Although there is a general tendency for larger rootlets to have longer central tissue projections, this association is rather weak and variable. Correlation analysis shows that the proportion of the variance (r^2) of central tissue projection length attributable to a linear relationship with rootlet diameter or cross sectional area varies from 14 to 66%. This suggests that any tendency for the two parameters to be closely related is disturbed by other, more obscure factors. For example, the proximal and distal limits of neighbouring central tissue projections are commonly at closely similar levels, even though their rootlets have widely differing cross sectional areas. It is therefore possible that factors unrelated to rootlet size, such as rootlet proximity, may in some way tend to maintain these limits level with one another during development.

9.2.3. L5 ventral rootlets

The early development of the L5 transitional zone resembles that of C7, outlined above (Fraher & Kaar, 1986). Between birth and 6 days, a distally tapering central tissue projection extends progressively further into the free rootlet (Fig. 30i,j). As a result, the proximal part of the free rootlet and all of the emergent rootlet generally come to consist entirely of central nervous tissue. The appearance of the transitional zone changes markedly between 6 and 12 days. The central tissue projection becomes retracted and splayed out (Fig. 30k), while its distal surface becomes highly irregular and obliquely set relative to the long axis of the rootlet. As a result the projection comes to lie largely within the emergent rootlet. However, it then elongates distally again. The resulting projection is irregular and tapers distally (Fig.

301). With maturation, this extends progressively further into the free rootlet.

Myelination commences in both central and peripheral parts of the L5 transitional zone at 3 days. Its progress is described elsewhere (Fraher & Kaar, 1984; Kaar & Fraher, 1985; Fraher et al., 1988a). At 3 and 6 days, the central ends of most myelinating transitional internodes lie in open-sided grooves up to 10 μm long on the projection surface. With the retraction of the transitional zone between 6 and 12 days, the central ends of the transitional internodes come to lie in cylindrical invaginations up to 20 μm deep into the projection, but do not extend deep to the plane of the spinal cord surface. At 20 days in more distal emergent and free parts of the rootlet, a substantial proportion lie in grooves which are open ventrally. At 300 days the central ends of most peripheral internodes again lie in open-sided grooves (Figs. 10b, 12).

The surface of the central tissue projection consists of a layer of astrocyte processes from 3 days on. Immature oligodendrocyte perikarya first occur in the projection at 12 days. At that stage large numbers of oligodendrocyte perikarya are aggregated immediately central to the transitional zone almost to the exclusion of astrocytes.

The increases in length of the central tissue projection which occurs up to 6 days and again after 12 days postnatum are probably due to distal growth and reorganisation of astrocyte processes rather than to migration of astrocyte cell bodies, since the majority of the latter continue to lie in the spinal cord as changes in length occur. The cylindrical invaginations in which the proximal ends of peripheral transitional internodes lie, develop during the stage of proximal

relocation of the zone both at lumbar and cervical levels (Fraher, 1978; Fraher & Kaar, 1982). They may develop due to distal extension of astrocyte processes, rather than as a result of active proximal invagination or growth of transitional Schwann cells (Fraher & Kaar, 1986). The changes which characterise lumbar zone development support this hypothesis, for the following reasons. Firstly, if the proximal ends of Schwann cells were to become invaginated into the central nervous system they would be surrounded by complete sleeves of astrocyte processes from the beginning. This is not the case. Instead, they rest in grooves on the astrocytic surface of the projection at 6 days, the lips of which subsequently gradually enfold and eventually encircle them. Secondly, the invaginations which are occupied only by collagen fibrils may reflect a general tendency for astrocyte processes to form sleeves around structures at the central tissue projection surface. This variation from the general behaviour pattern is analogous to that of Schwann cells which, while they normally envelop axons in tubular cytoplasmic channels continuous with the extracellular space only through the mesaxonal space, may envelop collagen fibrils in a similar fashion (Gamble, 1964; Gamble & Eames, 1966; Carlsen & Behse, 1980).

9.3. Cranial Nerves

9.3.1. Cochlear nerve

The cochlear nerve contains an extensive central tissue projection. This extends distally along the nerve for a considerable distance which, however, varies between species (Skinner, 1931; Tarlov, 1937a,b; Wulfhekel, 1969; Ross & Burkel, 1971; Chandross, Adams & Bear, 1977;

Chandross, Bear & Montgomery, 1977; Bridger & Farkashidy, 1980; Berthold et al., 1984). Its development was examined in the rat from the 15 day fetal stage up to maturity (Fraher & Delanty, 1987) at the light microscopic level.

The development of the central tissue projection is continuous but can be divided into four stages (Fig. 30a-d): Stage 1 involves initial central tissue outgrowth into the nerve from 15 to 17 days fetal, when a short projection is established (Fig. 30a). During Stage 2 growth is suspended or there is relative proximal regression. This takes place over the last four days of fetal life. Around birth growth recommences. At this time, the central-peripheral interface assumes the general form which it retains during the subsequent period of most rapid elongation. Thus, its distal surface becomes convex, moreso medially than laterally and it comes to lie medially and caudally within the nerve. It therefore becomes asymmetrical in shape (Fig. 30b). The cellularity of the projection is very low at first (Fig. 29e,h) but increases with age (Fig. 29f). However, it remains less than that of the part of the nerve composed of peripheral nervous tissue. Stage 3, when pronounced glial outgrowth into the nerve takes place (Figs. 29f,g, 30b-d) begins after birth and continues at a diminishing rate into adult life. Stage 4 involves definitive organisation of the central tissue projection, during which it takes on its mature form. This is completed between 6 and 13 days postnatum and overlaps with Stage 3.

Between 2 and 6 days postnatum the nerve segment consisting entirely of central tissue is established. This increases very rapidly in length after birth (Fig. 30b-d; Table 8). By 3 days it has reached the internal auditory meatus. By 4 days the most central part of the

nerve, and by 6 days its subarachnoid segment are made up entirely of CNS tissue. After this its growth rate decreases (Table 8). This may involve interstitial growth of the initially short central segment, or active regression distally of peripheral tissue, vacating axon segments which are enveloped by distal migration of central tissue.

It is noteworthy that the asymmetry of the central tissue projection develops during the late stages of fetal life. It thus anticipates the definite arrangement and is maintained throughout the phase of rapid elongation.

With maturation, the projection comes to occupy a progressively increasing proportion of the length of the modiolus. It may be that the length of that peripheral segment of the nerve between the projection and the ventromedial part of the basal turn of the spiral ganglion decreases over this period by 50 to 75%. If this true decrease in the length of the peripheral segment of a nerve really occurs, it is highly unusual in peripheral nerve development.

9.4. Central-Peripheral Tissue Relationships and Differential Growth

During transitional zone maturation a number of different developmental processes take place concurrently. Because these occur in the same location, interaction takes place between them. They include: the arrival of astrocytes in the zone and the elaboration of a thick layer of interwoven astrocyte processes which defines the CNS-PNS interface; the formation of complex Schwann cell clusters; the separation from these of transitional Schwann cells which subsequently segregate and myelinate peripheral axon segments; the distal extension of transitional oligodendrocytic glial units along the central axon

segments, and the formation of the transitional node. During transitional zone development, central and peripheral nervous tissues undergo considerable relative movements. Both oscillate proximally and distally along the fibre bundles so that the interface between them changes continually in position as they establish their mutual territories. Some patterns are evident in the alternation of these distal growth and proximal regression phases. Different combinations of these processes are found during the development of the various transitional zones examined.

The distal growth phases of the central tissue projections into the L5 ventral and C7 dorsal rootlets resemble one another in some respects. In both, the most rapid growth occurs between 3 and 6 days. The proximal regression phase which follows this takes place somewhat earlier (between 6 and 12 days) in the former than in the latter in which it occurs between 12 and 20 days. After this, projection length again increases, but at a rate which becomes progressively less with time in both locations. Both projections differ fundamentally in their development from the transitory outgrowth found in the cervical ventral rootlet (Fraher, 1978a; Fraher & Kaar, 1982), which is present only for a short period immediately after birth. Although the growth phases of the cochlear central tissue projection resemble in some respects those of L5 ventral and C7 dorsal rootlets, there are substantial differences as well. The period of most rapid outgrowth is between birth and 4 days postnatum in the cochlear nerve, and so is slightly earlier than that in the other two locations. Furthermore, it follows the proximal regression phase, instead of preceding it as in the other two. In addition, the most rapid outgrowth occurs in the cochlear

nerve one week after the projection first appears, whereas it occurs at the beginning of the outgrowth period in the other two nerves.

A proximal regression phase, whereby the central tissue projection becomes shorter, is a general feature of development in many nerves. The results of quantitative studies on spinal nerve roots (Fraher & Kaar, 1982, 1986; Fraher & Sheehan, 1987) are consistent with the hypothesis that proximal regression results from differential distal overgrowth of central tissue during development. This may also cause the disappearance of the projection into the C7 ventral rootlet. Regression of the projection into the cochlear nerve could result from the rapid increase which takes place during later fetal stages in the size of the closely related inferior cerebellar peduncle. As a result of this process, segments of the nerve or rootlet which lie originally in the subarachnoid space may also be engulfed and come to lie deep to the surface of the neuraxis. Schwann cells in engulfed segments may be stripped distally as the central tissue expands along the axon bundles and appear as the clusters (Fraher & Rossiter, 1983a,b) or sleeves (Fraher & Kaar, 1986) characteristic of the proximal segments of C7 and L5 ventral rootlets, respectively.

At later stages, once the transitional Schwann cells have segregated axon segments and established 1:1 relationships with them, and when transitional nodal maturation is under way, Schwann cells become invaginated progressively deeper below the cord surface as the transitional zone appears to sink into it. Such invagination could be caused by differential growth of the structures in the region of the zone. It could result, for example, if the increase in length of the intramedullary part on the axon failed to keep pace with the radial

growth of the spinal cord around it. Also, proliferation of the astrocyte processes of the zone could result in their becoming piled up around the central end of the transitional Schwann cell. Alternatively, the Schwann cell could invaginate the zone as its central end elongates and actively extends centrally along its axon. The qualitative difference in the morphology of the mature C7 ventral rootlet transitional zone compared with the others, whereby it comes to lie largely deep to the plane of the surrounding cord surface, shows that special conditions operate in the ventral cervical region which favour the passive development of Schwann cell invaginations deep to the cord surface (Fraher & Kaar, 1986).

The differential growth processes which operate during maturation of the C7 dorsal rootlet transitional zone produce a markedly different end result from that in the ventral rootlets of the same segment. The glial dome which begins to project into dorsal rootlets during the first week after birth persists into adult life (Tarlov, 1937a,b; Steer, 1971; Gamble, 1976; Berthold & Carlstedt, 1977a-c; Carlstedt, 1977b; Snyder, 1977; Fraher & Sheehan, 1987). These changes imply that peripheral nervous tissue withdraws distally and/or that central tissue actively migrates distally and becomes organised to build up the proximal part of the rootlet. It appears that these events, as well as considerable elongation of the projection, take place in the absence of substantial numbers of mitoses. It is therefore likely that cell migration, increase in cell size and elaboration of cytoplasmic processes play an important part in central tissue projection development. Furthermore, astrocyte process organisation may be plastic, since the developing projection successively expands distally, retracts somewhat and expands again.

The tissue dynamics involved in the growth of the dorsal rootlet and the proximal part of the root are therefore complex.

The level of complexity of the vagal transitional zone is compatible with extensive cellular and tissue movement during morphogenesis (Rossiter & Fraher, 1990), qualitatively different from that occurring in developing cervical (Fraher, 1978a) and lumbar (Fraher & Kaar, 1986) ventral rootlets, or in cervical (Fraher & Sheehan, 1987) and sacral (Carlstedt, 1981) dorsal rootlets. Unlike the arrangement in the other locations, Schwann cell somata and collagen come to lie at considerable distances below the surface of the neuraxis at vagal levels. This may involve invasion of the brainstem by peripheral nervous tissue, and/or overgrowth of peripheral rootlet segments by central tissue, resulting in the formation of peripheral tissue insertions. It may also involve distal migration of central nervous tissue into the rootlets to form projections, like that which takes place in C7 dorsal rootlets. However, any such movement is more complex than in C7, since the vagal projection is traversed by strands of peripheral tissue, a feature absent from C7 projections.

The structure of the mature vagal transitional zone may shed some light on these possibilities. For example, the preferential occurrence of peripheral tissue insertions in rootlets containing numerous contiguous unmyelinated axon bundles suggests that these could provide a migratory route along which Schwann cells gain access to the rootlet segment proximal to the developing astroglial barrier of the central tissue projection. This could take place if the Schwann cells migrated centrally within the axon bundle before it had been invaded by the astrocyte processes which form the matrix segregating its fibres.

Alternatively, the developing astrocytic barrier separating the CNS and PNS around the periphery of the bundles could be incomplete, allowing Schwann cells to migrate centrally. The deficiencies in the barrier of the mature peripheral tissue insertion could represent a persistence of this. Experimental studies support this possibility. These indicate that astrocyte processes forming the CNS-PNS barrier normally prevent such central migration (Gilmore, Sims & Heard, 1982; Blakemore, 1983; Sims & Gilmore, 1983; Harrison & Pollard, 1984; Harrison, 1985; Perry & Hayes, 1985; Blakemore, Crang & Curtis, 1986; Gilmore & Sims, 1986). Another possibility is that Schwann cells invade the CNS by following the perivascular route provided by the numerous blood vessels which traverse the transitional zone with the vagal rootlets. However, this is not necessarily the case, because (i) peripheral tissue insertions occur in rootlets which are not accompanied by blood vessels and (ii) blood vessels commonly pass between the CNS and PNS with developing cervical ventral rootlets (Kaar & Fraher, 1987) and these entirely lack peripheral tissue insertions. Another possible mechanism by which peripheral tissue insertions may develop is through overgrowth of differentiated peripheral rootlet segments by developing brainstem tissue, such as the inferior cerebellar peduncle. This would appear to be unlikely because of the greater number of peripherally enveloped fibres in the peripheral tissue insertion compared with the central tissue projection, the absence of cellular connective tissue components from the peripheral tissue insertion and the seeming absence of axons which were myelinated by Schwann cells over the whole length of the transitional zone (Rossiter & Fraher, 1990). At any rate, if such overgrowth does occur, it is not a simple process. It could occur at a

relatively early stage when Schwann cells are not definitively associated with axon segments. It could be part of the extensive cell migration and differential growth which occur in the developing brainstem. For example, the bulbopontine extension which is derived from the alar lamina involves cell migration ventrally in the region of the emergent zones of the glossopharyngeal, vagus and cranial accessory nerves (Hamilton, Boyd & Mossman, 1964). Furthermore, structures such as the tractus solitarius become submerged in the brainstem due to overgrowth by cells in the same region (Baxter, 1953). The formation of peripheral tissue insertions could take place as part of this process. Their probable occurrence in relation to glossopharyngeal rootlets supports this possibility. Another possibility is that Schwann cells in the peripheral tissue insertion develop in situ. This could occur if part of the neural crest does not separate from the neural tube during early development, as is the case with neuronal precursors of the trigeminal mesencephalic nucleus. Alternatively, the Schwann cells could be of intrinsic, i.e. neural tube, origin. Such a possibility was suggested by Weston (1970).

The occurrence and pattern of alternation of central and peripheral myelin sheaths on vagal axons suggest that Schwann cells and oligodendrocytes intermingle and have access to presumptively myelinated smaller axons in the developing zone. The likelihood of this is further strengthened by the geometry of peripheral tissue insertions and islands in two ways. Firstly, their endoneurial tissue and nerve fibres enveloped by myelinating or non-myelinating Schwann cells are partially or completely subdivided into fascicles by astrocyte processes, which take the place of sheath or perineurial cells in the rootlets. This

shows that central and peripheral nervous tissues intermingle in vagal rootlets. Secondly, bundles of centrally myelinated fibres commonly form bridges of CNS tissue running longitudinally through the insertion or island. This suggests that they may have been encircled by PNS tissue during development. The occurrence of PNS islands also shows that Schwann cells under normal developmental conditions can maintain a viable peripheral nervous environment within the confines of the CNS. Furthermore, the existence of cross connections between these islands and peripheral tissue insertions of neighbouring rootlets suggests that Schwann cells can migrate within the developing CNS. The presence of substantial amounts of collagen within them, in the absence of any fibroblasts, is further evidence that Schwann cells may produce collagen under normal in vivo conditions (Causey & Barton, 1959; Nathaniel & Pease, 1963; Bunge et al., 1980; Bunge & Bunge, 1984).

9.5 Glial Islands

As the CNS-PNS interface oscillates distally and proximally within the developing rootlet it displays transient, often marked, irregularities. Nevertheless, it generally retains its integrity and the central and peripheral tissue compartments both remain discrete. However, two classes of exception to this arrangement have been described. The first of these is represented by the peripheral tissue islands which are completely isolated from continuity with the main bulk of PNS tissue. The second consists of glial islands which occur in the rootlet or even in the root at a sometimes considerable distance beyond the CNS-PNS interface, lacking all connection with the CNS itself. It is likely that these arise when central nervous tissue elements lose

continuity with the glia limitans of the developing transitional zone during the distal phase of oscillation, and migrate peripherally along the rootlet. The marked irregularity of the surface of the developing CNS-PNS interface is compatible with such a sequence of events.

Glial islands have been described at the light microscopic level in human cranial nerves (Tarlov, 1937a,b) and at the electron microscope level in the Macaque trigeminal sensory root (Maxwell et al., 1969). These consist principally of astrocytic material. However, they also contain oligodendrocytes which myelinate axons traversing them. It is likely therefore that both types of glial cell or their precursors migrate distally and intermingle with peripheral nervous tissue during development. Maxwell et al. (1969) consider the possibility that the apparent islands may be in fact peninsulate extensions of the central tissue projection of the trigeminal sensory root. Whether or not that is the case, at least some glial islands in the rat are discrete and unconnected to the central nervous tissue of the transitional zone (Fig. 2). This was shown to be the case for glial islands in cervical (Fraher, 1974) and lumbar (Bristol & Fraher, unpublished observations) ventral rootlets examined by means of alternate sequential series of thin and semithin sections. In contrast to those described by Tarlov (1937a,b) and by Maxwell et al. (1969), ultrastructural examination shows that these glial islands consist only of astrocytic tissue. Each is completely surrounded by a continuous basal lamina. Its structure resembles that of an immature transitional zone. The astrocyte perikarya give rise to large numbers of processes which are interwoven in a haphazard and disorganised manner, though they tend to be arranged in a more orderly fashion in the vicinity of the axons which

traverse the island. Occasionally a process is arranged as a short segment of a spiral around the axon, suggesting that the axon may exert some organising influence upon it. These axon segments are unmyelinated throughout the extent of the island, despite the fact that they are heavily myelinated by Schwann cells both proximal and distal to it. The Schwann paranodes bounding the unmyelinated segment have an appearance identical to those of the PNS generally and are invaginated into the glial island for up to 10μm, as at ventral cervical transitional zones. The unmyelinated stretch of axon is commonly over 100μm long. It has a dense undercoat and resembles a nodal axon over its entire length. That the axon segments traversing these glial islands remain bare indicates that astrocytes present an effective barrier to Schwann cell extension along axons, a feature which is normally manifested at the CNS-PNS interface.

10. SUMMARY AND CONCLUSIONS

The transitional zone is that length of rootlet containing both central and peripheral nervous tissue. The CNS-PNS interface may be defined as the basal lamina covering the intricately interwoven layer of astrocyte processes which forms the CNS surface and which is pierced by axons passing between the CNS and PNS. Study of transitional zone development defines morphologically the growth, relative movement and interaction of central and peripheral nervous tissues as they establish their mutually exclusive territories on either side of the CNS-PNS boundary, and helps to explain the wide variations in the form of the mature transitional zone.

Nerve rootlets at first consist of bundles of bare axons. These become segregated by matrices of fine Schwann cell processes peripherally and of astrocyte processes centrally. The latter may prevent Schwann cell invasion of the CNS. Astrocyte processes branch profusely and come to form the principal central nervous tissue component of the transitional zone. Developmental changes in the transitional zone vary markedly between nerves, reflecting differences in its final morphology. Widespread relative movements and migration of CNS and PNS tissues take place during development, so that the central-peripheral interface changes shape and position, commonly oscillating along the proximodistal axis of the rootlet. For example, developing cervical ventral rootlets contain a transient central tissue projection, while that of lumbar ventral rootlets and to a lesser extent that of cervical dorsal rootlets alternately increase and decrease in length. In the developing cochlear nerve, a central tissue projection is present before birth, but regresses somewhat before a marked

outgrowth of central nervous tissue along the nerve takes place, which reaches into the modiolus during the first week postnatum. During development, some astrocytic tissue may even break off and migrate distally into the root, giving rise to one or more glial islands within it.

During the period immediately preceding birth, Schwann cells come to be present in very large numbers in that part of the rootlet immediately distal to the CNS-PNS interface, the proximal rootlet segment. Here they form prominent sleeves or clusters of closely packed cells which intertwine with and encapsulate one another on the rootlet surface. Such Schwann cell overcrowding in the proximal rootlet segment could result in part from distal overgrowth of the rapidly expanding CNS around axon bundles, which might strip the Schwann cells distally off the bundle segments so engulfed. Most cells comprising the clusters or sleeves separate from them to segregate and envelop axon segments in the proximal rootlet segment in the manner characteristic of Schwann cells. Others lose axonal contact and lie dormant in the segment. Morphological and morphometric analysis of the developing transitional zone and proximal rootlet segment are thus consistent with marked dynamic interactions between the central and peripheral tissues on either side of the CNS-PNS interface.

The transitional node is located at the CNS-PNS interface. The level along the axon at which it differentiates may be determined by the astrocytes forming the interface, either directly, or indirectly by determining the central limit of the Schwann cell, in close relation to which the node differentiates. This supports the possibility that node location may be influenced by extra-axonal factors. The presumptive bounding oligodendrocyte probably plays little or no part in this, since

it is usually separated by a long unmyelinated segment from the presumptive node at this stage. Developmental changes in the nodal axon resemble those of peripheral rather than central nodes. The ensheathing cells do not substantially modify their appearance during node development in response to their unique relationship with one another at the transitional node, though a variety of differences in detail are found. Astrocyte processes and basal lamina come to form a progressively more complete barrier within the transitional node gap between the CNS and PNS environments, as maturation progresses. They also come to form a gradually more extensive tubular sleeve into which the transitional Schwann cell paranode is invaginated. Stereological analysis is consistent with this being due to distal overgrowth of central nervous tissue. At the deep end of the invagination they give rise to a ring of processes which forms a collar projecting into the node gap. The production by individual astrocytes of sleeve and node gap processes as well as those contributing to the glia limitans contradicts the binary classification of astrocytes according to which each produces only one type of process. Instead it suggests that the astrocyte is multipotential insofar as it may produce a variety of processes serving a number of different structural roles, each appropriate to the location of the cell.

Ventral motoneuron node packing density in the lumbar transitional zone is likely to be seven times greater than in the ventral root and five times greater than in bundles of these axons in the spinal cord. The fact that nodes are longitudinally offset relative to one another reduces or excludes crosstalk between them, since they are further apart than if they all lay in the same transverse plane of the

rootlet. However, they are not regularly spaced in the transitional zone. Three-dimensional reconstructions show that they are commonly clustered. Nodes of large and of small fibres tend to be preferentially clustered, each with others of its own class.

The position and form of the mature transitional zone both vary markedly between nerves. For example, in lower cervical ventral rootlets the zone is to a large extent sunken below the surrounding cord surface and, though the CNS-PNS interface is irregular in shape, it is approximately parallel to this. By contrast, it lies almost entirely within lumbar ventral rootlets which contain a central tissue projection commonly over 100 μm long. Lower cervical dorsal rootlets contain large dorsoventrally flattened wedge-shaped central tissue projections which may show up to two orders of branching distally. The transitional zones of cranial nerves vary widely in form. Those of abducent rootlets, which are small, lie in the plane of the surrounding brainstem surface and resemble those of lower cervical ventral rootlets. That of the trochlear nerve contains an extensive central tissue projection, resembling that of a lower cervical dorsal rootlet. This might suggest that the presence or absence of a central tissue projection in a motor nerve could be related to the dorsoventral position of the attachment to the neuraxis of the nerve containing it. However, spinal accessory rootlets, which are attached to the upper cervical spinal cord midway between the dorsal and ventral spinal rootlets, have transitional zones closely resembling those of ventral rather than dorsal cervical rootlets and are not intermediate in form between the two, as might be predicted according to the above hypothesis. Oculomotor rootlets vary markedly in size. The larger ones tend to contain prominent central

tissue projections, while in some, though not all, of the smaller ones the transitional zone resembles that of the lower cervical ventral rootlets, which are of similar size. Thus, despite the close similarities between the three nerves innervating the extraocular muscles, their transitional zones differ markedly from one another. Among the sensory cranial nerve rootlets, the cochlear nerve trunk contains a very long central tissue projection, which comprises the entire nerve trunk. The transitional zone lies towards the distal end of this, where the cochlear nerve branches spring from its surface. The sensory root of the trigeminal nerve is particularly large and also contains a central tissue projection which comprises its entire cross section over a considerable distance. The dorsolateral vagal rootlets are also large and contain prominent central tissue projections. Hypoglossal rootlets resemble those of the oculomotor nerve. Examination of a variety of cranial nerve rootlets therefore suggests that the presence or absence of a central tissue projection and therefore the location of the transitional zone within the rootlet or at the surface of the neuraxis, respectively, may be associated with rootlet size. Such a relationship would be in accord with differences in transitional zone morphology between dorsal and ventral rootlets at lower cervical cord levels and within upper thoracic ventral rootlets. The presence of long central tissue projections in lumbar ventral rootlets is the sole exception to the otherwise rather well-defined association between transitional zone morphology and rootlet size. These studies clearly show that there is no rostrocaudal gradient of transitional zone size and structure along the neuraxis.

Central tissue projections almost always lie eccentrically in the rootlet, closer to that surface of the the rootlet which lies nearest the neuraxis. This enables transitional nodes to be spaced widely apart, reducing or excluding crosstalk between them. Where many small cervical or cranial motor rootlets emerge from the neuraxis, the rootlet traverses an extensive pad of intricately interwoven astrocyte processes which extends into the area of cord surface surrounding the emergent zone of the rootlet. Few astrocytic perikarya occur either in these pads or in small central tissue projections. Instead they lie in the CNS adjacent to the rootlet and give rise to processes which extend into the transitional zone. Large projections contain numerous astrocyte and also oligodendrocyte perikarya and resemble CNS tissue generally.

The transitional zones of dorsolateral vagal rootlets present an order of complexity greater than found elsewhere. A typical rootlet contains a transitional zone over 300 μm long, consisting of a central tissue projection extending distally into the rootlet beyond the brainstem surface, and a peripheral tissue insertion extending centrally for a longer distance along the rootlet, deep into the brainstem. The peripheral tissue insertion is continuous with the peripheral tissue of the free rootlet through channels traversing or running parallel to the central tissue projection. Accordingly, the vagal CNS-PNS interface is topologically much more complex than those found elsewhere. In some rootlets the peripheral tissue in the brainstem constitutes an isolated island deep within the neuraxis. The CNS-PNS transition of vagal axons reflects this complexity. About one fifth of all of those which are myelinated alternate, in many cases more than once, between the CNS and PNS tissue compartments. These are myelinated by Schwann cells

distal to the transitional zone, by oligodendrocytes in the central tissue projection and by one or more short intercalated Schwann internodes in the peripheral tissue insertion. In addition, the majority of unmyelinated axon bundles alternate between central and peripheral tissue compartments, also commonly more than once. Around one fifth of peripherally unmyelinated axons have an oligodendrocytic sheath in the central compartment. Of those axons possessing more than one intercalated Schwann internode, over one quarter display alternation of myelinated and unmyelinated segments in the peripheral tissue insertion.

Astrocytes in the vagal transitional zone segregate PNS tissue, a role played by sheath cells further peripherally in the vagal rootlets, as in the PNS generally. Astrocytes form the thick multi-layered surface limiting membrane of the central tissue projection and also the barrier between the peripheral tissue insertion and the surrounding brainstem, which consists only of an attenuated layer of processes. This barrier is deficient in places, where oligodendrocytic myelin sheaths are directly exposed to the endoneurial space of the peripheral tissue insertion and in some instances are apposed to myelinating or non-myelinating Schwann cells. Such communication between the central and peripheral compartments is unique to the vagal transitional zone. The findings are consistent with a range of possible events during development, for example: considerable migration and intermingling of central and peripheral tissues, possible overgrowth of rootlet segments by developing myelencephalic tissue, failure of part of the neural crest to separate form the developing neural tube, and the origin of peripheral tissue insertion Schwann cells from the neural tube, or combinations of these factors.

The marked offsetting of transitional nodes in the longitudinal and transverse planes of the transitional zone may have a number of mechanical advantages. Nodes are likely to be weak points along nerve fibres since they lack the strength provided by cytoplasm. Because of its fluid crystalline nature it is likely that the myelin sheath provides the fibre with little tensile strength. Offsetting of nodes may circumvent their vulnerability to traction-induced stress and the greater tendency to snap if all lie in the same plane. Continuity of Schwann cell and astrocytic basal laminae and their cross-linkage by collagen fibrils may provide further mechanical strength. The astrocytic invagination may act as a suction cup, resisting distraction of the Schwann internode, the central end of which is inserted into it. The cellular sheaths surrounding lumbar ventral roots are continuous with the pia mater and the free rootlets comprising them traverse the space between the most superficial pial layer and the glia limitans. This continuity may also help to strengthen the junctional region between the CNS and PNS in general. Further mechanical strength may be provided by the insertion of endoneurial collagen fibril bundles into clefts between the astrocyte processes of the glia limitans and by the intricate interdigitation of rootlet sheath cells with astrocytes in some sites.

Rootlet sheaths are fenestrated, so that their endoneurial spaces are continuous with the subpial space. The spaces between the rootlets contain numerous capillaries and postcapillary venules which communicate freely with vessels in the subjacent spinal cord in the great majority of nerves examined. Vascularity of the transitional zone increases considerably during the period when transitional nodes of small fibres become mature, which is likely to coincide with increased

neural activity. The transitional zone continues to be richly vascularised throughout life, a feature which supports the high level of metabolic activity associated with the particularly high density of nodes which it contains.

ACKNOWLEDGEMENTS

The author is indebted to Cambridge University Press, Blackwell Scientific Publications, Elsevier Science Publishers and Chapman & Hall for permission to reproduce material published in the Journal of Anatomy, Neuropathology and Applied Neurobiology, Journal of the Neurological Sciences and the Journal of Neurocytology, respectively. The author is grateful to Ms. B. Rea and Mr. D. O'Leary for technical assistance in producing this article and to Ms. M. Bogan for typing the manuscript. The work reported here was supported by grants from the Medical Research Council (later the Health Research Board) of Ireland, the Multiple Sclerosis Society of Ireland and the Wellcome Trust.

REFERENCES

Aguayo, A.J., Bray, G.M., Terry, L.C. and Sweezey, E. (1976) Three dimensional analysis of unmyelinated fibres in normal and pathologic autonomic nerves. J. Neuropathol. Exper. Neurol. **35**, 136-151.

Allt, G. (1969) Ultrastructural features of the immature peripheral nerve. J. Anat., Lond. **105**, 283-293.

Baxter, J.S. (1953) Frazer's Manual of Embryology. pp. 144-146, London: Balliere, Tindall & Cox.

Berthold, C.-H. (1968a) Ultrastructure of the node-paranode region of mature feline ventral lumbar spinal root fibres. Acta Soc. Med. Upsal. **73**, 37-70.

Berthold, C.-H. (1968b) Ultrastructure of postnatally developing feline peripheral nodes of Ranvier. Acta Soc. Med. Upsal. **73**, 145-166.

Berthold, C.-H. (1974a) A comparative morphological study of the developing node-paranode region in lumbar spinal roots. I. Electron microscopy. Neurobiol. **4**, 82-104.

Berthold, C.-H. (1974b) A comparative morphological study of the developing node-paranode region in lumbar spinal roots. II. Light -microscopy after OTAN - staining. Neurobiol. **4**, 117-131.

Berthold, C.-H. and Carlstedt, T. (1977a) Observations on the morphology at the transition between the peripheral and the central nervous system in the cat. II. General organisation of the transitional region in S_1 dorsal rootlets. Acta Physiol. Scand., Suppl. **446**, 23-42.

Berthold, C.-H. and Carlstedt, T. (1977b) Observations on the morphology at the transition between the peripheral and the central nervous system in the cat. III. Myelinated fibres in S_1 dorsal rootlets. Acta Physiol. Scand., Suppl. **446**, 43-60.

Berthold, C.-H. and Carlstedt, T. (1977c) Observations on the morphology at the transition betwen the peripheral and the central nervous system in the cat. V. A light microscopical and histochemical study of S_1 dorsal rootlets in developing kittens. Acta Physiol. Scand., Suppl. **446**, 73-85.

Berthold, C.-H., Carlstedt, T. and Corneliuson, O. (1984) Anatomy of the nerve root at the central-peripheral transitional region. In: Peripheral Neuropathy, Vol. 1, 2nd ed. pp. 156-170. Eds. P.J. Dyck, P.K. Thomas and E.H. Lambert. Philadelphia: W.B. Saunders and Co.

Bieger, D. and Hopkins, D.A. (1987) Viscerotopic representation of the upper alimentary tract in the medulla oblongata in the rat: the nucleus ambiguus. J. Comp. Neurol. **262**, 546-62.

Blakemore, W.F. (1983) Remyelination of demyelinated spinal cord axons by Schwann cells. In: Spinal Cord Reconstruction, pp. 281-291 Eds. C.C. Kao, R.P. Bunge, and P.J. Reier. Raven Press: New York.

Blakemore, W.F., Crang, A.J. and Curtis, R. (1986) The interaction of Schwann cells with CNS axons in regions containing normal astrocytes. Acta Neuropathol. 71, 295-300.

Blakemore, W.F. and Patterson, R.C. (1975) Observations on the interactions of Schwann cells and astrocytes following X-irradiation of neonatal rat spinal cord. J. Neurocytol. 4, 573-85.

Bondareff, W. and McLone, D.G. (1973) The external glial limiting membrane in Macaca: Ultrastructure of a laminated glioepithelium. Am. J. Anat. 136, 277-96.

Braak, E. (1975) On the fine structure of the external glial layer in the isocortex of man. Cell and Tissue Res. 157, 367-90.

Bridger, M.W.M. and Farkashidy, J. (1980) The distribution of neuroglia and Schwann cells in the 8th nerve of man. J. Laryngol. Otolaryngol. 94, 1353-1362.

Bristol, D.C. and Fraher, J.P. (1987) A morphometric study of the CNS-PNS transitional zone in rat lumbar ventral roots. J. Anat. 152, 236.

Bristol, D.C. (1989) Aspects of the ventral rootlet transitional zone in the rat. A morphometric and morphological analysis of the L_4 ventral rootlet transitional zone and the distribution of transitional nodes of Ranvier within it. Ph.D. Thesis, National University of Ireland.

Bristol, D.C. and Fraher, J.P. (1989) Experimental traction injuries of ventral spinal nerve roots. A scanning electron microscopic study. Neuropathol. Appl. Neurobiol. 15, 549-561.

Bunge, R.P. and Bunge, M.B. (1984) Tissue culture observations relating to peripheral nerve development, regeneration and disease. In: Peripheral Neuropathy, Vol. 1. pp. 378-399. Eds. P.J. Dyck, P.K. Thomas, E.H. Lambert and R. Bunge. W.B. Saunders Co: Philadelphia.

Bunge, M.B., Williams, A.K., Wood, P.M., Uitto, J. and Jeffrey, J.J. (1980) Comparison of nerve cell and nerve cell plus Schwann cell cultures, with particular emphasis on basal lamina and collagen formation. J. Cell Biol. 84, 184-202.

Caley, D.W. and Maxwell, D.S. (1970) Development of the blood vessels and extracellular spaces during postnatal maturation of rat cerebral cortex. J. Comp. Neurol. 138, 31-48.

Carlsen, F. and Behse, F. (1980). Three dimensional analysis of Schwann cells associated with unmyelinated nerve fibres in human sural nerve. J. Anat. **130**, 545-557.

Carlstedt, T. (1977a) Observations on the morphology at the transition between the peripheral and the central nervous system in the cat. I. A preparative procedure useful for electron microscopy of the lumbosacral dorsal rootlets. Acta Physiol. Scand., Suppl. 446, 5-21.

Carlstedt, T. (1977b) Observations on the morphology at the transition between the peripheral and the central nervous system in the cat. IV. Unmyelinated fibres in S_1 dorsal rootlets. Acta Physiol. Scand., Suppl. **446**, 61-71.

Carlstedt, T. (1981) An electron-microscopical study of the developing transitional region in feline S_1 dorsal rootlets. J. Neurol. Sci. **50**, 357-372.

Causey, G. and Barton, A.A. (1959) The cellular content of the endoneurium of peripheral nerve. Brain, **82**, 594-598.

Chandross, R.J., Adams, J.B. and Bear, R.S. (1977) Discontinuous transition of myelin structure at the junction between central and peripheral components of the eighth cranial nerve, as disclosed by X-ray diffraction. J. Comp. Neurol. **177**, 11-16.

Chandross, R.J., Bear, R.S. and Montgomery, R.L. (1977) An X-ray diffraction comparison of myelins from the human nervous system. J. Comp. Neurol. **177**, 1-10.

Cox, D.R. (1966) Notes on the analysis of mixed frequency distributions. Br. J. Math. statist. Psychol. **19**, 39-47.

Dempster, A.P., Laird, N.M. and Rubin, D.B. (1977) Maximum likelihood from incomplete data via the EM algorithm. Jl. R. statist. Soc. B. **39**, 1-38.

Fedoroff, s. (1986) Prenatal ontogenesis of astrocytes. In: Cellular Neurobiology: A Series. Astrocytes Vol. 1. Development, Morphology and Regional Specialization of Astrocytes. pp. 35-74 Eds. S. Federoff and A. Vernadakis. Academic Press: Orlando.

Foncin, J.F. (1961) Structure fine de la zone de passage radiculo-medullaire. Rev. Neurol., **105**, 509-513.

ffrench-Constant, C. and Raff, M.C. (1986) Evidence that the oligodendrocyte-type 2-astrocyte cell lineage is specialized for myelination. Nature **323**, 335-8.

Fraher, J.P. (1973) A quantitative study of anterior root fibres during early myelination. II. Longitudinal variation in sheath thickness and axon circumference. J. Anat., Lond. **115**, 421-444.

Fraher, J.P. (1974) A numerical study of cervical and thoracic ventral nerve roots. J. Anat., Lond. **118**, 127-142.

Fraher, J.P. (1978a) The maturation of the ventral root-spinal cord transitional zone. J. Neurol. Sci. **36**, 427-449.

Fraher, J.P. (1978b) Quantitative studies on the maturation of central and peripheral parts of individual ventral motoneuron axons. II. Internodal length. J. Anat., Lond. **127**, 1-15.

Fraher, J.P. (1989) Axon-myelin relationships in rat cranial nerves III, IV, and VI: A morphometric study of large- and small-fibre classes. J. Comp. Neurol. **286**, 384-390.

Fraher, J.P. and Bristol, D.C. (1990) High density of nodes of Ranvier in the CNS-PNS transitional zone. J. Anat., Lond. **170**, 131-137.

Fraher, J.P. and Delanty, F.J.N. (1987) The development of the central-peripheral transitional zone of the rat cochlear nerve. A light microscopic study. J. Anat. **155**, 109-18.

Fraher, J.P. and Kaar, G.F. (1982) The maturation of the ventral root-spinal cord transitional zone. Part 2. A quantitative ultrastructural study of the dynamics of its early development. J. Neurol. Sci. **53**, 63-75.

Fraher, J.P. and Kaar, G.F. (1984) The transitional node of Ranvier at the junction of the central and peripheral nervous systems: an ultrastructural study of its development and mature form. J. Anat. **139**, 215-238.

Fraher, J.P. and Kaar, G.F. (1985) The development of alpha and gamma motoneuron fibres in the rat. II. A comparative ultrastructural study of their central and peripheral myelination. J. Anat., Lond. **141**, 89-103.

Fraher, J.P. and Kaar, G.F. (1986) The lumbar ventral root-spinal cord transitional zone in the rat. A morphological study during development and at maturity. J. Anat., Lond. **145**, 109-122.

Fraher, J.P., Kaar, G.F., Bristol, D.C. and Rossiter, J.P. (1988a) Development of ventral spinal motoneurone fibres: a correlative study of the growth and maturation of central and peripheral segments of large and small fibre classes. Prog. Neurobiol. **31**, 199-239.

Fraher, J.P. and Rossiter, J.P. (1983a) Cell clusters on fetal rat ventral roots: prenatal development. J. Anat., Lond. **136**, 111-128.

Fraher, J.P. and Rossiter, J.P. (1983b) Cell clusters on rat ventral roots: postnatal development. J. Anat., Lond. **137**, 555-571.

Fraher, J.P. and Rossiter, J.P. (1991) Myelin-axon relationships established by rat vagal Schwann cells deep to the brainstem surface. J. Comp. Neurol. **304**, 253-260.

Fraher, J.P. and Sheehan, M.M. (1987) The CNS-PNS transitional zone of rat cervical dorsal roots during development and at maturity. A morphological and morphometric study. J. Anat., Lond. **152**, 189-203.

Fraher, J.P., Smiddy, P.F. and O'Sullivan, V.R. (1988b) The central-peripheral transitional regions of cranial nerves. Oculomotor nerve. J. Anat., Lond. **161**, 103-113.

Fraher, J.P., Smiddy, P.F. and O'Sullivan, V.R. (1988c) The central-peripheral regions of cranial nerves. Trochlear and abducent nerves. J. Anat. **161**, 115-123.

Gamble, H.J. (1964) Comparative electron-microscopic observations on the connective tissues of a peripheral nerve and a spinal nerve root in the rat. J. Anat., Lond. **98**, 17-25.

Gamble, H.J. (1976) Spinal and cranial nerve roots. In: The Peripheral Nerve Ed. D.N. Landon. Chapman and Hall: London.

Gamble, H.J. and Eames, R.A. (1966) Electron microscopy of human spinal nerve roots. Arch. Neurol. **14**, 50-53.

Gilmore, S.A. and Sims, T.J. (1986) The role of Schwann cells in the repair of glial cell deficits in the spinal cord. In: Neural Transplantation and Regeneration, pp. 245-269 Eds. G.D. Das. and R.B. Wallace. Springer-Verlag: New York.

Gilmore, S.A., Sims, T.J., and Heard, J.K. (1982) Autoradiographic and ultrastructural studies of areas of spinal cord occupied by Schwann cells and Schwann cell myelin. Brain Res. **239**: 365-375.

Guyton, A.C. (1981) Textbook of Medical Physiology. 6th Ed. W.B. Saunders Co.: Philadelphia.

Hamilton, W.J., Boyd, J.D. & Mossman, H.W. (1964) Human Embryology, pp. 336-339. Heffer: Cambridge.

Hannah, R.S. and Nathaniel, E.J.H. (1974) The postnatal development of blood vessels in the substantia gelatinosa of rat spinal cord - an ultrastructural study. Anat. Rec. **178**, 691-710.

Harrison, B.M. (1985) Schwann cell and oligodendrocyte remyelination in lysolecithin-induced lesions in irradiated rat spinal cord. J. Neurol. Sci. **67**, 143-159.

Harrison, B.M., and Pollard, J.D. (1984) Pattern of Schwann cell remyelination in a spinal cord lesion. Neurosci. Lett. **52**: 275-280.

Haug, H. (1971) Die membrana limitans gliae superficialis der sehrinde der katze. Z. Zellforsch. mikr. Anat. **115**, 79-87.

Hildebrand, C. (1971a) Ultrastructural and light microscopic studies of the nodal region on large myelinated fibres of the adult feline spinal cord white matter. Acta physiol. Scand. Suppl. **364**, 43-80.

Hildebrand, C. (1971b) Ultrastructural and light microscopic studies of the developing feline spinal cord white matter. I. The nodes of Ranvier. Acta physiol. Scand. Suppl. **364**, 81-108.

Hirano, A. and Dembitzer, H.M. (1978) Morphology of normal central myelinated axons. In: Physiology and Pathobiology of Axons, pp. 65-82 Ed. S.G. Waxman. Raven Press: New York.

Kaar, G.F. (1984) Development of the transitional region between central and peripheral nervous systems. A morphological and quantitative study of the L5 ventral root. Ph.D. Thesis, National University of Ireland.

Kaar, G.F. and Fraher, J.P. (1985) The development of alpha and gamma motoneuron fibres in the rat. I. A comparative ultrastructural study of their central and peripheral axon growth. J. Anat., Lond. **141**, 77-88.

Kaar, G.F. and Fraher, J.P. (1986) The sheaths surrounding the attachments of rat lumbar ventral roots to the spinal cord: a light and electron microscopical study. J. Anat., Lond. **148**, 137-146.

Kaar, G.F. and Fraher, J.P. (1987) The vascularization of the central-peripheral transitional zone of rat lumbar ventral rootlets: a morphological and morphometric study. J. Anat., Lond. **150**, 145-154.

Kaar, G.F., O'Sullivan, V.R. and Fraher, J.P. (1983) Combined vascular perfusion and in situ fixation of rat spinal nerve roots. Ir. J. Med. Sci. **152**, 222.

Kalia, M. and O'Sullivan, J.M. (1982) Brainstem projections of sensory and motor components of the vagus nerve in the rat. J. Comp. Neurol. **211**, 238-264.

Kidd, G.J. and Heath, J.W. (1988) Double myelination of axons in the sympathetic nervous system of the mouse. II. Mechanisms of formation. J. Neurocytol. **17**, 264-276.

Lundborg, G. and Brånemark, P.-I. (1968) Microvascular structure and function of peripheral nerves. Adv. Microcirc. **1**, 66-68.

Matthews, M.A. and Duncan, D. (1971) A quantitative study of morphological changes accompanying the initiation and progress of myelin production in the dorsal funiculus of the rat spinal cord. J. Comp. Neurol. **142**, 1-22.

Maxwell, D.S., Kruger, L. and Pineda, A. (1969) The trigeminal nerve root with special reference to the central-peripheral transitional zone: An electron microscopic study in the macaque. Anat. Rec. **164**, 113-126.

Miceli, M.O. and Malsbury, C.W. (1985) Brainstem origins and projections of the cervical and abdominal vagus in the golden hamster: a horseradish peroxidase study. J. Comp. Neurol. **237**, 65-76.

Miller, R.H. (1988) Astrocyte heterogeneity in the vertebrate central nervous system. In: The Making of the Nervous System, pp. 268-281. Eds. J.G. Parnavelas, C.D. Stern and R.V. Stirling. Oxford University Press.

Miller, R.H., Fulton, B.P. and Raff, M.C. (1989) A novel type of glial cell associated with nodes of Ranvier in rat optic nerve. Eur. J. Neurosci. **1**, 172-80.

Miller, R.H. and Raff, M.C. (1984) Fibrous and protoplasmic astrocytes are biochemically and developmentally distinct. J. Neurosci. **4**, 585-592.

Moll, C. and Meier, C. (1983) The central-peripheral transition zone of the cervical spinal nerve roots in Jimpy mutant and normal mice. Acta Neuropathol. **60**, 241-251.

Nathaniel, E.J. and Nathaniel, D.R. (1963) Electron microscopic observations on the dorsal root-spinal cord junction. J. Cell Biol., **19**, 122.

Nathaniel, E.J.H. and Pease, D.C. (1963) Collagen and basement membrane formation by Schwann cells during nerve regneration. J. Ultrastr. Res. **9**, 550-560.

Němeček, S., Pařízek, J., Špaček, J. and Němečková, J. (1969) Histological, histochemical and ultrastructural appearance of the transitional zone of the cranial and spinal nerve roots. Folia Morphol. **17**, 171-181.

Nugent, S.G. O'Sullivan, V.R. Fraher, J.P. and Rea, B.B. (1991) Central-peripheral transitional zone of the spinal accessory nerve in the rat. J. Anat., Lond. **175**, 19-25.

Obersteiner, H., and Redlich E. (1894) Über Wesen und Pathogenese der Tabischen Hinterstrangsdegeneration. Arb. Neurol. Inst. Univ. Wien, 1-3:158-172.

Olsson, Y. (1975) Vascular permeability in the peripheral nervous system. In: Peripheral Neuropathy. Ed. P.J. Dyck, P.K. Thomas and E.H. Lambert. W.B. Saunders Co: Philadelphia.

Pannese, E., Ledda, M. and Matsuda, S. (1988) Nerve fibres with myelinated and unmyelinated portions in dorsal spinal roots. J. Neurocytol. **17**, 693-700.

Perry, V.H. and Hayes, L. (1985) Lesion-induced myelin formation in the retina. J. Neurocytol., **14**: 297-307.

Peters, A., Palay, S.L. and Webster, H. DeF (1976) The Fine Structure of the Nervous System: The Neurons and Supporting Cells, pp. 233-244. W.B. Saunders: Philadelphia.

Phelps, C.H. (1972) The development of the glio-vascular relationship in the rat spinal cord. Z. Zellforsch. mikr. Anat. **128**, 555-563.

Poritsky, R. (1969) Two and three dimensional ultrastructure of boutons and glial cells on the motoneuronal surface in the cat spinal cord. J. Comp. Neurol. **135**, 423-452.

Privat, A. and Rataboul, P. (1986) Fibrous and protoplasmic astrocytes. In: Cellular Neurobiology: A Series. Astrocytes, Vol. 1, Development, Morphology and Regional Specialization of Astrocytes, Vol. 1, pp. 105-129. Eds. S. Fedoroff, and A. Vernadakis. Academic Press: Orlando.

Raine, C.S. (1984) Morphology of myelin and myelination. In: Myelin, 2nd ed. pp. 1-50, Ed. P. Morell. Plenum Press: New York.

Raff, M.C. (1989) Glial cell diversification in the rat optic nerve. Science **243**, 1450-1455.

Risling, M., Fried, K., Hildebrand, C. and Cukierman, A. (1986) Unmyelinated axons in the feline trigeminal motor root. Anat. Rec. **214**, 198-203.

Ross, M.D. and Burkel, W. (1971) Electron microscopic observations of the nucleus, glial dome and meninges of rat acoustic nerve. Am J. Anat. **130**, 73-92.

Rossiter, J.P. (1989) The CNS-PNS transitional region of the vagus nerve. A morphological study in the adult rat. Ph.D. Thesis, National University of Ireland.

Rossiter, J.P. and Fraher, J.P. (1990) Intermingling of central and peripheral nervous tissues in rat dorsolateral vagal rootlet transitional zones. J. Neurocytol. **19**, 385-407.

Samorajski, T. and Friede, R.L. (1968) A quantitative electron microscopic study of myelination in the pyramidal tract of the rat. J. Comp. Neurol. **134**, 323-338.

Sasaki, M. and Ide, C. (1989) Demyelination and remyelination in the dorsal funiculus of the rat spinal cord after heat injury. J. Neurocytol. **18**, 225-239.

Schonbach, J., Hu, K.H. and Friede, R.L. (1968) Cellular and chemical changes during myelination: Histologic, autoradiographic, histochemical and biochemical data on myelination in the pyramidal tract and corpus callosum of rat. J. Comp. Neurol. **134**, 21-38.

Schlaepfer, W.W., Freeman, L.A., and Eng, L.F. (1979) Studies of human and bovine spinal nerve roots and the outgrowth of CNS tissues into the nerve root entry zone. Brain Res., **177**, 219-219.

Sims, T.J. and Gilmore, S.A. (1983) Interactions between intraspinal Schwann cells and the cellular constituents normally occurring in the spinal cord: an ultrastructural study in the irradiated rat. Brain Res. **276**, 17-30.

Sims, T.J., Gilmore, S.A., Waxman, S.G. and Klinge, E. (1985) Dorsal-ventral differences in the glia limitans of the spinal cord: an ultrastructural study in developing normal and irradiated rats. J. Neuropathol. & Exp. Neurol. **44**, 415-29.

Sindou, M., Quoex, C. and Baleydier, C. (1974) Fiber organisation at the posterior spinal cord-rootlet junction in man. J. Comp. Neurol. **153**, 15-26.

Skinner, H.A. (1931) Some histologic features of the cranial nerves. Arch. Neurol. Psychiat. **25**, 356-372.

Skoff, R.P., Knapp, P.E. and Bartlett, W.P. (1986) Astrocytic diversity in the optic nerve: A cytoarchitectural study. In: Cellular Neurobiology: A Series. Astrocytes: Development, Morphology and Regional Specialization of Astrocytes, Vol. 1. pp. 269-291. Eds. S. Fedoroff and A. Vernadakis. Academic Press: Orlando.

Smith, R.S., Chan, H. and Schaap, C.J. (1985) Intermittent myelination of small-diameter sciatic axons in Xenopus laevis. J. Neurocytol. **14**, 269-278.

Snyder, R. (1977) The organization of the dorsal root entry zone in cats and monkeys. J. Comp. Neurol. **174**, 47-69.

Steer, J.M. (1971) Some observations on the fine structure of rat dorsal spinal nerve roots. J. Anat., Lond. **109**, 467-486.

Stensaas, L.J. and Stensaas, S.S. (1968) Astrocytic neuroglial cells, oligodendrocytes and microgliacytes in the spinal cord of the toad. II. Electron microscopy. Zeitschrift für Zellforschung und Mikroskopische Anatomie **86**, 184-213.

Sturrock, R.R. (1981). A quantitative and morphological study of vascularisation of the developing mouse spinal cord. J. Anat. **132**, 203-221.

Sturrock, R.R. (1982) Gliogenesis in the prenatal rabbit spinal cord. J. Anat., Lond. **134**, 771-793.

Suarez, I. and Fernandez, B. (1983) Structure and ultrastructure of the external glial layer in the hypothalamus of the hamster. J. Hirnforsch. **24**, 99-109.

Sunderland, S. (1978) Nerves and Nerve Injuries. Churchill Livingstone: Edinburgh.

Tarlov, I.M. (1937a) Structure of the nerve root. I. Nature of the junction between the central and the peripheral nervous system. Arch. Neurol. Psychiat. **37**, 555-583.

Tarlov, I.M. (1937b) Structure of the nerve root. II. Differentiation of sensory from motor roots; observations on identification of function in roots of mixed cranial nerves. Arch. Neurol. Psychiat. **37**, 1338-1355.

Thomas, P.K. (1963) The connective tissue of peripheral nerve: an electron microscopic study. J. Anat., Lond. **97**, 35-44.

Uehara, M. and Ueshima, T. (1988) Scanning electron microscopy of the superficial glial limiting membrane in the cat brain and spinal cord. Jap. J. Vet. Sci. **50**, 115-124.

Virchow, R. (1858), Ruckenmark und Gehirn. In: Die Cellularpathologie in ihrer Begrundung auf Physiologische und Pathologische Gewebelehre. pp. 238-254: Berlin: Hirschwald

Wagner, H.-J., Barthel, J. and Pilgrim, C. (1983) Permeability of the external glial limiting membrane of rat parietal cortex. Anat. & Embryol. **166**, 427-437.

Waxman, S.G. (1986) The astrocyte as a component of the node of Ranvier. Trends Neurosci. **9**, 250-253.

Waxman, S.G. and Black, J.A. (1984) Freeze-fracture ultrastructure of the perinodal astrocyte and associated glial junctions. Brain Res. **308**, 77-88.

Webster H. de F. (1971) The geometry of peripheral myelin sheaths during their formation and growth in rat sciatic nerves. J. Cell Biol. **48**, 348-367.

Weston, J.A. (1970) The migration and differentiation of neural crest cells. Adv. Morphogen. **8**, 41-114.

Wiley-Livingston, C.A. and Ellisman, M.H. (198O) Development of axonal specialisations defines nodes of Ranvier and precedes Schwann cell myelin elaboration. Devl. Biol. **79**, 334-355.

Williams, V. (1976) Intercellular relationships in the external glial limiting membrane of the neocortex of the cat and rat. Am. J. Anat. **144**, 421-432.

Wolff, J. (1965) Electronenmikroskopische Untersuchungen uber Struktur und Gestalt von Astrozytenforsatzen. Z. Zellforsch. mikr. Anat. **66**, 811-825.

Wulfhekel, U. (1969) Der Übergang der zentralen in die periphere Struktur von Hirnnerven bei den niederen Wirbeltieren. Acta anat. **74**, 183-196.

Yokota, R. (1984) Occurrence of long non-myelinated axonal segments intercalated in myelinated, presumably sensory axons: electron microscope observations in the dog atrial endocardium. J. Neurocytol. **13**, 127-143.

TABLE 1

PATTERNS OF ALTERNATION OF CENTRAL AND PERIPHERAL MYELIN SHEATHS ON AXONS FOUND IN A SAMPLE OF 91 VAGAL FIBRES TRAVERSING THE TRANSITIONAL ZONE

Alternation	Frequency %
S-O-S_i-O	84.6
S-O-S_i-S_i-O	5.5
S-O-S_i-S_i-S-O	3.3
S-O-S_i-S_i-S_i-S_i-O	1.1
S-O-S_i-O-S_i-O	2.2
S-O-S_i-O-S_i-S_i-O	3.3

S, transitional Schwann cell internode; S_i, intercalated Schwann cell internode; O, one or more oligodendrocyte internodes.

From Rossiter and Fraher (1990)

TABLE 2

NODE DENSITY

a

MEAN NODE DENSITY (±S.E.M.) AT THE TRANSITIONAL ZONES (TZ), IN THE INTRAMEDULLARY BUNDLES (IMB) AND VENTRAL ROOTS (VR)

Ratios between densities and overall mean values (± s.e.m.) are also given.

Node density (± s.e.m.) (nodes/$10^5 \mu m^3$)			Ratios	
TZ*	IMB*	VR+	TZ/IMB	TZ/VR
13.8 ± 1.5	6.6 ± 0.8	2.0 ± 0.2	2.3	7.8

* Mean of 25 values
\+ Mean of 36 values

b

DENSITY IN THE TRANSITIONAL ZONE (TZ) (D_{tz}) AND IN THE CENTRAL TISSUE PROJECTION (CTP) (D_{ctp}).

Representative values for small (S; 15 fibres or fewer), medium (M; 16-30 fibres) and large (L; more than 30 fibres) rootlets.

Rootlet type	Mean No. of fibres	D_{tz} (nodes/$10^5 \mu m^3$)	D_{ctp} (nodes/$10^5 \mu m^3$)
S	12	22.4	36.4
M	21	10.3	17.6
L	42	10.2	18.6

c

MEAN (±s.d.) OVERALL VALUES FOR PROXIMAL, MIDDLE AND DISTAL THIRDS OF THE TZ.

Rootlet segment	D_{tz} (nodes/$10^5 \mu m^3$)	D_{ctp} (nodes/$10^5 \mu m^3$)
proximal third	11.2 (± 8.1)	13.2 (± 10.1)
middle third	14.0 (± 7.3)	26.3 (± 15.9)
distal third	15.8 (± 13.1)	72.5 (± 36.7)

From Bristol and Fraher (1989)

TABLE 3

NEAREST NEIGHBOUR DISTANCES

a

Nearest neighbour distances for L5 transitional nodes, based on 439 values for large and 300 for small fibres. Overall mean values (± s.e.m.) for proximal, middle and distal thirds of the TZ and for the TZ as a whole.

Nearest neighbour distance (μm)			
proximal third	middle third	distal third	whole TZ
18.1 (± 3.5)	12.2 (± 1.3)	11.9 (± 1.2)	12.8 (± 0.4)

b

Numbers and percentages of small-small, large-large and small-large nearest neighbour pairs, for all nodes, regardless of nearest neighbour distance (NND), and for nodes with NNDs of less than 10 μm.

Nearest neighbour pairing	All nodes		nodes with NND < 10 μm	
	no.	%	no.	%
small - small	145	19.6*	89	28.6**
large - large	251	34.0*	81	18.5+
small-large	343	46.4*	141	45.3

* percentage of all nodes (n = 739)
** percentage of all small nodes (n = 300)
\+ percentage of all large nodes (n = 439)

From Bristol & Fraher (1989).

TABLE 4

Rootlets	Mean Transitional Zone Length
Oculomotor nerve	50 μm
Trochlear nerve	296 μm
Trigeminal nerve	335 μm (CTP length 880 μm)
Abducent nerve	25 μm
Facial nerve	520 μm (CTP length 610 μm)
Cochlear nerve	565 μm (CTP length 1530 μm)
Vagus nerve	300 - 700 μm (CTP length 150 μm)
C2 ventral	44 μm
C7 ventral	32 μm
Upper thoracic ventral	240 μm
L4 ventral	160 μm
L5 ventral	70 μm
C7 dorsal	427 μm

TABLE 5. DATA FOR CAPILLARIES AND POSTCAPILLARY VENULES (PCVs) RELATED TO L5 VENTRAL ROOTLETS AT THE AGES INDICATED

		Capillaries				PCV	
Age (days)	Rtlt CSA	no/rtlt	% length	dist (μm)	diam (μm)	no/rtlt	diam (μm)
20f	51.8	1.1	57	8.8	7.4	0.4	10.9
1	100.4	1.1	41	11.5	8.1	0.7	11.6
3	150.5	0.9	63	16.6	7.5	0.3	15.7
6	334.9	1.1	51	13.5	8.4	0.4	17.6
12	542.0	1.2	48	17.8	7.4	0.5	16.9
20	618.8	1.5	92	23.7	7.6	0.2	13.4
300	2372.6	1.4	96	39.5	8.5	0.5	30.0

20f: 20 days fetal
Rtlt CSA: rootlet cross sectional area
No/rtlt: mean number per rootlet
%length: mean percentage of rootlet length related to capillaries
dist: mean distance from capillary to rootlet centre
diam: mean capillary diameter (μm)

From Kaar and Fraher (1987)

TABLE 6. STEREOLOGICALLY DERIVED DATA QUANTIFYING DEVELOPMENTAL CHANGES IN THE TISSUE COMPONENTS OF THE C7 VENTRAL ROOTLET TRANSITIONAL ZONE DURING ITS PERIOD OF MOST RAPID MATURATION

Level	Age (days)	Interstitium	Astrocyte	Oligodendrocyte	Schwann cell	Myelin*		Axon
						sc	ol	
Outer third	1	15.4	18.7	0	42.2	1.0	-	15.6
	4	14.1	38.0	5.8	7.3	1.2	1.0	24.6
	12	18.2	29.0	6.5	10.0	7.1	2.9	23.0
Middle third	1	4.3	43.5	7.8	0.01	-	0.2	35.8
	4	7.0	40.8	11.2	0.1	0.1	2.6	33.3
	12	8.1	40.5	6.2	4.6	5.1	3.3	27.3
Inner third	1	4.6	33.8	12.0	0.0	-	0.2	43.9
	4	5.4	47.9	7.1	0.0	-	2.5	34.2
	12	8.7	46.1	6.1	3.7	3.5	5.0	23.1

* sc: Schwann cell myelin; ol: oligodendrocyte myelin

From Fraher and Kaar (1982).

TABLE 7. GROWTH RATES OF C7 DORSAL ROOTLET CROSS SECTIONAL AREA (CSA) AND CENTRAL TISSUE PROJECTION (CTP) LENGTH

	CSA ($\mu m^2/100$)		CTP length (μm)	
Age (Days)	Mean CSA (±s.d.)	Δ/day	Mean Length (± s.d.)	Δ/day
6	93(±34)		126(±34)	
		7.2		17
12	136(±81)		200(±90)	
		2.3		-6
20	154(±133)		181(±103)	
		4.3		2.5
70	367(±173)		308(±132)	
		0.3		0.5
300	444(±97)		427(±77)	

CSA: mean rootlet cross sectional area (expressed as $\mu^2/100$)

mean CSA: mean rootlet CSA at the specified age;
Δ/day: daily increase in CSA over interval;
mean length: mean CTP length at the specified age;
Δ/day:daily increase in length over the interval.

From Fraher & Sheehan (1987).

TABLE 8. GROWTH RATES OF CENTRAL TISSUE PROJECTION (CTP) AND TRANSITIONAL ZONE (TZ) LENGTH IN COCHLEAR NERVE

	CTP		TZ	
Age	Length (μm)	Δ/day	Length (μm)	Δ/day
Newborn	125		125	
		140		20
2	405		165	
		103		150
4	610		465	
		12		-21
13	720		275	
		6.3		3.4
72	1090		475	
		2.0		1.4
171	1290		615	
		1.2		-0.3
371	1530		565	

Length: mean length at the age indicated;
Δ/day: daily increase over the interval.
From Fraher & Delanty (1987).

FIGURES

Fig. 1 (a,b) Diagrammatic view of the ventral cord surface showing the general arrangement at (a) cervical and (b) lumbar spinal levels of ventral rootlets (r), aggregated rootlet bundles (ARB) and dorsal (DR) and ventral (VR) roots.

(c-e) Diagrammatic longitudinal section of a rootlet passing between the CNS and PNS showing (c) its intramedullary (I), emergent (E, dots) and free (F) segments; (d) the transitional zone (TZ) and central tissue projection (CTP); and (e) a myelinated fibre possessing myelin sheaths produced by a transitional oligodendrocyte (TO) centrally and by a transitional Schwann cell (TSC) peripherally, with the transitional node intervening at the CNS-PNS interface (arrowheads).
CNS tissue: shaded.

a: From Bristol & Fraher (1989).

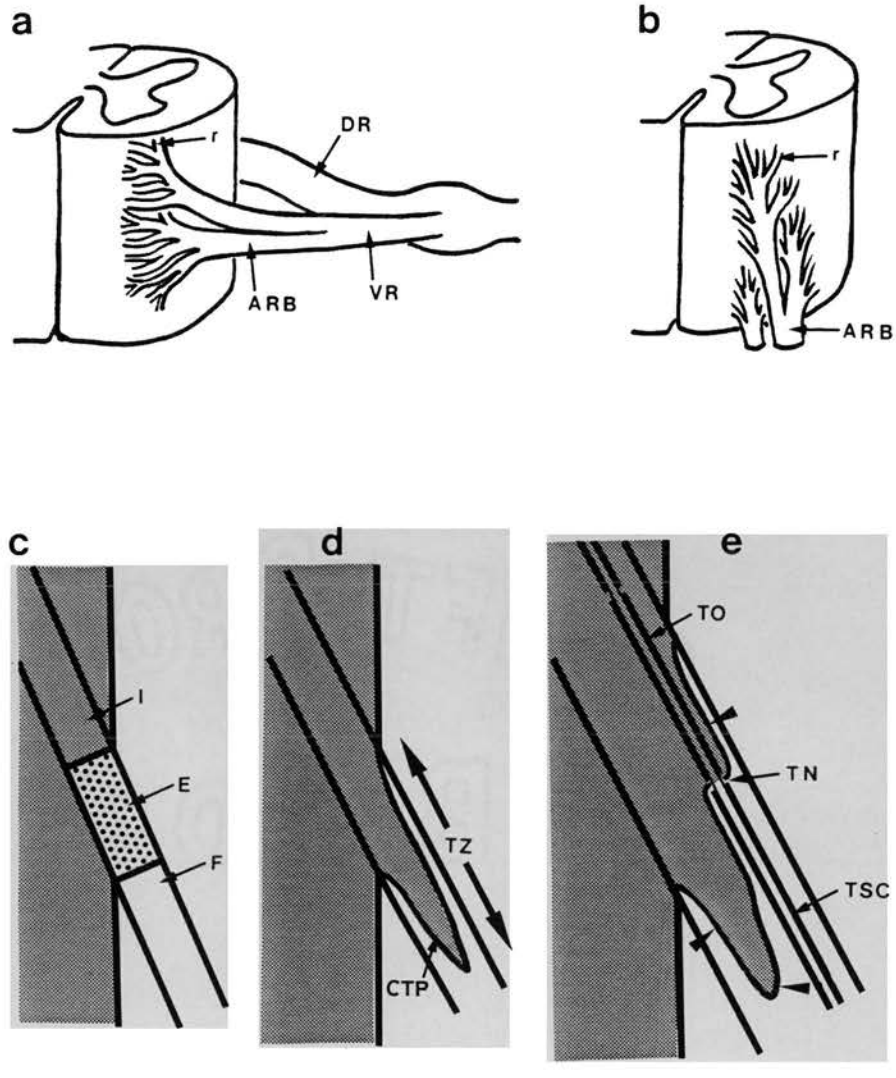

FIG. 1

Fig. 2 Diagrammatic sections longitudinal to rootlets and at right angles to the CNS surface, showing the eight principal types of transitional zone and a glial island. (See Section 3.1).

TYPES OF TRANSITIONAL ZONE

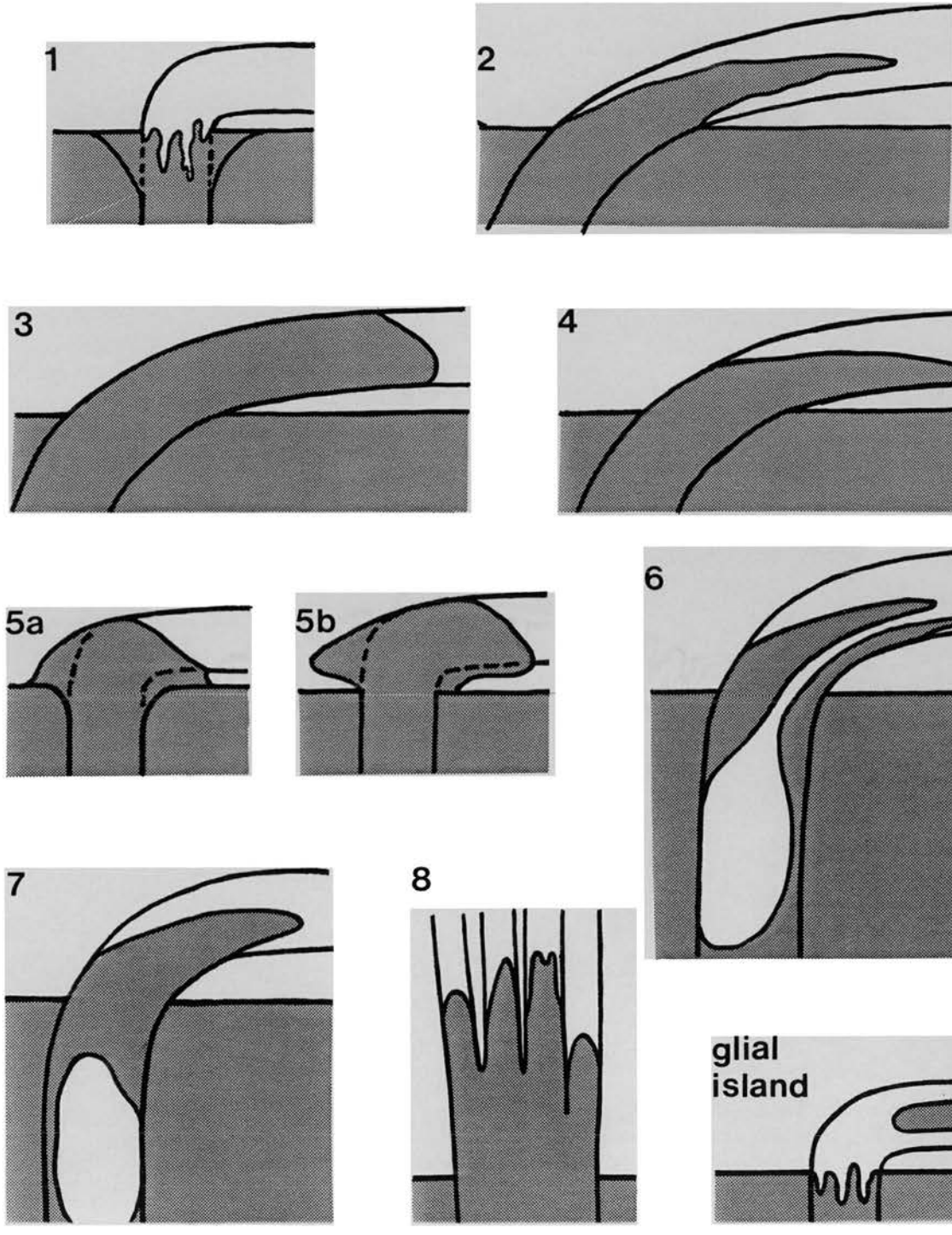

FIG. 2

Fig. 3 (a-d) Light micrographs of sections at right angles to the CNS surface through rootlets possessing type 1 transitional zones.

(a) Abducent rootlet emerging from the brainstem through a circumscribed pad of thickened glia limitans. Transitional node arrowed.

(b) Small abducent rootlet showing a fibre with a transitional node (arrowed) deep to the CNS surface.

(c,d) Semiserial sections through a spinal accessory transitional zone showing a rootlet traversing a thick astrocytic pad (c, asterisk) within which the transitional nodes are located (d).

(e) Light micrograph of a longitudinal section through the type 2 transitional zone of a C7 dorsal rootlet. The central tissue projection (outlined) contains pale astrocytic perikarya.

(f-h) Light micrographs of serial transverse sections through the type 3 transitional zone of an oculomotor rootlet at (f) emergent and (g,h) free levels. The rootlet consists entirely of CNS tissue at the levels shown and is surrounded by a thick astrocytic sleeve.

Scale bars: 20μm.
a,b: From Fraher et al. (1988c); c,d: from Nugent et al. (1991); e: From Fraher & Sheehan (1987); f-h: from Fraher et al. (1988b).

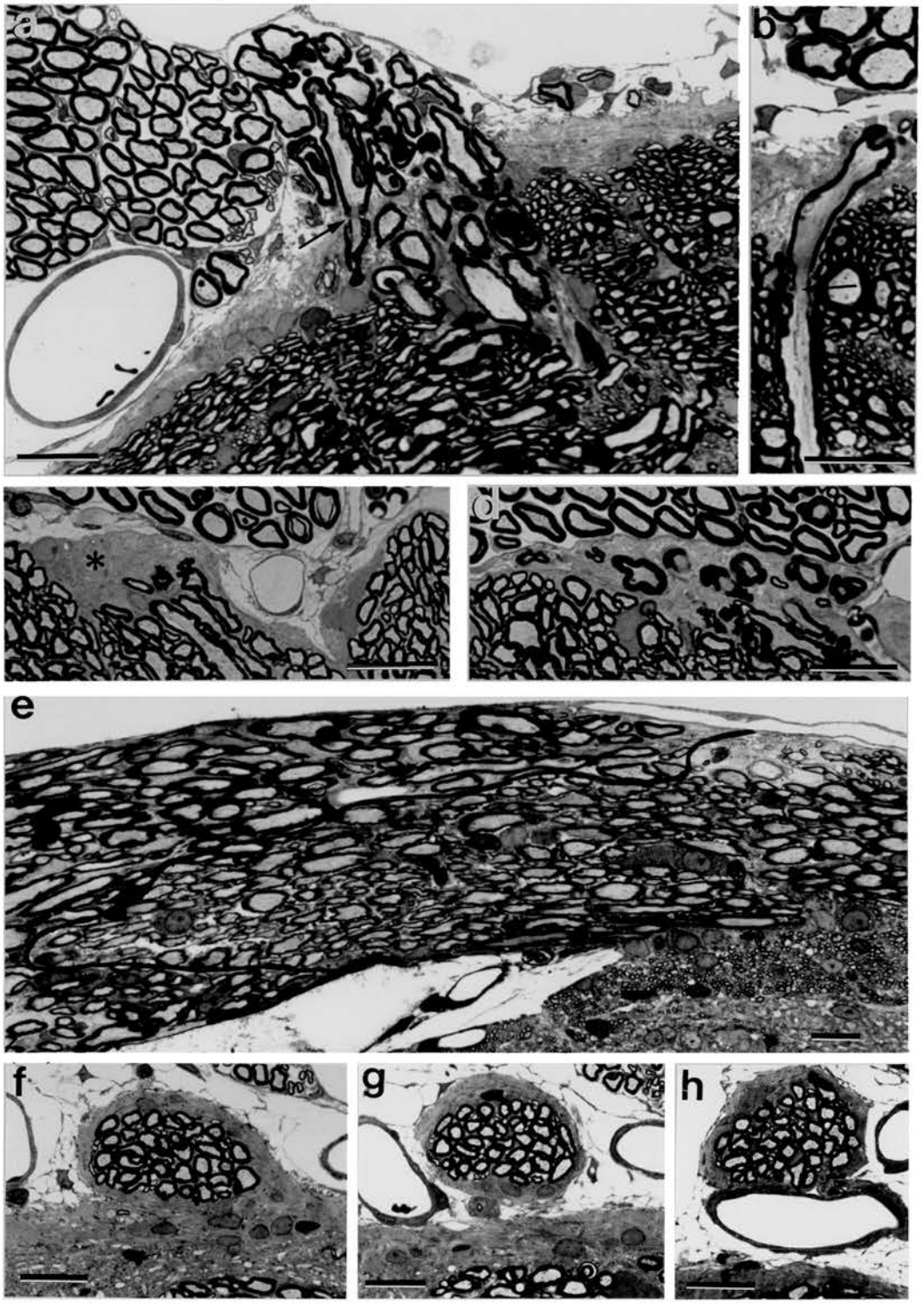

FIG. 3

Fig. 4 (a-d) Longitudinal (a) and semiserial transverse (b-d) sections through type 4 transitional zones in oculomotor rootlets. The central tissue projection is outlined in (a). The projection coincides with the dorsal and collateral surfaces of the rootlet (c). Peripheral tissue extends centrally on the superficial aspect of the proximal part of the emergent segment (b, arrowhead).

(e) Longitudinal section through the type 5a transitional zone of an oculomotor rootlet which emerges through a wedge-shaped thickening of the glia limitans.

(f-h) Semiserial light micrographs of a (pale) transversely sectioned dorsolateral vagal rootlet, (f) emerging through the brainstem surface and (g,h) at progressively deeper levels within the inferior cerebellar peduncle.
Brainstem surface: arrowheads.

Scale bars: 30μm.
a-e: from Fraher et al. (1988b); f,h: from Rossiter & Fraher, (1990); g: from Fraher & Rossiter (1991).

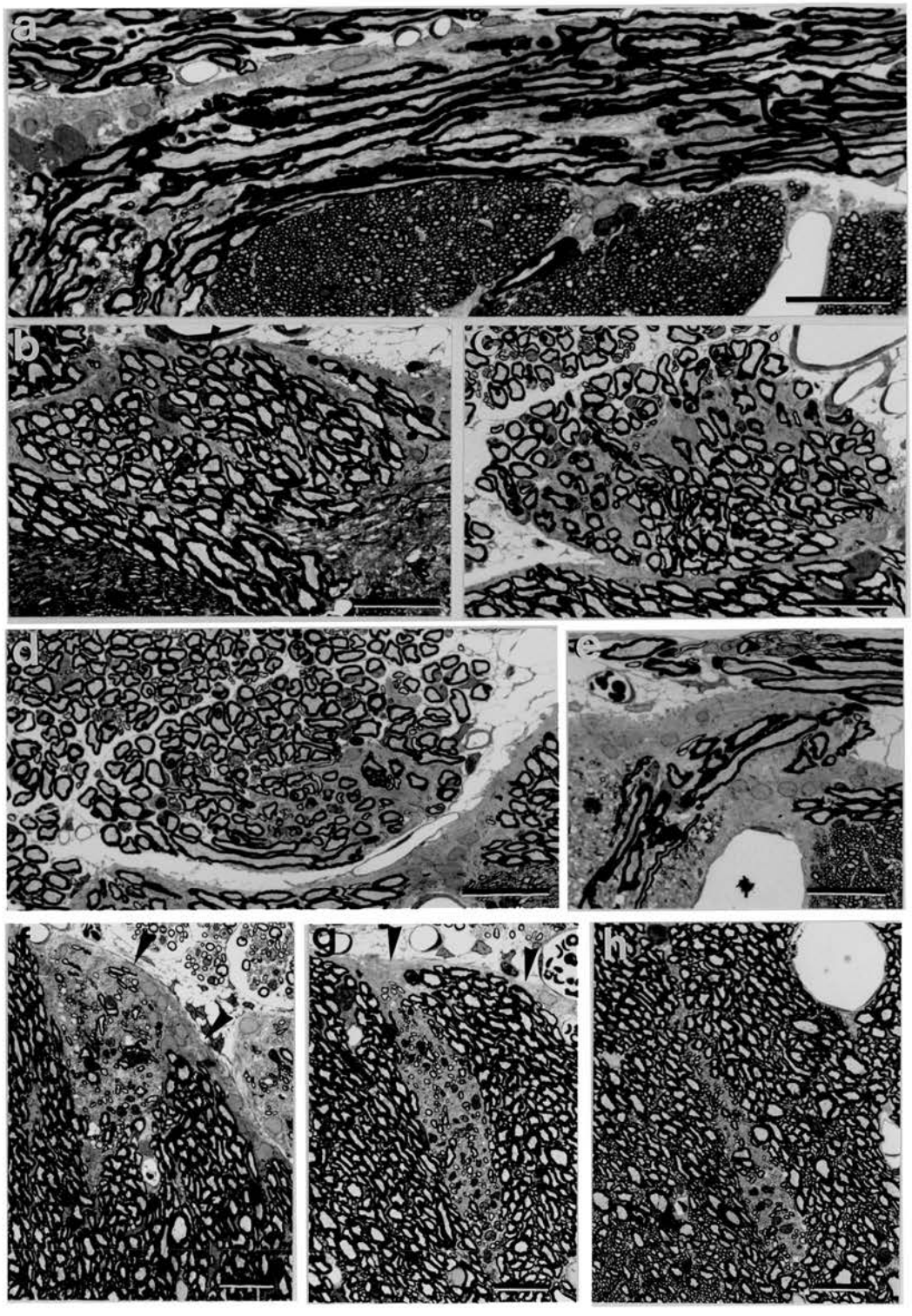

FIG. 4

Fig. 5 Diagrams showing the relationship of astrocytic tissue to myelinated fibres in a type 1 transitional zone in planes longitudinal (ls) and transverse (ts) to the rootlet as shown in (a). The central end of each transitional Schwann cell myelin sheath (S) is invaginated below the plane of the CNS surface (b). Each invagination is walled by astrocyte processes or perikarya, arranged like a honeycomb (c). The basal lamina covering the Schwann cell is continuous with that lying on the astrocyte processes lining the invaginations at the level of the transitional node (N), central to which the myelin sheath is formed by a transitional oligodendrocyte (O). A fringe of slender glial processes (F) projects distally for a short distance beyond the plane of the surrounding CNS surface.
Astrocytic tissue: shaded.
Myelin: black.
Basal lamina: dashed lines.

Fig. 6 (a) Transverse section through a glial fringe element consisting of three astrocyte processes contained within the same basal lamina.

(b) Transverse section through a developing transitional zone, containing both myelinated and nonmyelinated axons, surrounded by astrocyte perikarya (asterisks).

(c-e) Astrocytes in central tissue projection.
(c) Large, transversely orientated primary process stemming from an astrocyte perikaryon at the surface of the projection.

(d-e) Transversely orientated flattened process stemming from a perikaryon within the projection, reaching the projection surface, where (e) it bifurcates.

Scale bars: a,c: 1μm; b,d,e: 5μm.
a,b: from Fraher (1978a); a,b: from Fraher (1978a).

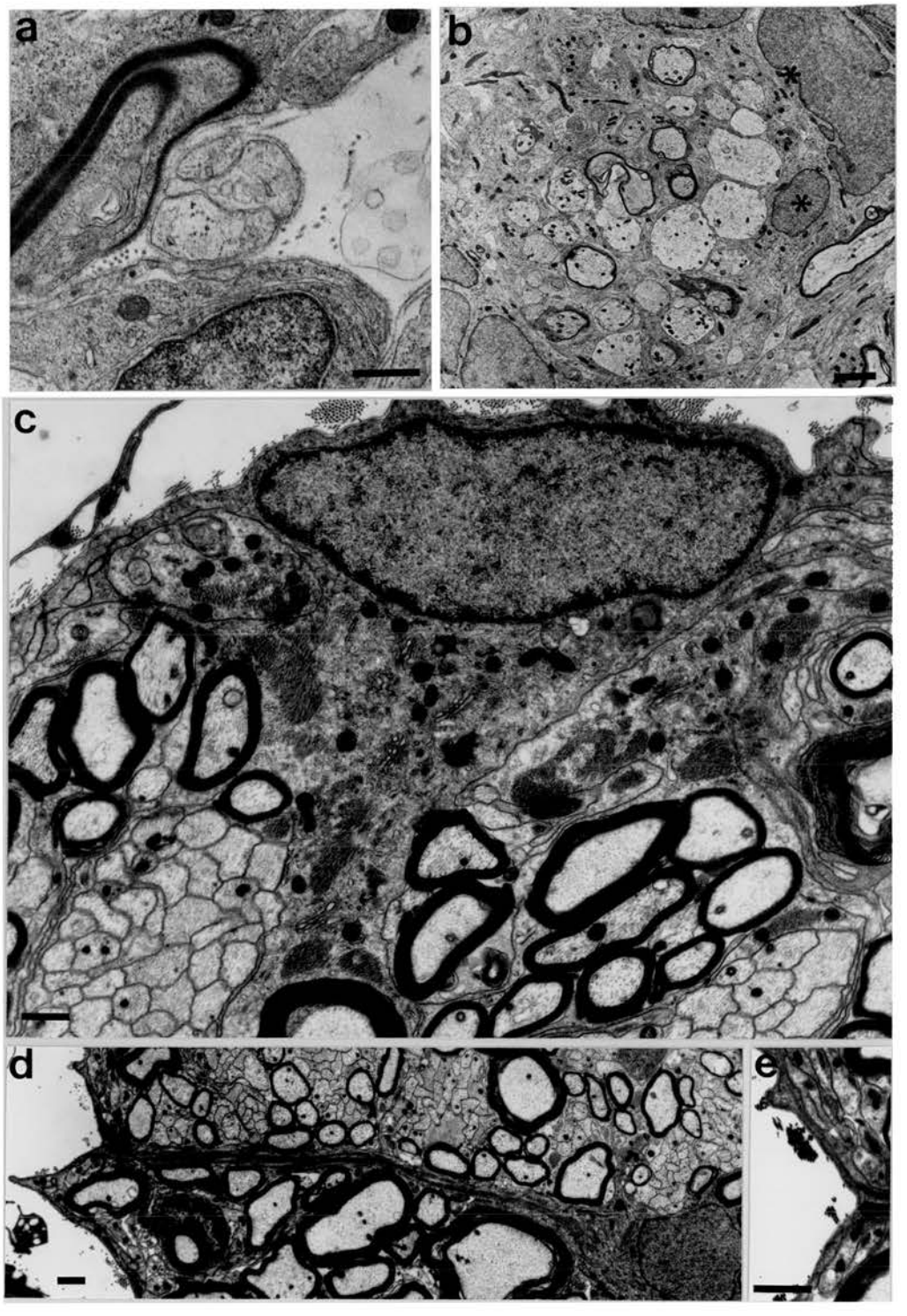

FIG. 6

Fig. 7 (a,b) Schematic diagrams illustrating arrangement of cytoplasmic processes arising from astrocyte perikarya.

(a) A transversely orientated cylindrical primary process (1) gives rise to fine longitudinally running processes (2) and terminates in a laminar end-foot (3).

(b) A large transversely orientated laminar primary process (4) gives rise to a longitudinally orientated secondary process (5). A longitudinally orientated primary process (6) arises from one end of the perikaryon. Laminar processes (7) arise from primary and secondary processes and from the perikaryon.

From Rossiter & Fraher, 1990.

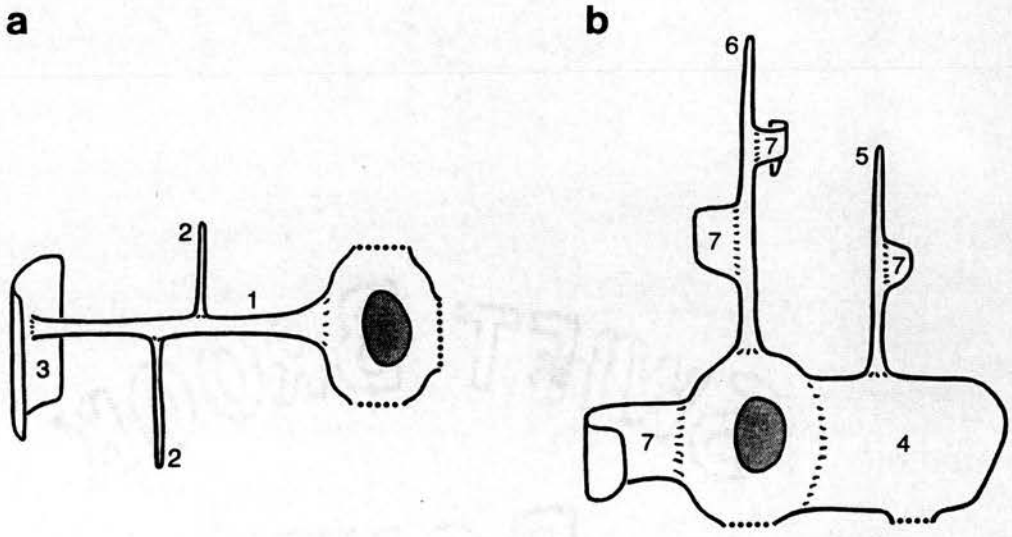

FIG. 7

Fig. 8 Astrocytic tissue in the CTP and PTI.

(a,b) Electronmicrographs showing differing arrangements of astrocytic processes forming the CTP surface. arrows: desmosomes; arrowheads: gap junctions.

(c) Glia limitans of brainstem consisting of two or three simply arranged layers of processes.

(d) A transversely sectioned peripheral tissue insertion showing astrocyte proceses forming an open network.

(e) Astrocytic processes forming a partition within a peripheral tissue insertion.

(f) Showing a deficiency in the astrocytic boundary of a peripheral tissue insertion. An unmyelinated axon enveloped by an intercalated Schwann cell (above) is separated from an oligodendrocytic myelin sheath (below) only by basal lamina (arrowhead).

Scale bars: a-e: 1 μm; f: 0.1 μm.

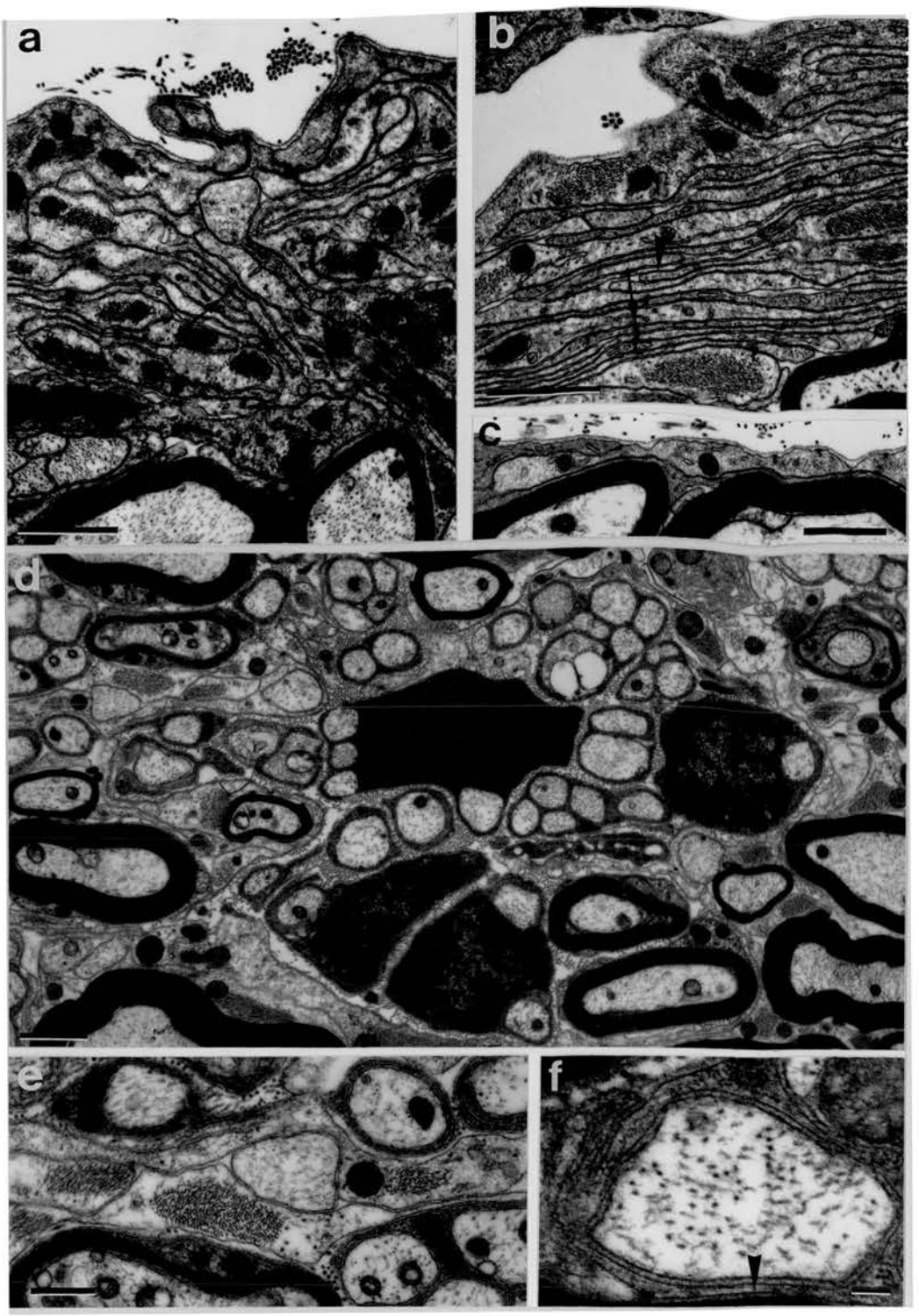

FIG. 8

Fig. 9 (a) Diagram of a dorsolateral vagal rootlet showing the planes of transverse sections (b,c) through its central tissue projection (small arrowheads) and peripheral tissue insertion (large arrowheads), respectively

(b) Transverse section through central tissue projection, showing bundles of PNS tissue, consisting of myelinated (arrow) or nonmyelinated fibres (asterisk) or both, traversing the central tissue projection in tunnels or in grooves (arrowheads) on its surface.

(c) Transverse section through peripheral tissue insertion surrounded by CNS tissue and bounded by an astrocytic limiting membrane (outlined), from which incomplete partitions extend inwards partly subdividing the insertion. The insertion is irregular in outline and may be traversed by finger-or bridge-like projections (double arrow) or long invaginations of CNS tissue (double arrowhead). The limiting membrane may be deficient in places (arrow), where an unmyelinated axon bundle is shown in close apposition to a fibre myelinated by an oligodendrocyte. A group of myelinated fibres and an unmyelinated fibre bundle are shown in one of the partial subdivisions of the insertion.

CNS tissue: shaded; individual astrocyte profiles not shown; PNS tissue: unshaded.

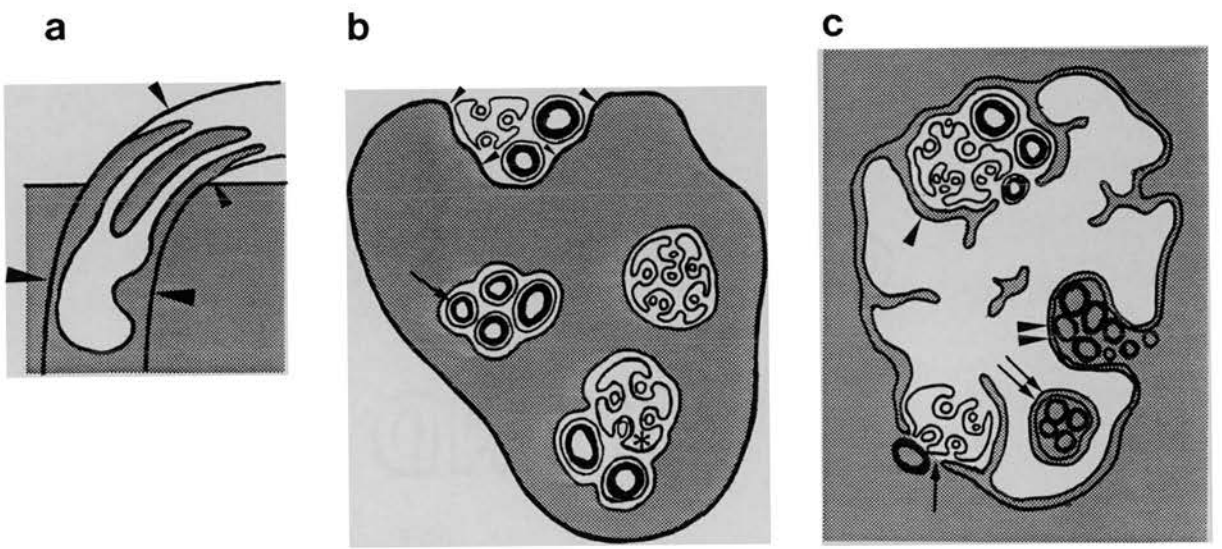

FIG. 9

Fig. 10 Electronmicrographs showing relationships of transitional Schwann cell internodes to the astrocytic tissue of the transitional zone.

(a,b) Transversly sectioned myelinated fibres lying (a) in an invagination (arrowheads) lined by basal lamina and containing collagen fibrils, and (b) in a groove on the surface of a central tissue projection.

(c) Longitudinal section through a transitional internode, transitional node and part of an oligodendrocytic paranode.

(d) Transverse section through the transitional internode of a small myelinated fibre which shares a deep groove on the CTP surface (arrowheads) with a group of unmyelinated axons which are enveloped and isolated from each other by a matrix of branching processes arising from a Schwann cell perikaryon.

(e) Transverse section through astrocyte processes (asterisks) which form basal lamina-covered complexes with Schwann cell-enveloped unmyelinated axons and which are closely related to transitional internodes of small myelinated fibres at a level distal to the CTP.

Scale bars: 1 μm.
b: from Fraher & Sheehan (1987); c-e: from Rossiter & Fraher (1990).

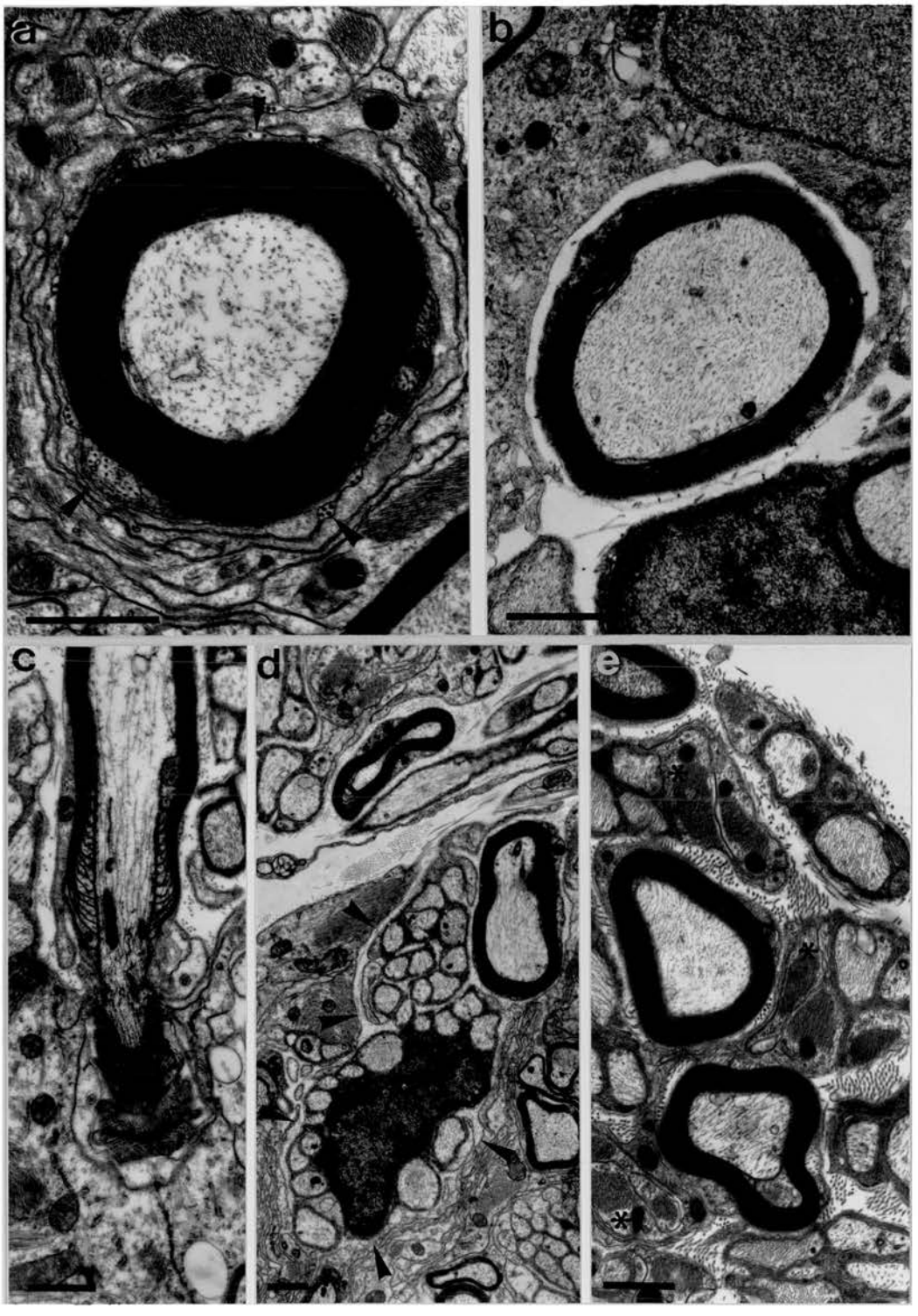

FIG. 10

Fig. 11 Scanning electron micrographs of experimentally avulsed cervical ventral rootlets showing the honeycomb-like arrangement of astrocytic tissue at the transitional zone.

(a) Ventral cord surface showing normal arrangement of root components (right) and avulsion site (left).

(b) A number of rootlets have been avulsed; the surrounding pia mater (asterisks) is intact.

(c) A wedge-shaped central tissue projection of a type 5 rootlet, showing the honeycomb with the torn ends of an axon (arrow) and of a myelinated fibre (double arrow) protruding into the depths of one space.

(d) Honeycomb spaces showing circumferentially ridged walls (arrowheads) and portions of an axon torn at the transitional node (arrow) protruding into the depths of one space.

(e) The locus of a single avulsed rootlet showing a ruptured axon (arrow) projecting into the honeycomb.

Scale bars: a,b: 200 μm; c,d: 10 μm; e: 20 μm.
b,e: from Bristol & Fraher (1989).

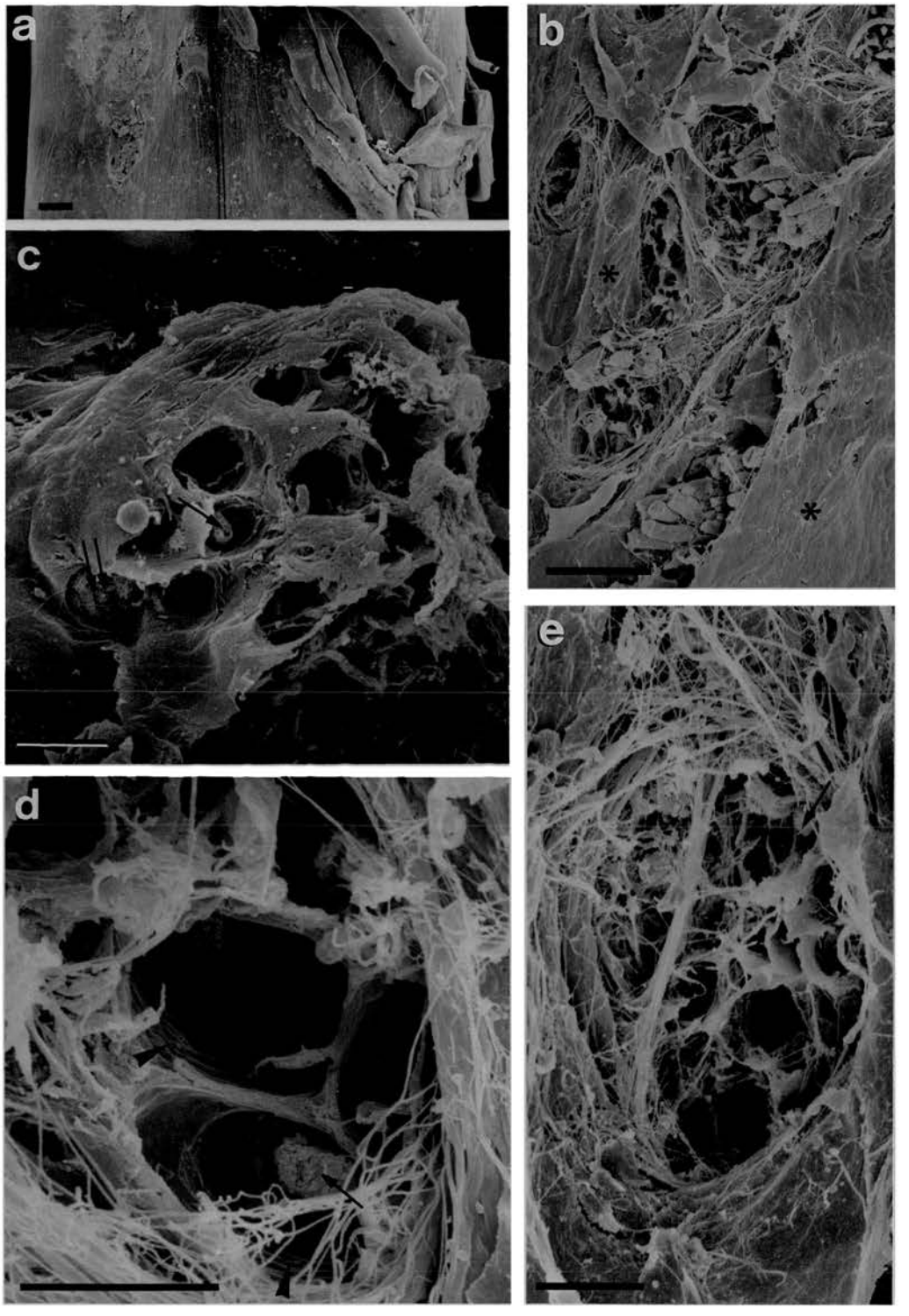

FIG. 11

Fig. 12 Diagrams showing the relationship of astrocytic tissue to myelinated fibres in a type 2 transitional zone in planes longitudinal (ls) and transverse (ts) to the rootlet, as shown in (a). The central end of each transitional Schwann cell myelin sheath (S) lies in a groove on the surface of the central tissue projection, the wall of which is formed by astrocyte processes. The basal lamina covering the Schwann cell is continuous with that of the astrocyte processes forming the groove at the transitional node (N), central to which the myelin sheath is formed by a transitional oligodendrocyte (O).
Astrocytic tissue: shaded.
Myelin: black.
Basal lamina: dashed lines.

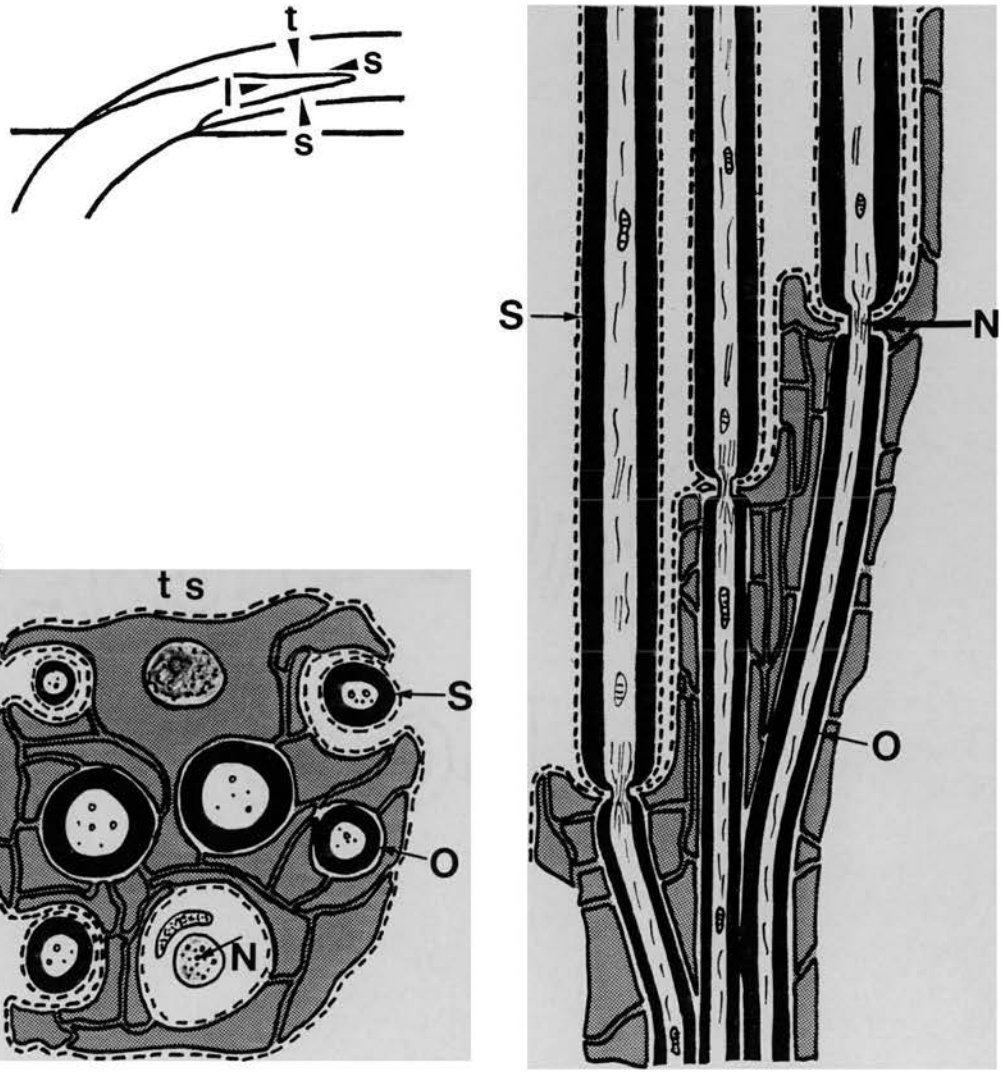

FIG. 12

Fig. 13 Diagrammatic longitudinal sections through the central-peripheral transition of:

(a) a single large unmyelinated fibre, along which an astrocytic collar extends superficial to the plane of the CNS surface (arrowheads) to contact the central end of the transitional Schwann cell;
(b) an unmyelinated axon bundle, the Schwann process enveloping which extend deep to the plane of the surrounding CNS surface (arrowheads) (See Text).

Schwann processes: black.
Astrocyte processes: shaded.
Basal lamina: dashed lines.

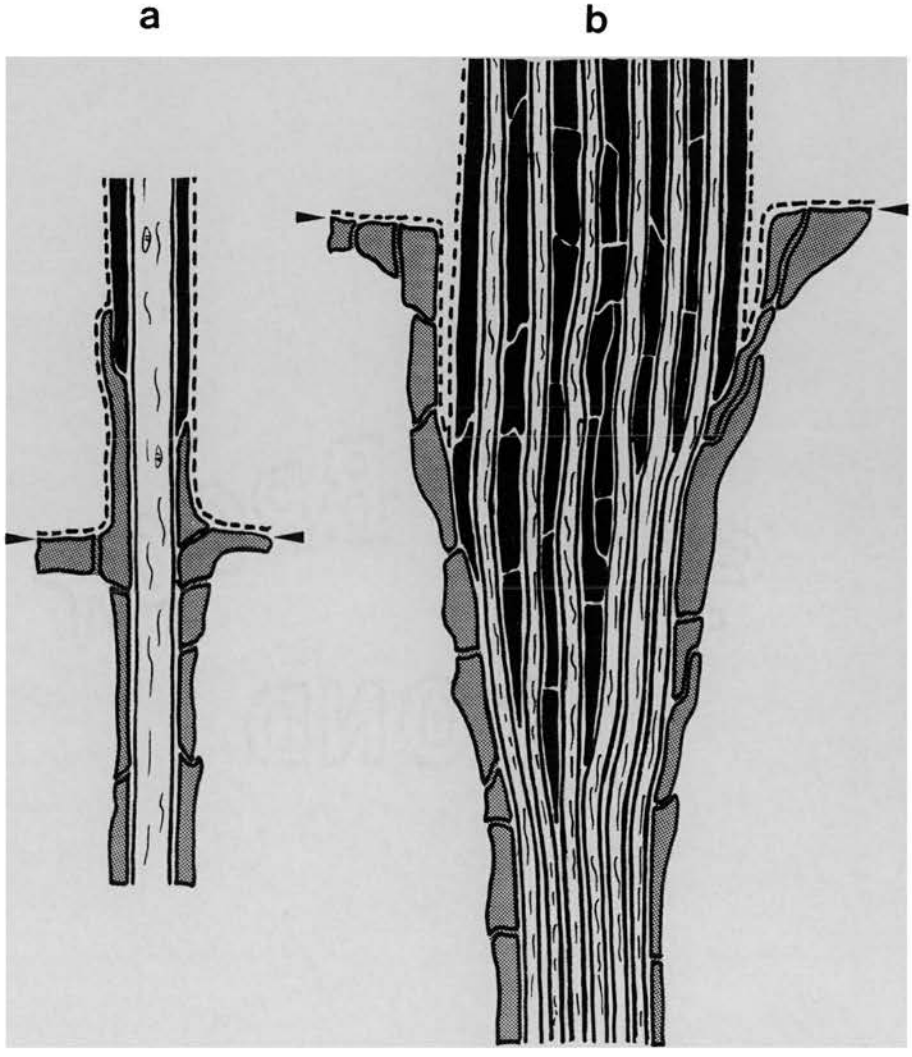

FIG. 13

Fig. 14 Electron micrographs of transversely sectioned unmyelinated fibres at the CNS-PNS transtional zone.

(a) A large unmyelinated fibre enveloped by a pale astrocytic sleeve distal to the plane of the CNS surface (see Fig. 13a).

(b) A large unmyelinated fibre distal to the plane of the CNS surface, enveloped by a sleeve consisting of pale astrocyte processes and the closely apposed central end of a transitional Schwann cell (arrowheads).

(c-f) Electron micrographs of a transversely sectioned unmyelinated axon bundle at progressively more central levels.

(c) Superficially, the cleft between astrocytic tissue and Schwann cell processes is bounded by basal lamina and contains collagen fibrils.

(d) More deeply, axons are still segregated by Schwann cell processes (arrows), but these are directly apposed to astrocytic processes (arrowheads).

(e) Schwann processes terminate first towards the bundle's surface and superficial axons (asterisks) are directly apposed to one another and to the surrounding astrocytic tissue.

(f) Schwann cell processes (arrows) lying towards the middle of the bundle extend furthest centrally.

Scale bars: 1 μm.
a,b: from Fraher (1978a); c,e,f: from Rossiter & Fraher (1990).

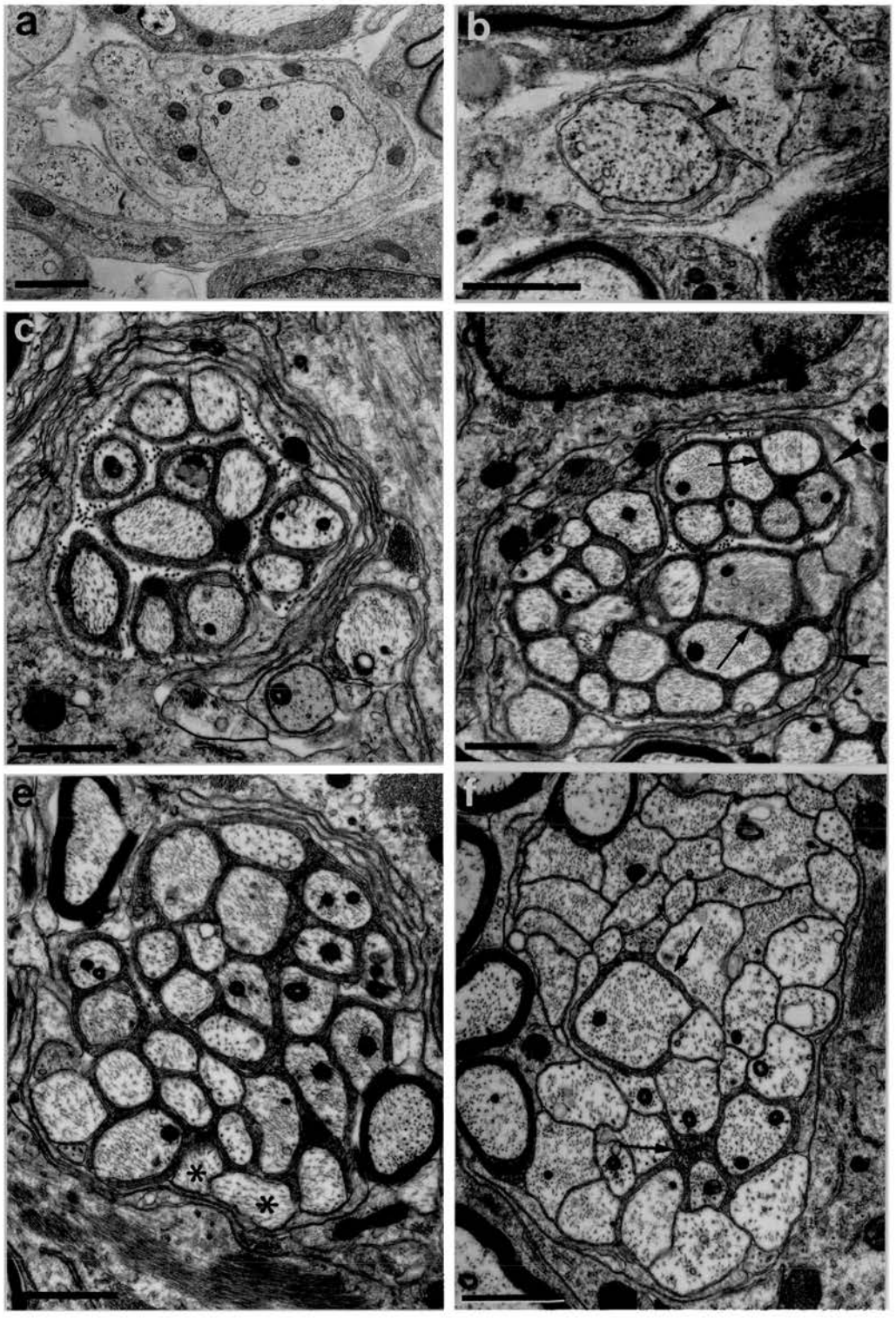

FIG. 14

Fig. 15 Diagrams showing examples of sections through the transitional zones of a number of spinal and cranial nerves in the planes indicated in (a), showing their essential structure.

(a) View of ventral aspect of brainstem and upper cervical spinal cord. Lines indicate planes of section of each nerve, identified according to the labels below.

(b-d) C2 ventral rootlet. Sections transverse to the plane of the spinal cord showing (b) emergent rootlet running caudally in an extension of the glia limitans; (c) running through a pedunculated central tissue projection which is closely apposed to a blood vessel (asterisk); and (d) two rootlets emerging through two fused projections which are separated from the underlying cord by a space (arrowed) containing pia mater.

(e) Lower cervical dorsal rootlet longitudinally sectioned as shown in the inset diagram, containing an irregular central tissue projection.

(f) Upper thoracic rootlets joining to form an aggregated rootlet bundle (asterisk) and containing central tissue projections some of which fuse.

(g) Oculomotor rootlets, longitudinally sectioned, showing the wide variety of transitional zone types which they contain.

(h) Abducent rootlets, longitudinally sectioned showing a caudal type 5a zone (left) and type 1 zones in intermediate and rostral (right) rootlets.

(i) Trigeminal sensory root, containing a type 3 zone with a smooth, convex distal surface.

(j) Cochlear nerve, containing a type 3 zone, from which cochlear nerve branches (arrows) consisting of PNS tissue arise directly.

(k) Trochlear nerve, longitudinal sectioned, containing a type 2 zone as it emerges, running transversely, on the dorsal aspect of the brainstem.

(l-n) Vestibular nerve showing (l) the dorsal division of the ganglion (right; crosses, D) and the ventral tongue-shaped central tissue projection (left; shaded). Rootlets emerging from the dorsal division of the ganglion follow variable, sometimes highly irregular, courses before entering the CNS (below). (m,n) sections at right angles to (l) in planes indicated by large and small arrowheads, respectively, show branches emerging from the ventral division of the ganglion (crosses, V), following a regular path and entering the stepped surface of the tongue-shaped central tissue projection (shaded). Within this they turn sharply to run parallel to its long axis and enter the brainstem.

(o) Longitudinal section through the type 8 transitional zone of the facial nerve, giving rise to individual branches or fascicles each containing its own central tissue projection.

(p,q) Longitudinal sections showing examples of hypoglossal rootlets which bend sharply as they pass between the CNS and PNS, containing (p) type 1 and (q) type 3 transitional zones.

(r,s) Longitudinal sections through spinal accessory zones showing emergent rootlets (r) some of which run for a considerable distance in the thickened glia limitans (arrowhead) before becoming free and (s) others possess a type 5a transitional zone.

Central nervous tissue: shaded;
Peripheral nervous tissue: unshaded.

e: based on Fraher & Sheehan (1987); f: from Fraher et al., 1988b; g,j: from Fraher et al. 1988c; q,r: based on Nugent et al. (1991).

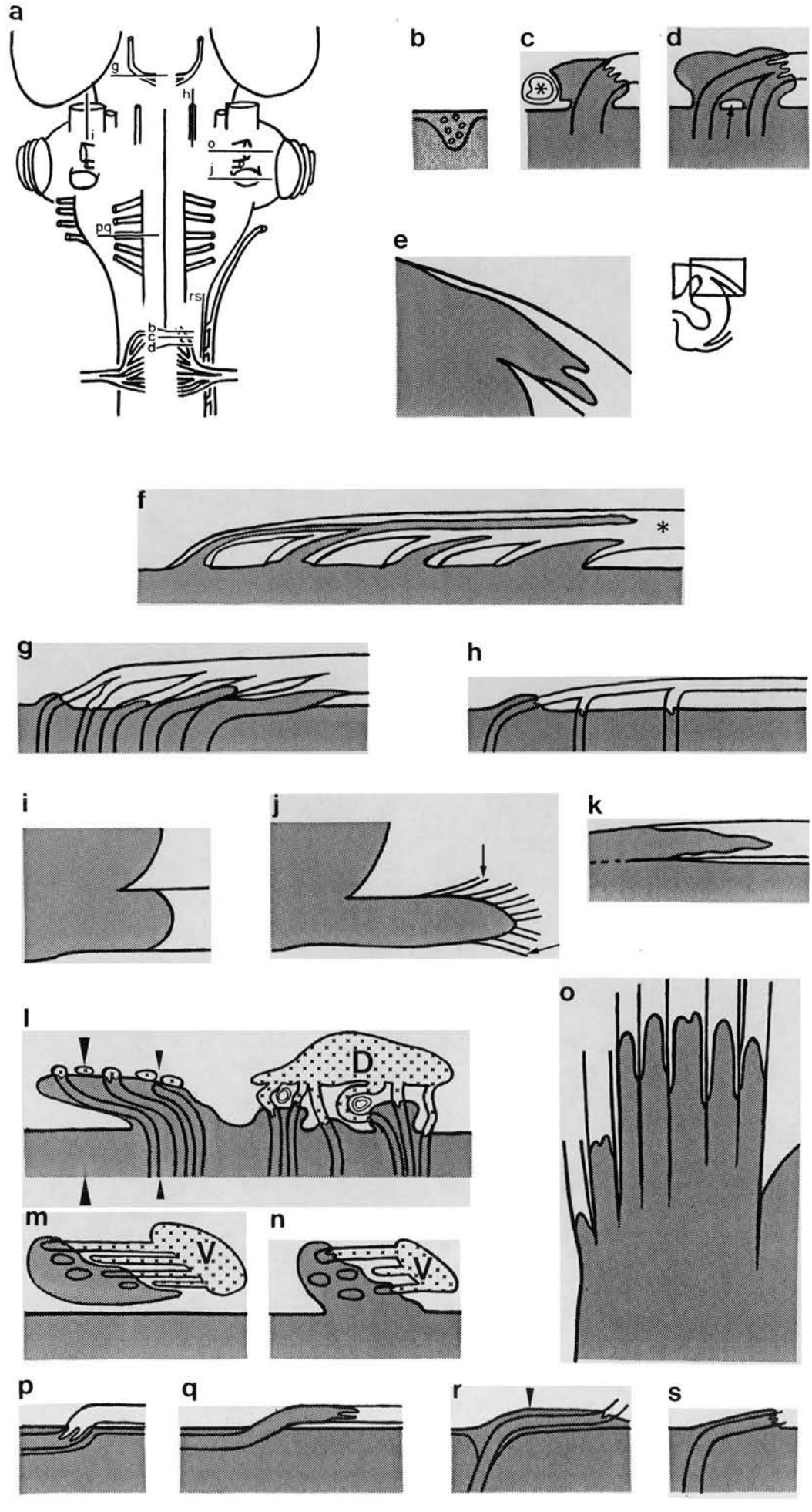

FIG. 15

Fig. 16 (a-c) Light micrographs of semiserial transverse sections at progressively more distal levels through a bundle (arrowed) of small, peripherally myelinated fibres in an upper thoracic ventral root (a) where all axons are unmyelinated within the central tissue projection, (b) where some are myelinated and (c) distal to the transitional zone where all are myelinated.

(d) The ventral division of the vestibular nerve (arrow) runs close to the cochlear nerve trunk which consists entirely of central nervous tissue over much of its length and contains numerous blood vessels (arrowheads).

(e) Enlargement of (a) showing cochlear branches consisting of (dark) peripheral nervous tissue arising directly from the (pale) central tissue projection. Occasional neuronal somata (arrowheads) lie in the projection.

Scale bars: a-c: 15μm; d: 200μm; e: 100μm.
d,e: from Fraher & Delanty, 1987.

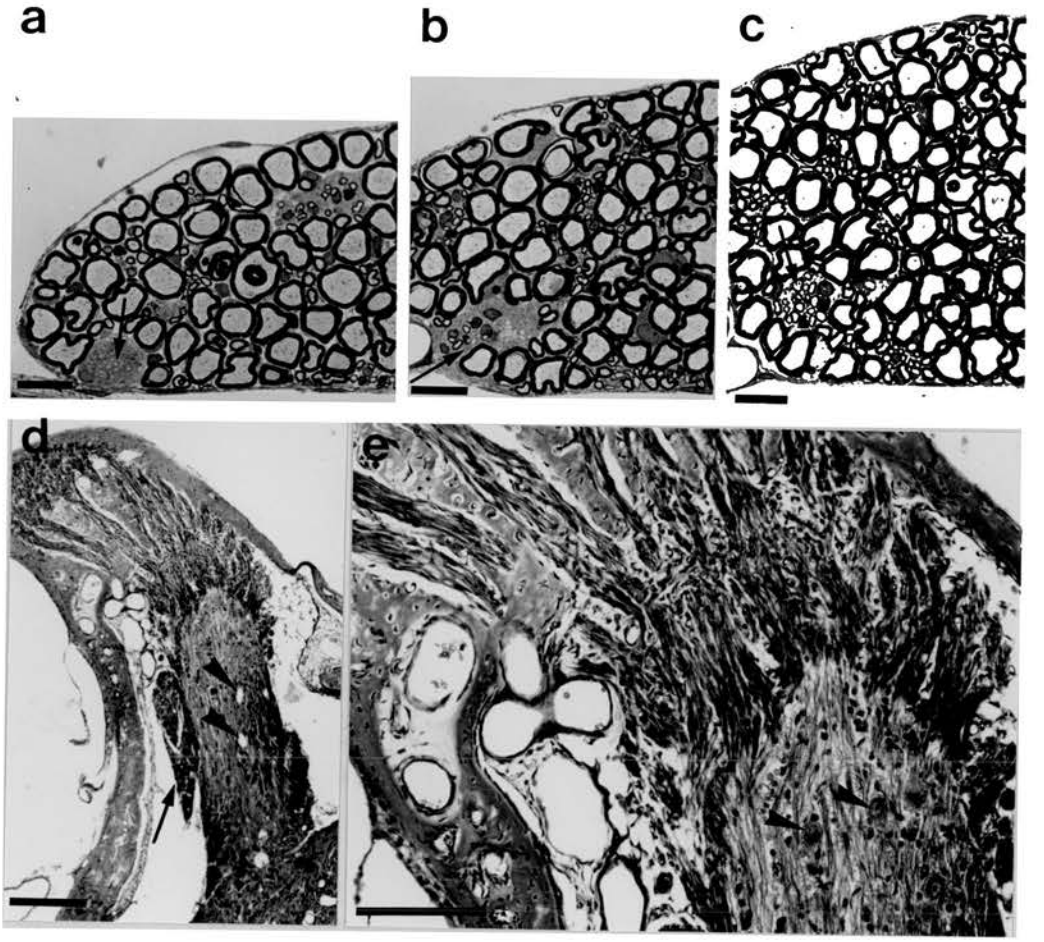

FIG. 16

Fig. 17 (a-i)

(a) Schematic transverse section through medulla oblongata, showing vagal rootlets emerging in dorsolateral, intermediate and ventrolateral positions. Three dorsolateral rootlets course through the spinal tract of the trigeminal nerve (V) and inferior cerebellar peduncle (P) and merge superficially to form an aggregated rootlet bundle (ARB).

(b) Schematic longitudinal section through a dorsolateral vagal rootlet and subjacent medulla oblongata (MO) showing the general form of the central tissue projection (CTP).

(c-f) Transverse sectional profiles through the rootlet at the levels shown in (b).

(g) Schematic longitudinal section through a vagal rootlet showing the general form of a peripheral tissue insertion (PTI) (asterisk) in its intramedullary segment.

(h,i) Transverse sectional profiles of the rootlet at the levels indicated in (g). Peripheral nervous tissue extends centrally in tunnels piercing the CTP and connects the PTI with the free rootlet distal to the CTP. An isolated island of peripheral tissue is apposed to the CTP (g,i, arrows). Ridge- and finger-like projections of central tissue extend into the PTI (g,h).

(j-l) Schematic longitudinal sections through dorsolateral vagal rootlets.

(j) Peripheral nervous tissue extends centrally into the PTI along a groove on the surface of the CTP (arrowheads).

(k) A peripheral tissue island (asterisk) lies deep to the brainstem surface within the intramedullary segment of the rootlet.

(l) Continuity of peripheral nervous tissue within the intramedullary segment of one rootlet (asterisk) with that superficial to the brainstem surface, is established only through a cross connection with the PTI of another rootlet (double asterisk).

CNS tissue: white; PNS tissue: shaded.

From: Rossiter & Fraher (1990).

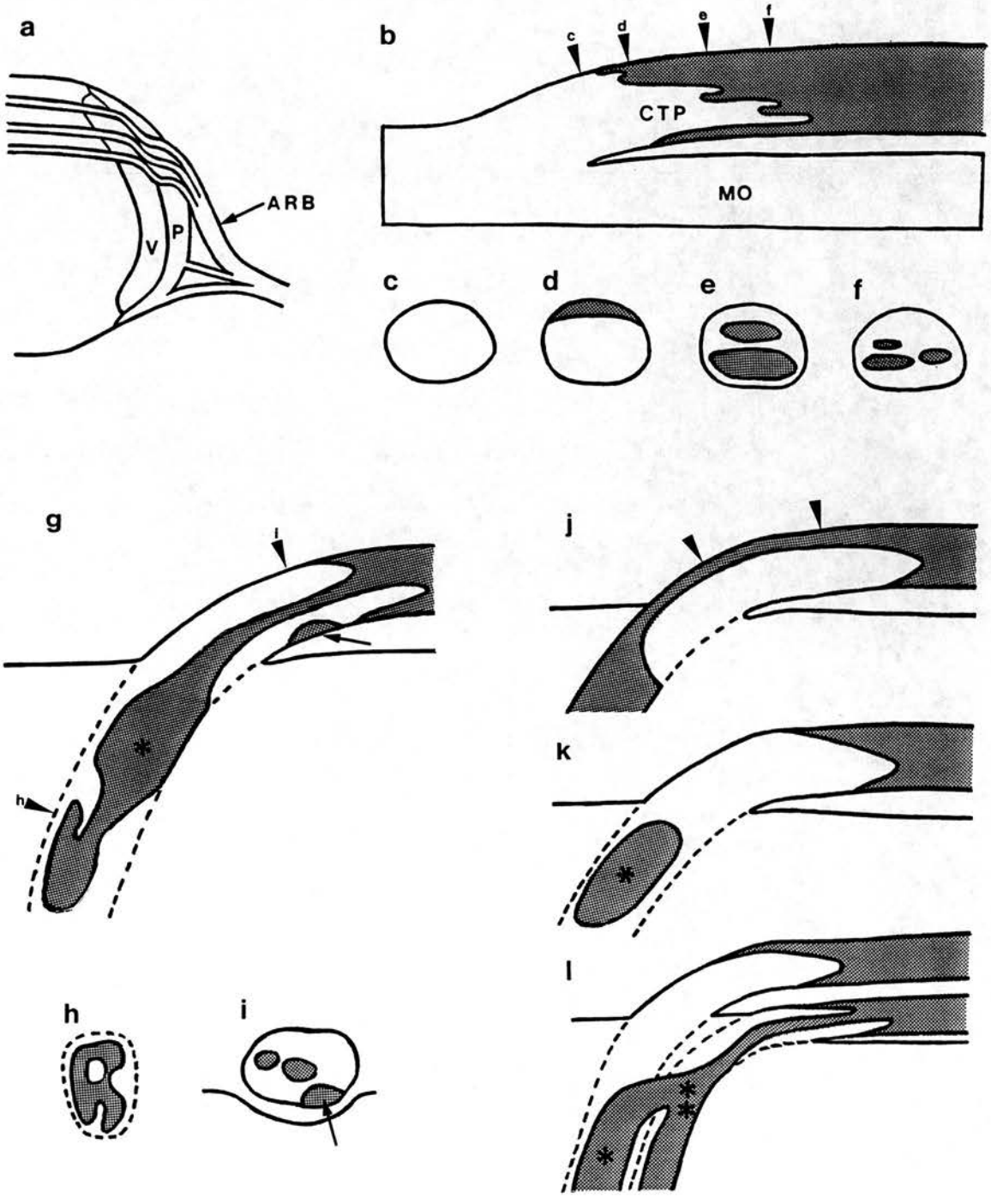

FIG. 17

Fig. 18 (a) Schematic longitudinal section through a dorsolateral vagal rootlet superficial to the brainstem surface (solid outline) and within the brainstem (dashed outline), showing patterns of peripheral-central transition of myelinated fibres.

Fibre 1 enters the CNS directly. Fibres 2-5 are enveloped by alternating central and peripheral myelin sheaths and have one intercalated peripheral internode or more in the PTI.

Schematic transverse sections (1-4) show relationships of Schwann cell internodes to the central tissue projection at the levels of interruption of fibres 1 to 4 indicated (arrowheads) in (a).
Central tissue: white;
Peripheral tissue: shaded;
Schwann myelin sheaths: black;
Oligodendrocytic myelin sheaths: white;
Brainstem surface: arrows.

(b) Schematic longitudinal section through a dorsolateral vagal rootlet showing direct and alternating patterns of peripheral-central transition of unmyelinated axon bundles. For clarity the plexiform pattern of the bundles is greatly simplified.

Central tissue: white;
Peripheral tissue: shaded.
Bundle 1 enters the CNS directly towards the central end of the CTP.
Bundle 2 alternates three times between the CNS and PNS.

Bundle 3 traverses an endoneurial tunnel piercing the central tissue projection and enters the CNS directly at the central end of the PTI.
Bundles 4 and 5 alternate between the CNS and PNS in relation to the PTI and to an isolated island of peripheral tissue apposed to the central tissue projection surface, respectively.
From: Rossiter & Fraher (1990).

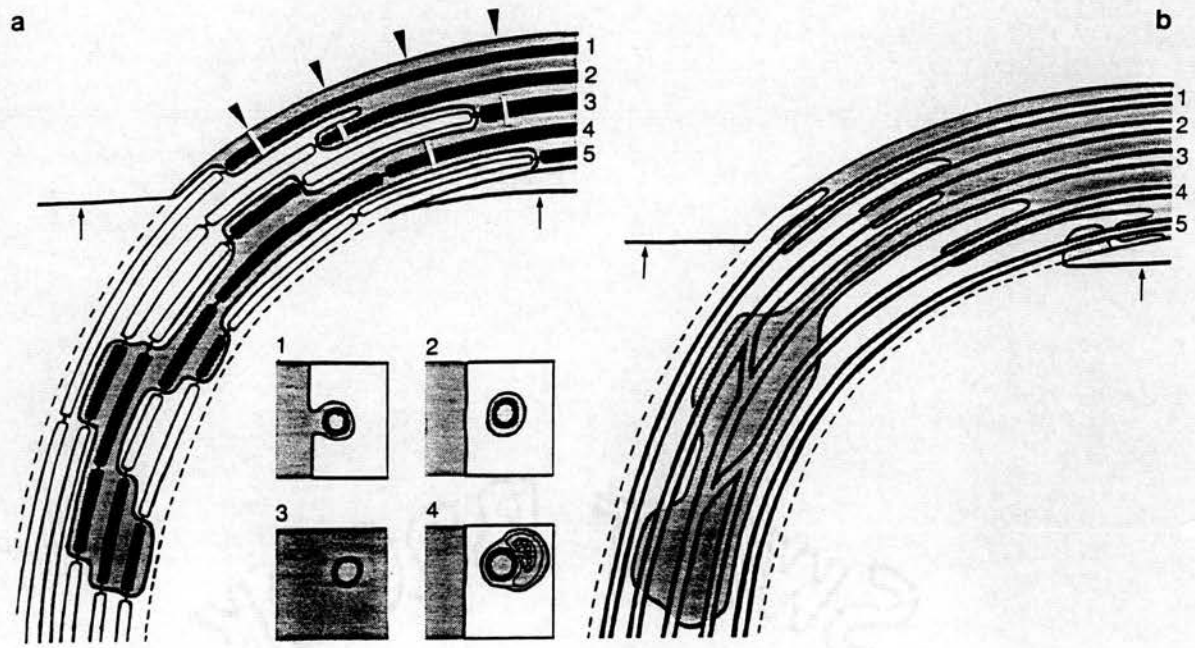

FIG. 18

Fig. 19 (a-d) Selected serial transverse sections of an axon illustrating alternation of central and peripheral myelin sheaths,

(a) at the level of the transitional Schwann cell perikaryon;

(b) within the central tissue projection the axon (asterisk) is enveloped by an oligodendrocytic myelin sheath apposed to those of two other centrally myelinated fibres;

(c) at the level of the intercalated Schwann cell perikaryon in the peripheral tissue insertion;

(d) where the axon (asterisk) has finally entered the CNS it is closely related to an oligodendroycte perikaryon and other centrally myelinated axons.

Scale bars: 1 μm.
From: Rossiter & Fraher (1990).

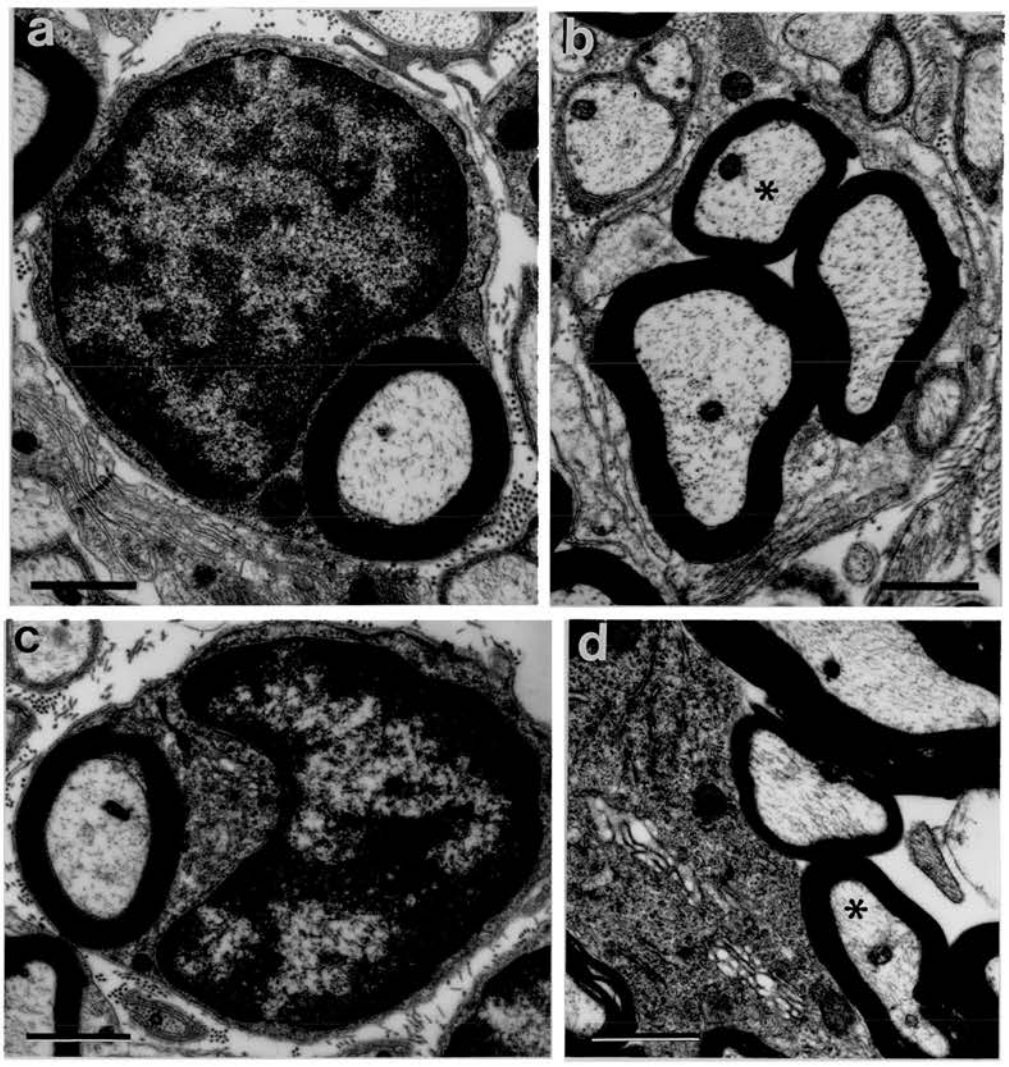

FIG. 19

Fig. 20 (a-d) Selected serial electronmicrographic transverse sections illustrating an axon (asterisks) that is unmyelinated peripheral and central to an intercalated Schwann cell myelinated segment:

(a) an unmyelinated segment is grouped with other unmyelinated axons enveloped by Schwann cell processes;

(b) a non-myelinating Schwann cell perikaryon envelops the unmyelinated axon segment;

(c) the intercalated myelinating Schwann cell perikaryon;

(d) a central unmyelinated segment of the axon within an unmyelinated bundle.

Scale bars: 1 μm.
From : Rossiter & Fraher (1990).

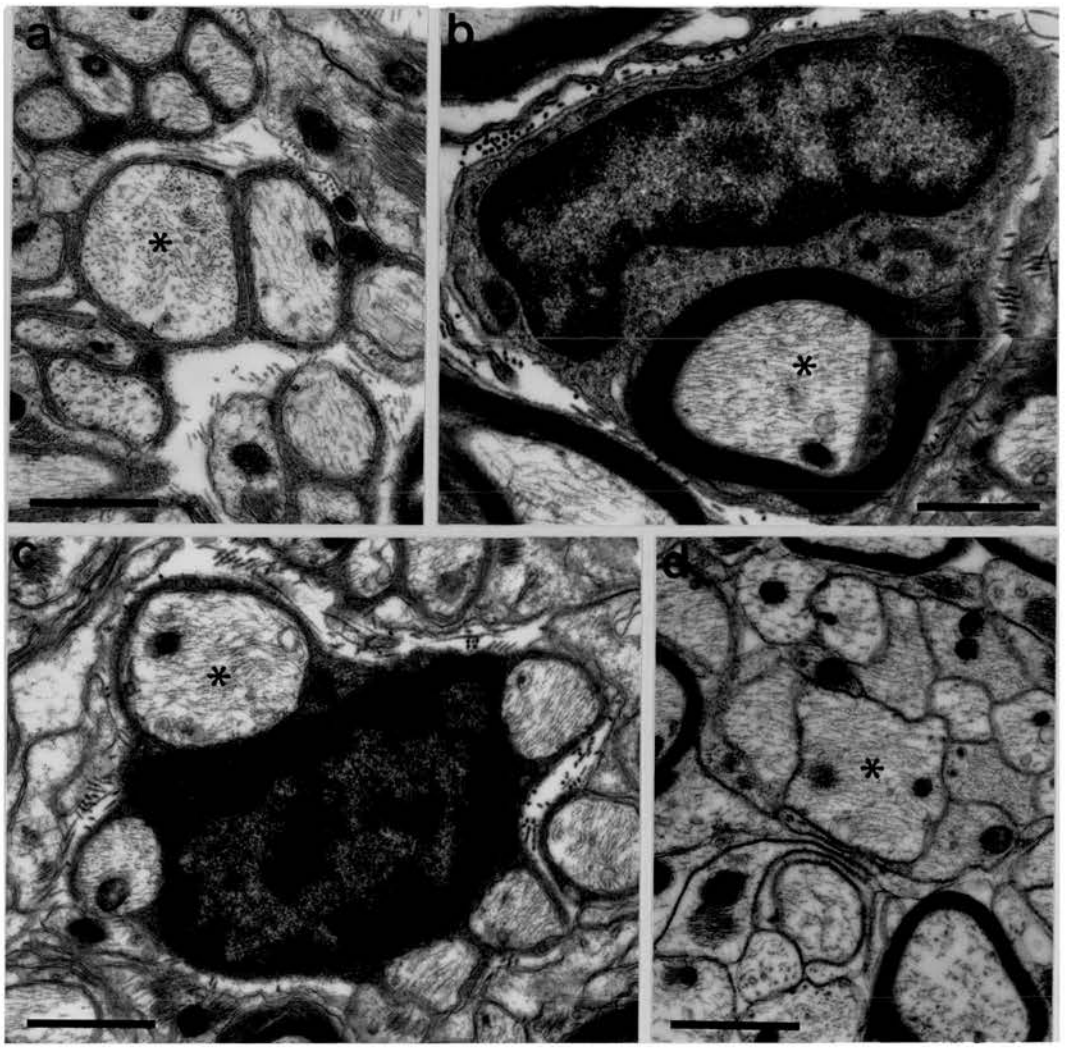

FIG. 20

Fig. 21 (a-d) Views of computerized three-dimensional representations of ventral, medial, dorsal and lateral aspects (a,b,c,d, respectively) of a central tissue projection showing the distribution of transitional nodes of large (unmarked pale spots) and small (pale spots containing solid circles) fibres.

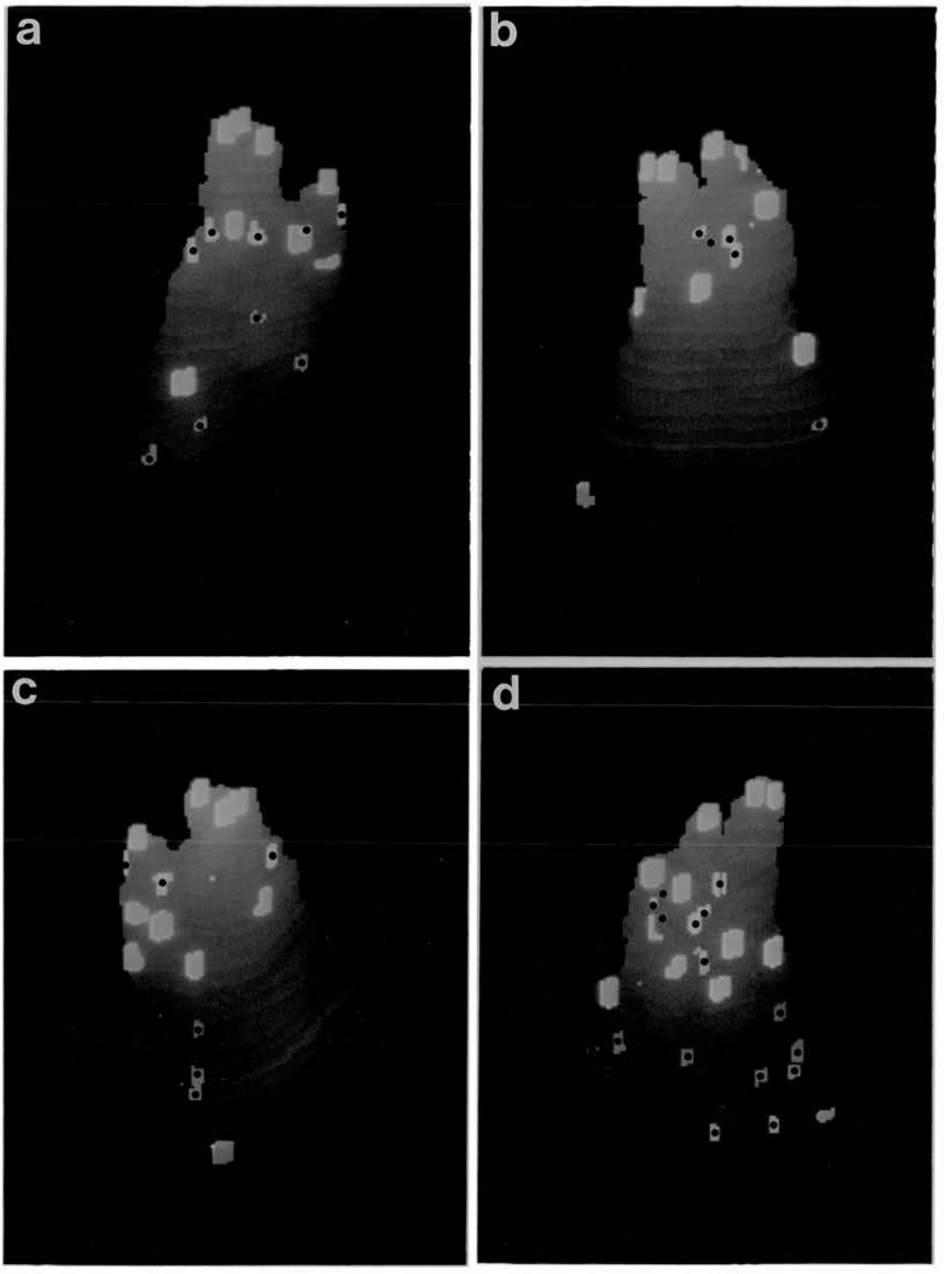

FIG. 21

Fig. 22 Diagrammatic sections through a Type 1 transitional zone of a a C2 ventral rootlet at right angles to the surface of the spinal cord (arrows), showing a plane projection of all of its transitional nodes (dots) relative to the median longitudinal plane of the intramedullary (broken lines) and free (solid lines) parts of the rootlet as it traverses the cord surface (arrows).

Left: lateral; right: medial.

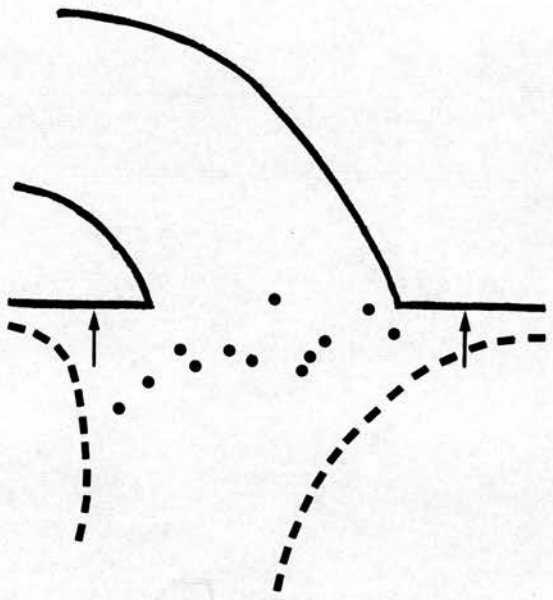

FIG. 22

Fig. 23 Rootlet sheaths.

(a) Diagram from a ventral viewpoint of an aggregated rootlet bundle (ARB) running superficial to the pia mater (shaded) and piercing the pia as it breaks up into its component rootlets which lie within the intrapial space before entering the CNS.

(b) Transverse section (in plane of large arrowheads in (a)) through the ARB (dotted) and the underlying CNS (shaded) as the ARB fuses with the pia mater (arrows).

(c) Transverse sections through the component rootlets (dotted) in the intra-pial space (arrow), which also contains bloodvessels (arrowheads).

(d) Diagrammatic longitudinal section through two rootlets (crosses) as they run between the superficial layer of the pia mater (arrowheads) right and the CNS (dotted) left. Rootlet sheaths are fenestrated (arrows). Through these the rootlet endoneurium communicates with the inter-radicular spaces which contains numerous blood vessels (asterisks), some of which enter the CNS with the rootlets and accompany their intramedullary segments as far as the grey matter.

(e,f) Diagrammatic transverse sections through (e) an aggregated rootlet bundle and (f) a cranial nerve rootlet, showing how extensively both, and in particular the latter, are subdivided by a network of attenuated cell processes.

(g,h) Diagrammatic longitudinal sections showing how, in some cranial nerves, a cytoplasmic compartment may contain only a single myelinated fibre. In some cases (g) the attenuated processes (shaded) bounding this end freely, short of the glia limitans (unshaded, below), while in others (f) they come into close apposition with it.

CNS surface: arrowheads.

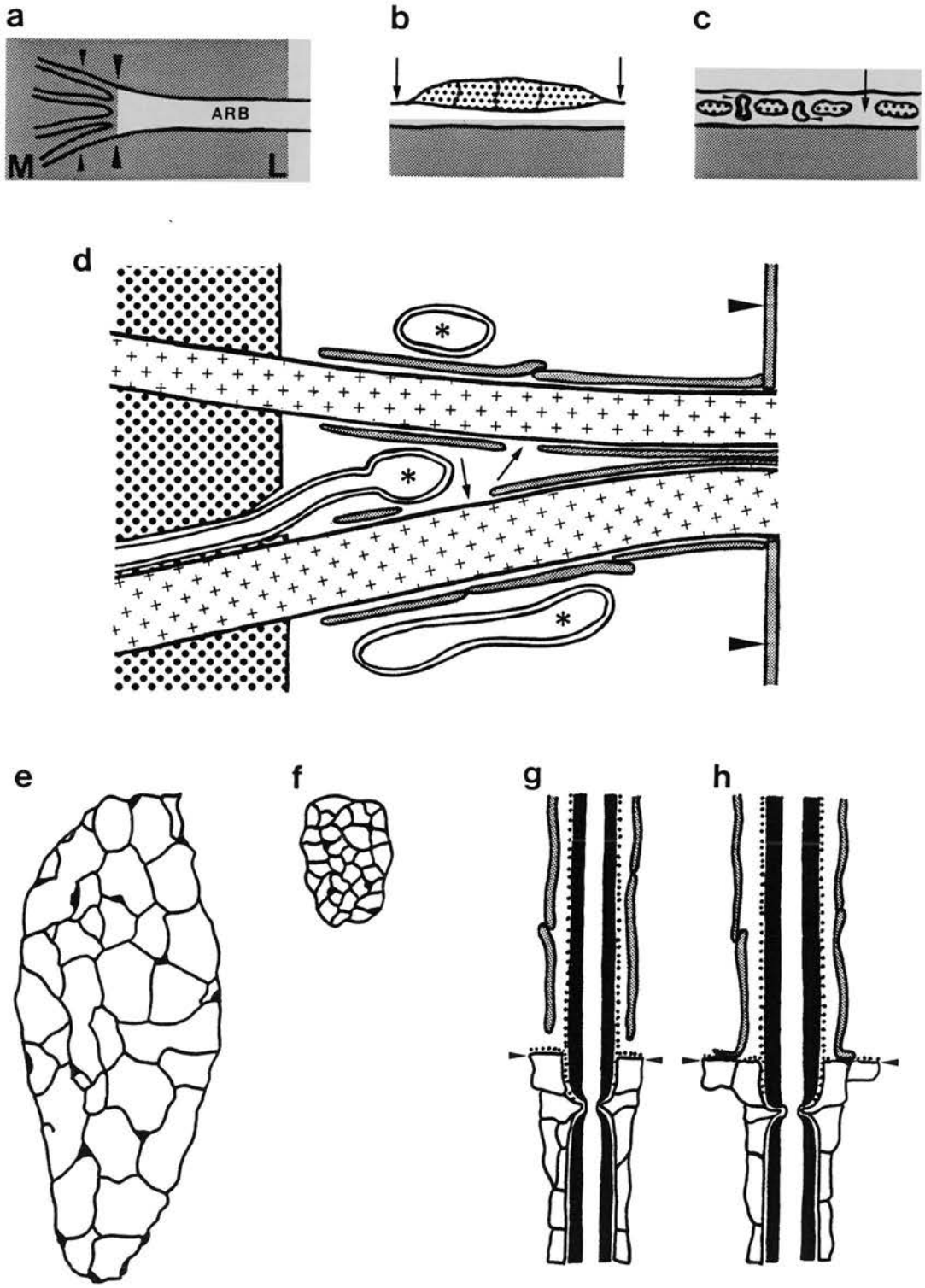

FIG. 23

Fig. 24 (a-c)

(a) Electronmicrograph showing the intimate inter-relationship between dark sheath cells of an abducent rootlet (above) with the glia limitans (below).

(b) Electronmicrograph of a transversely sectioned vestibular rootlet subdivided by a fine network of cytoplasmic processes into compartments, some containing only a single myelinated fibre, and others containing only collagen fibril bundles.

(c) Electronmicrograph showing a collagen fibril bundle in the space between the glia limitans (left) and the surface of the trochlear nerve (right) where the latter is composed of astrocytic processes.

Scale bars: 1 μm.

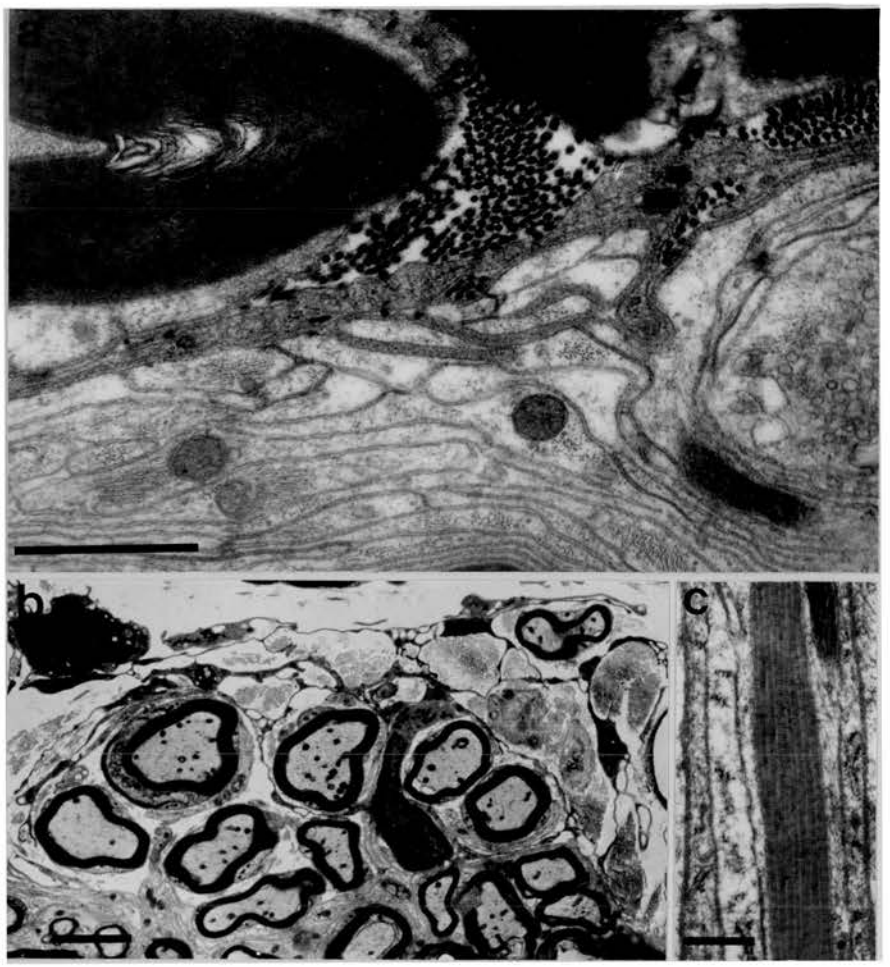

FIG. 24

Fig. 25 (a-c) Collagen fibril bundles related to transitional zones.

(a) Laminated bundles between adjacent surfaces of C7 dorsal root central tissue projections, where the latter are formed of astrocyte processes.

(b) Collagen fibril bundles (arrowed) extending into the glia limitans.

(c) Ring of collagen fibrils surrounding the attachment of a rootlet to the CNS, transversely sectioned in the angle between the former (arrowed, above) and the latter (arrowheads, below). Double arrowhead: pial cell.

(d,e) Bloodvessels at the transitional zone.

(d) Longitudinal section of lumbar spinal cord (below) and rootlets (above), showing a bloodvessel (asterisk) running from the inter-radicular space into the spinal cord accompanying a rootlet, of which the free (F), emergent (E) and intramedullary segments (I) are labelled.

(e) Tangential section through a 20 day fetal ventral root exit zone, showing ventral rootlets (asterisks) separated by inter-radicular spaces containing a rich network of bloodvessels.

Scale bars: a,b,c: 1 μm; d,e: 30μm.
a: from Fraher & Sheehan (1987); c: from Fraher & Kaar (1986); d: from Kaar & Fraher (1987); e: from Kaar & Fraher (1986).

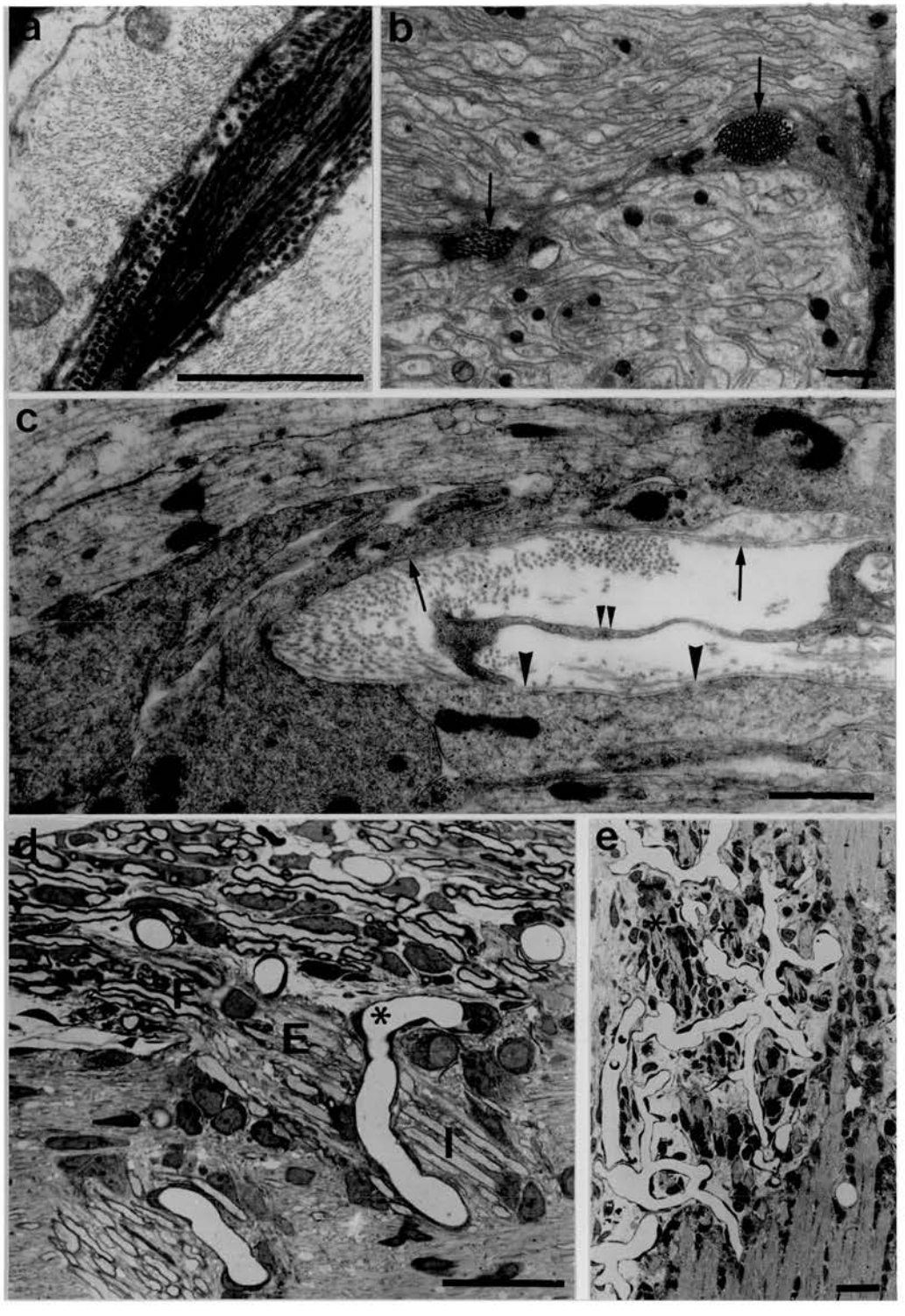

FIG. 25

Fig. 26 (a-e)

(a) Transverse section through a capillary in an inter-radicular space. Endothelial cell arrowed; Pericyte: asterisk. Note tight junction (arrowhead) where endothelial layers meet.

(b) Apposed margins of some endothelial cells are overlapped and irregular. Note obliquely sectioned plasma membranes (arrow).

(c) Apposed edges of some endothelial cells are tongued and grooved. Asterisk: lumen.

(d) Transverse section through a postcapillary venule. Its wall consists of inner endothelial (arrow) and outer pericyte (asterisk) layers.

(e) Electron micrograph showing the perivascular space around a postcapillary venule (below) traversing the spinal cord surface (above). Basal laminae (arrows) bound the space. Astrocyte processes: asterisks; pericyte: circle; endothelium: double asterisk.

Scale bars: a,d: 1 μm; b,c,e: 0.2 μm.
From: Kaar & Fraher (1987).

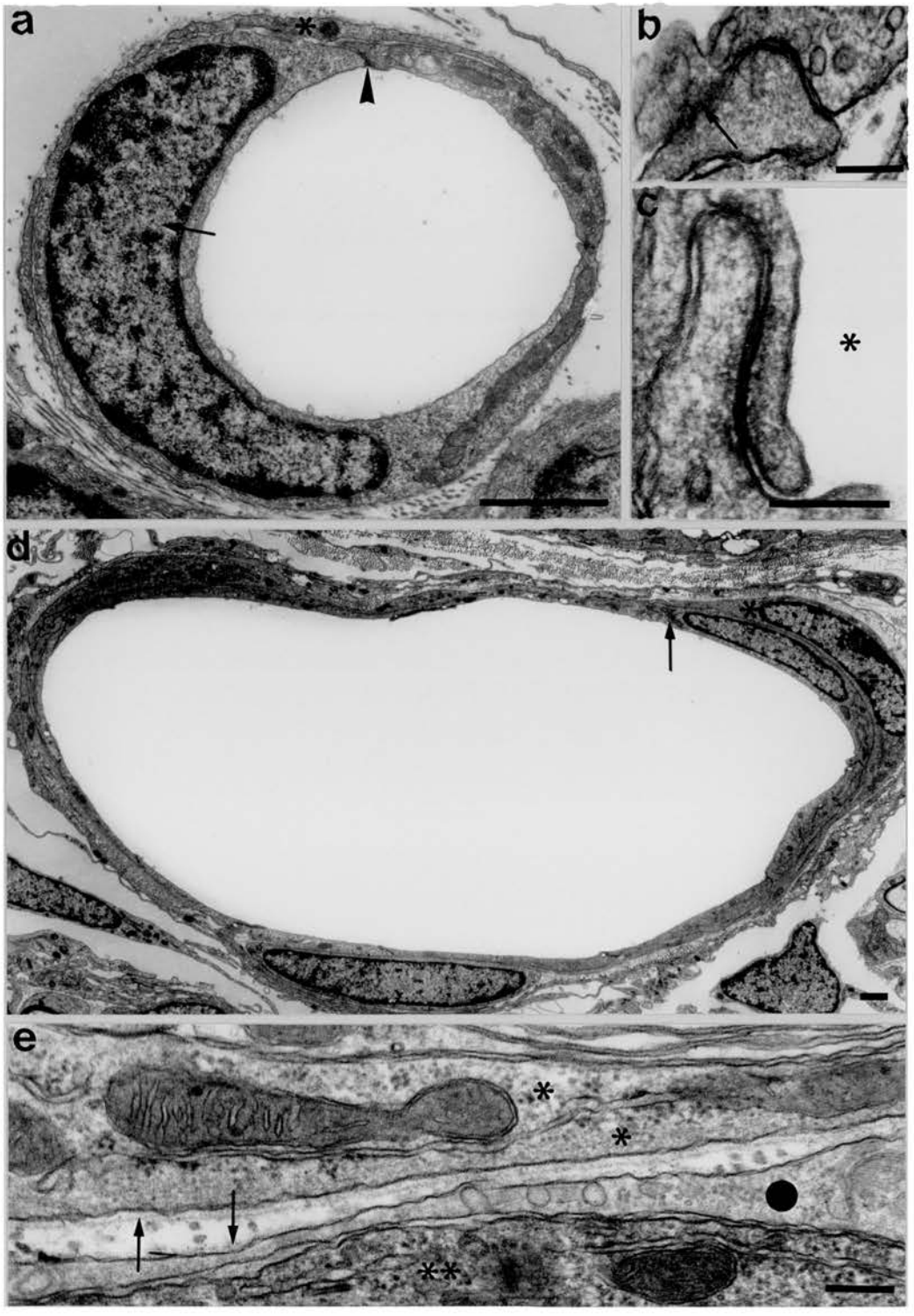

FIG. 26

Fig. 27 Ultrastructural features of developing transitional zone.

(a) Transversely sectioned axons segregated by matrix of astrocyte processes.

(b,c) Presumptive Schwann cells forming sleeves around (b) longitudinally and (c) transversely sectioned developing L5 rootlets. Within the rootlet (c) individual axons are segregated by a matrix formed of fine processes arising from the presumptive Schwann cells.

(d,e) Transverse sections through developing lower cervical transitional zones in planes tangential to the spinal cord surface, showing (d) a number of Schwann cell perikarya lying at or deep to the level of the spinal cord surface and (e) at a later stage the central ends of a transitional Schwann cell (asterisk) invaginated deep to the cord surface. Adjacent to it is an oligodendrocyte paranode (double asterisk).

(f) Transverse section through a developing myelinated axon in an invagination of the cord surface (arrowheads) containing basal lamina and bounded by astrocyte processes.

Scale bars: a, c: 1 μm; b,d,e,f: 5μm.
a,c: from Fraher & Rossiter (1983a); e,f: from Fraher (1978a).

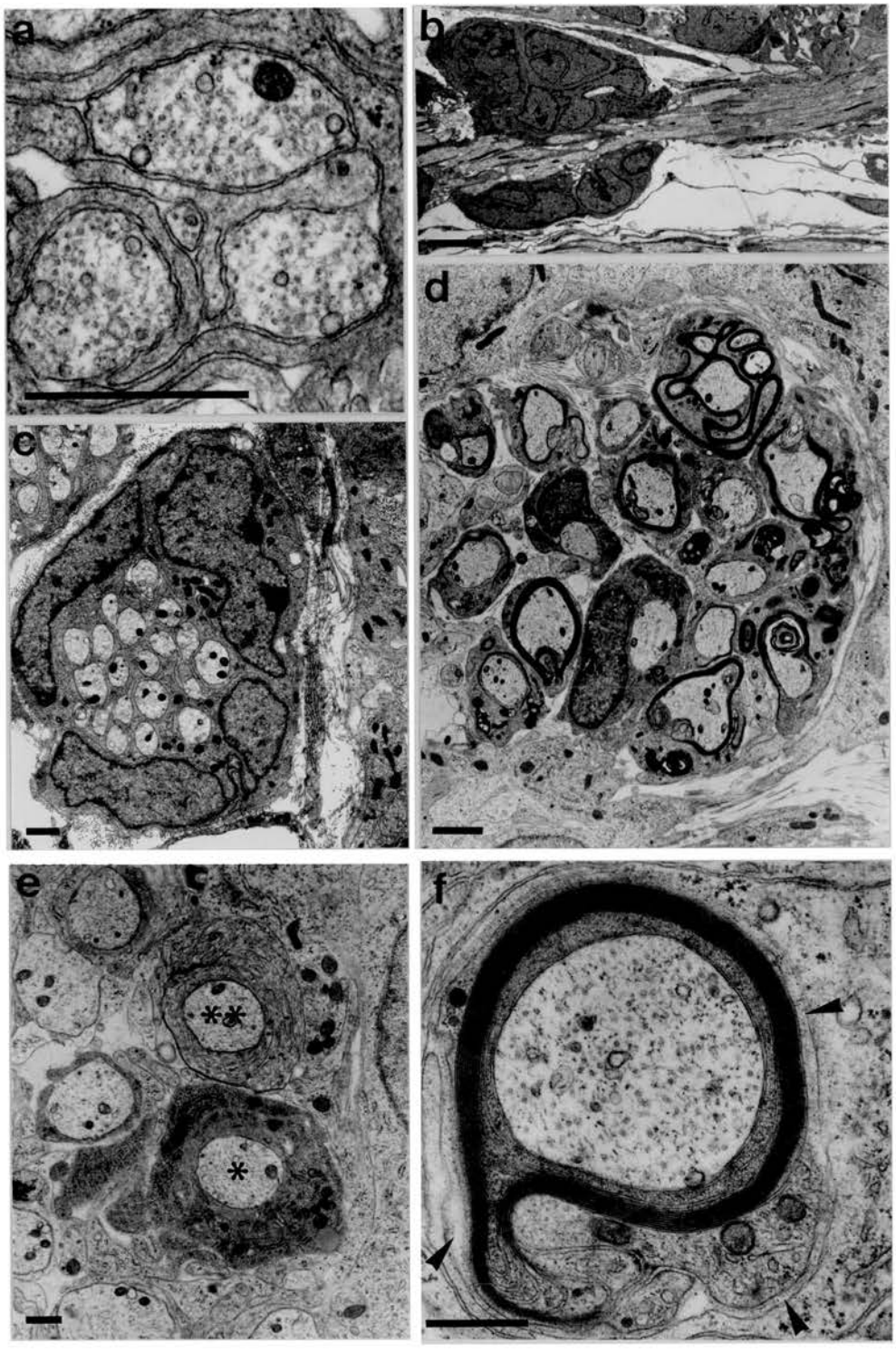

FIG. 27

Fig. 28 Diagrammatic longitudinal sections showing the segregation and myelination of developing axons traversing the CNS surface (arrowheads).

(a) Cluster of presumptive Schwann cells encapsulating one another. One is shown giving rise to a process entering the axon bundle (left) and beginning to segregate it. Another (above) is leaving the cluster and is beginning to envelop an axon.

(b) At a later stage one axon (left) is enveloped by a Schwann cell, the perikaryon of which lies in a depression on the CNS surface, while another (right) has elongated and its perikaryon has migrated distally beyond the CNS surface, but its central end continues to invaginate the CNS surface.

(c) The central end of a transitional Schwann cell, lying in its invagination has formed a number of turns of its mesaxon which are longitudinally sectioned (arrows).

(d,e) The myelin sheath has become compacted and with maturation (e) increases in thickness and becomes more deeply invaginated below the CNS surface than previously.

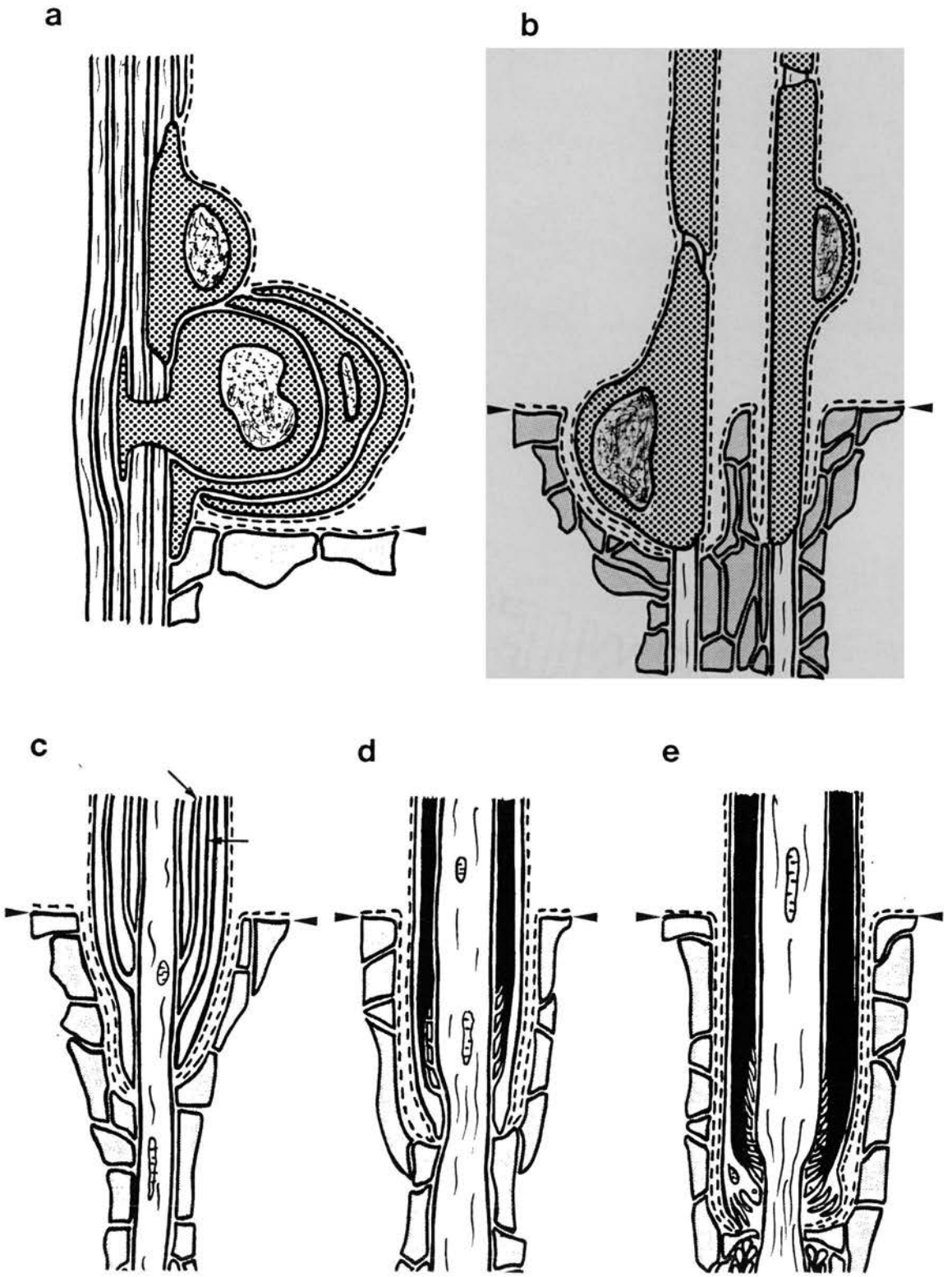

FIG. 28

Fig. 29 (a-d) Light micrographs of longitudinally sectioned C7 dorsal rootlets attached to the spinal cord (SC) at (a) 3, (b) 4, (c) 6 and (d) 12 days postnatum. At 4 days, note the epithelioid arrangement (arrow) of astrocyte perikarya in the central tissue projection.

(e-i) Light micrographs of sections through developing cochlear nerve.

(e) 16 day fetus. The central tissue projection (asterisk) is much less cellular than the peripheral segment of the nerve.

(f) 1 day postnatum. The central tissue projection (arrowhead) is more cellular than previously. Its distal limit (outlined) lies about half way along the segment of the nerve which lies in the subarachnoid space (S). Cochlear nerve bundles traverse loose tissue to reach the cochlear ganglion (arrow).
Left: medial; right: lateral.

(g) 6 days postnatum. The distal limit of the central tissue projection (outlined) lies in the modiolus. Peripheral branches (arrows) arise directly from the projection.

(h-i) 16 day fetus. Transverse sections (h) through the almost acellular central tissue projection (asterisk), where it is attached to the inferior cerebellar peduncle, (i) through the highly cellular peripheral tissue segment of the nerve (arrowheads) immediately distal to the central tissue projection.
M, medulla oblongata;
O, otic capsule;
ICP, inferior cerebellar peduncle;
S, subarachnoid space.

Scale bars: a-d: 20 μm; e-i: 100 μm.
a,c: from Fraher & Sheehan (1987); e-i: from Fraher & Delanty (1987).

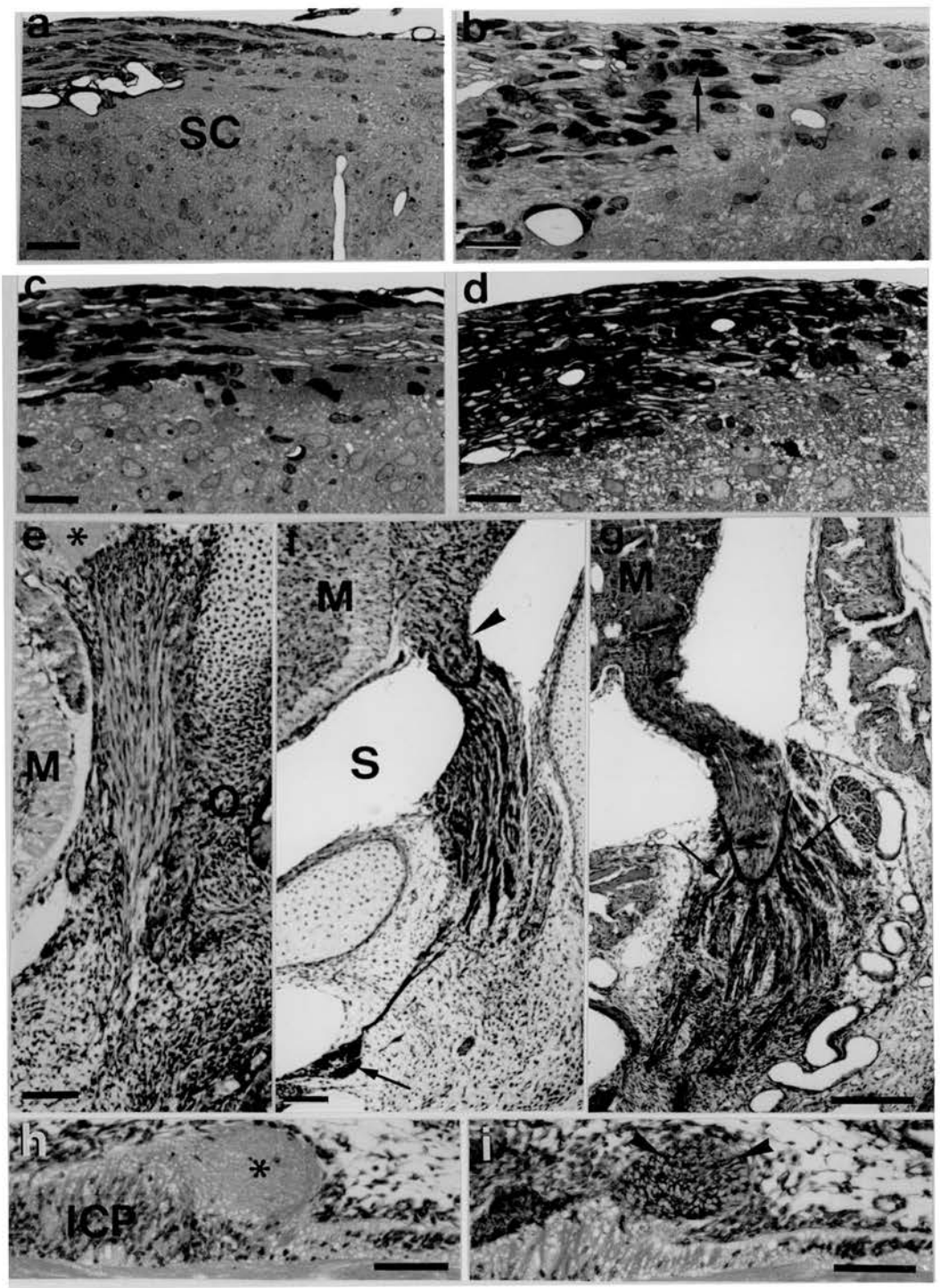

FIG. 29

Fig. 30 Diagrammatic longitudinal sections through developing transitional zones of

(a-d) Cochlear nerve, showing the progressive outgrowth of the central tissue projection into the modiolus between (a) 17 days fetal, (b) 1, (c) 6 and (d) 13 days postnatum;

(e-h) C7 dorsal rootlet, showing the form of the central tissue projection at (e) 3, (f) 6, (g) 12 and (h) 20 days postnatum (Note the proximal regression of the projection between 12 and 20 days);

(i-l) L5 ventral rootlet, showing the form of the central tissue projection at (i) birth, (j) 6, (k) 12 and (l) 20 days postnatum (Note the proximal regression of the projection between 6 and 12 days).

a-d: from Fraher & Delanty (1987); e-h: based on Fraher & Sheehan (1987); i-j: based on Fraher & Kaar (1986).

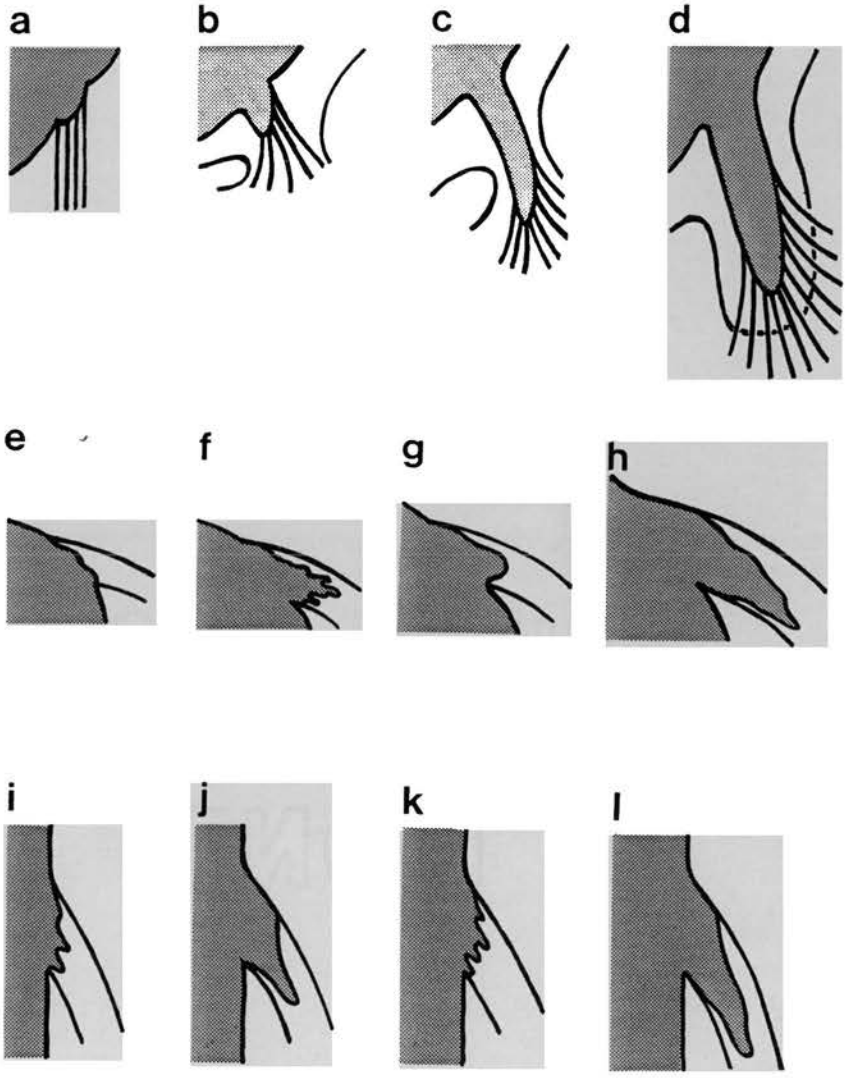

FIG. 30